THE AVOIDANCE RESPONSE OF PHYCOMYCES IN A CONTROLLED ENVIRONMENT

Thesis by
Paul Wells Meyer

In Partial Fulfillment of the Requirements
for the Degree of
Doctor of Philosophy

California Institute of Technology
Pasadena, California

1986

(Submitted December 6, 1985)

Acknowledgements

I wish to thank my advisor, Dr. Howard C. Berg, for his help with the design and construction of my experimental apparatus, for defining the experimental strategy needed to unlock the avoidance riddle, for his willingness to help with any problem on a moment's notice, his patience, and his example as a scientist and as a human being.

I also wish to thank the following people, in chronological order of appearance:

My parents, Peter Meyer and Patricia Brown.

Veit Elser, my roommate for two years as an undergraduate at Caltech, for help with courses in mathematical physics.

Dr. Hans Liepmann, my undergraduate adviser at Caltech, for introducing me to Max.

Dr. Max Delbrück, for inviting me to work in his lab as an undergraduate at Caltech in January, 1978, for his example as a scientist, and for trying to teach me how to think.

Manny Delbrück, for her interest in this research, and for including me in her family.

The members of my advisory committees: Dr. Howard Berg, Dr. Charles Brokaw, Dr. Jim Hudspeth, Dr. Henry Lester, Dr. Jerry Pine, and Dr. Jean-Paul Revel, for their advice, and for giving me a push at a critical moment in June, 1982.

Dr. Ed Lipson and Dr. Patricia Burke, for organizing the Cold Spring Harbor Phycomyces meeting in August, 1982, and the Caltech Division of Biology, for providing a travel allowance.

My fellow avoidance investigators Dr. Jean-François Lafay and Dr. Jean Matricon at the University of Paris, Dr. Igor Gamow at the University of Colorado, and Dr. Robert Cohen at the University of Florida, for useful discussions.

Ivan Matus, for finally doing the definitive experiments, and for many helpful discussions.

Diana Brooks, for her patience, encouragement, and help with communication skills.

Dr. Norman Brooks, for his friendly advice in March, 1984.

Markus Meister, for applying his mathematical and physical insight to this problem, and for his invaluable suggestions on finding particular solutions to Laplace's equation.

I would also like to acknowledge the financial support of the National Science Foundation through a three year graduate fellowship, the National Institutes of Health through an NRSA training grant, and Caltech through the Mc Callum fund, several Graduate Research and Teaching Assistantships, and Special Institute Fellowships.

ABSTRACT

If an object is placed 1 mm away from the growing zone of a Phycomyces sporangiophore growing in air, then after 2 to 6 min the sporangiophore bends away from the object, without ever touching it, at a rate of about 1°/min. The sporangiophore stops bending after about 30 min. This is called the avoidance response of Phycomyces.

How does the sporangiophore detect the object? It seems likely that a chemical mechanism is involved, since other physical stimuli (light, electric and magnetic fields) have already been ruled out.

A simple mechanism was proposed 10 years ago, in which the ambient air currents near the surface of an object modify the distribution of a hypothetical, short-lived effector gas emitted by the sporangiophore. However, the avoidance response occurs at its usual rate in the complete absence of ambient air currents. Thus, the suppression of air currents near the surface of a solid object cannot provide the signal for the response.

The avoidance rate depends significantly on the recent history of the experimental chamber, on the length of time the sporangiophore has spent inside the experimental chamber, and on other factors. By carefully controlling environmental variables, the variation in avoidance rate of different sporangiophores in successive experiments can be held to less than ±10%. This allows accurate determination of the distance dependence of the response, and accurate comparison of different types of barriers.

The rate of the response falls off above 90 % relative humidity - but does not fall to zero. Surprisingly, the sporangiophore avoids a thin, 120 μm diameter parallel wire placed 0.5 mm away at about the same rate as it avoids another sporangiophore placed at the same distance. Also, the distance dependence of the avoidance response appears to be much weaker than previously reported, and the response may depend on the chemical composition of the object, in contrast to previous reports. These findings, combined with the results of calculations presented in Appendix 3, argue strongly against the hypothesis that the barrier acts merely by reflecting a diffusible substance emitted by the sporangiophore.

The only remaining viable chemical mechanism for the avoidance response requires that the signal molecule emitted by the sporangiophore be adsorbed by the surface of the avoided object for a nonzero length of time, and not just be reflected by it. Three new versions of this hypothesis are presented which are consistent with the experimental results.

Table of Contents

CHAPTER	TITLE	PAGE
	Acknowledgement	ii
	Abstract	iv
	List of Illustrations	ix
	Glossary	xi
1	Introduction	1
2	History	9
	(I) Discovery of the avoidance response in Phycomyces	9
	(II) Responses to water vapor	11
	(III) Discovery of olfactory chemotropism in Phycomyces	13
	(IV) Zinc and aluminum	16
	(V) Sporangiophore flaring	17
3	General Methods	18
	(I) Culture conditions	18
	(II) Experimental procedure	19
	(III) Apparatus for the avoidance response	24
	(A) Mechanical design	24
	(B) Temperature control	28
	(IV) Measurement of air movements	38
	(V) Measurement and control of relative humidity	42
	(A) Experimental procedure	42
	(B) Correction for cooling the base of the apparatus	43
	(C) Direct measurement of the relative humidity	45
	(VI) Cleaning the apparatus	47
	(VII) Barrier preparation	49

CHAPTER	TITLE	PAGE
4	Experiments, Results and Interpretations	50
	(I) Outline of the results and interpretations	50
	(A) The Growth-Promoter Reflection Model ...	52
	(B) The Wind Gradient Model	53
	(C) The Growth-Inhibitor Adsorption Model ...	54
	(D) The Atmospheric Growth-Inhibitor Model	55
	(E) The Barrier Emission Model	55
	(II) Avoidance in the absence of ambient wind	56
	(III) Reproducible avoidance rates	58
	(A) Environmental controls	59
	(B) Experimental procedure	60
	(C) Data analysis.....	62
	(D) Results obtained with reproducible avoidance rates.....	67
	(IV) Humidity dependence	73
	(V) Inhibition of the avoidance response by cleaning the apparatus	75
	(VI) Time dependence of the response	79
	(VII) Recent results supporting the new working hypothesis	83
	(A) Dependence on chemical composition ...	83
	(B) Avoidance of thin wires	85
	(C) Distance dependence in a wind-free environment	86

CHAPTER	TITLE	PAGE
5	Discussion	87
	Appendices	90
	1. Derivation of the corrected growth rate	90
	2. Derivation of the corrected bending rate, in the plane of bending	93
	3. Mathematical modeling of the response	96
	(I) Introduction	96
	(II) Solutions to Laplace's equation in open air: emission or adsorption of a gas by a sphere	98
	(III) Solutions to Laplace's equation in open air: emission or adsorption of a gas by a thin cylinder	104
	(IV) Plane and wire barriers	109
	References	135

List of Illustrations

NUMBER	TITLE	PAGE
1	Scale drawing of a sporangiophore	2
2	Photograph of the experimental setup	22
3	Cross-sectional view of the environmental chamber	25
4	Temperature-sensing bridge and amplifier circuit	29
5	Current amplifier for heater coil	31
6	Triac drive circuit for room air heater	35
7	Wind velocity inside the chamber as a function of vertical thermal gradient	41
8	Data from a typical experiment	65
9	Avoidance rate at 0.5, 1.0, and 2.0 mm from the barrier	68
10	Avoidance rate as a function of the time delay between the positioning of the barrier and the first measurement of the horizontal position of the sporangium	69
11	Avoidance rate as a function of stalk diameter	71
12	Aiming error as a function of the initial angle of the sporangiophore with respect to the barrier	72
13	Avoidance rate as a function of relative humidity	74
14	Typical avoidance response after cleaning the chamber with alkaline detergent, and typical response without cleaning	76
15	Avoidance rate as a function of the elapsed time during the experiment	80

NUMBER	TITLE	PAGE
16	View of the sporangiophore (a), the vertical component of its growth rate as a function of bending angle (b), and the vertical elevation along the growing zone as a function of bending angle (c)	92
17	The path of the sporangium as viewed from above (a), and the vertical and horizontal components of the growing zone (b), viewed in the plane of bending	95
18	The coordinate system used in the calculations	97
19	The concentration of an emitted precursor gas and an adsorbed effector gas	103
20	The concentration of a gas emitted by a thin cylinder	108
21	The concentration of the effector gas in the Growth-Promoter Reflection Model	118
22	The concentration of the inhibitor in the Inhibitor Adsorption Models	128
23	The concentration of the effector in the Barrier Emission Model	133
24	Summary of the concentration and flux differences predicted for the five proposed models for the avoidance response	134

Glossary

a = sporangiophore radius, cm

α = sporangiophore bending angle, °

c = effector gas concentration, molecules/cm^3

c_P = precursor gas concentration, molecules/cm^3

c_O = effector gas concentration at the surface of the growing zone, molecules/cm^3

c_{OP} = precursor gas concentration at the surface of the growing zone, molecules/cm^3

c_∞ = background gas concentration, molecules/cm^3

$\Delta c/c$ = fractional difference in the concentration of effector gas across the growing zone, i.e., $\Delta c/c = [\, c(\theta = \pi) - c(\theta = 0)\,] / c(\theta = \pi/2)$.

$\Delta F/F$ = fractional difference in flux of effector gas into the growing zone, i.e., $\Delta F/F = [\, F(\theta = \pi) - F(\theta = 0)\,] / F(\theta = \pi/2)$.

d = distance from the sporangiophore axis to a plane barrier (or to the axis of a parallel wire), cm

D = diffusion coefficient of effector gas, cm^2/sec

D_P = diffusion coefficient of precursor gas, cm^2/sec

F = flux, positive away from the growing zone, molecules/cm^2/sec

k = adsorption rate constant, cm/sec

L = length of sporangiophore growing zone, cm

R_d = $(D\tau)^{1/2}$ = decay length of effector gas, cm

R_{dp} = $(D_P\tau_P)^{1/2}$ = decay length of precursor gas, cm

R_{MAX} = the distance at which the effector concentration is maximum, in the "growth-inhibitor adsorption" model

ρ = distance to the axis of a thin wire barrier, cm

ρ_o = radius of a thin wire barrier, cm

τ = decay time of effector gas, sec

τ_P = decay time of precursor gas, sec

U = air velocity, cm/sec

v = growth rate of sporangiophore, μm/min

θ = aiming error angle, or azimuthal angle around the axis of the growing zone, °

ϕ = azimuthal angle around the axis of a thin wire barrier

1. Introduction

The mycelium of the fungus Phycomyces sends up, into the air, a long thin tube about 0.1 mm in diameter, called a sporangiophore. The sporangiophore develops at its tip a spherical sporangium about 0.5 mm in diameter, containing approximately 10^5 asexual spores. Growth of the sporangiophore occurs in a tapered zone extending 2 to 3 mm below the base of the sporangium. When the sporangiophore is mature (stage 4b, about 2 cm long), it grows steadily at about 3 mm/hr, and twists clockwise, when viewed from above, at about 2 revolutions/hr. It normally reaches a height of 10 cm or more. A scale drawing of a sporangiophore is shown in Fig. 1.

If an object is placed 1 mm away from the growing zone of a sporangiophore, then after 2 to 6 min the sporangiophore bends away from the object, without ever touching it, at a rate of about 1°/min. See Fig. 1. The sporangiophore stops bending after about 30 min. This is called the avoidance response of Phycomyces.

The avoidance response was discovered independently by Elfving (1881) and by Wortmann (1881), and then ignored until 1962.

Elfving (1890) reported that sporangiophores bent toward pieces of rosin, tree pitch, or rusted iron placed directly above a growing Phycomyces culture. This "positive aerotropic bending," as he called it, was studied extensively by him, Steyer (1901), and Errera (1892). The sporangiophores bent toward strongly reducing metals and toward odor sources (e.g., volatile organic compounds, ozone, mineral acids). This work is discussed by Elfving (1917). The pre-1925 avoidance literature, published mainly in German, is reviewed further in Chapter 2.

Fig. 1. Scale drawing of a sporangiophore

The lower drawing shows the stalk, growing zone, and sporangium of a stage IVb Phycomyces sporangiophore viewed from the side. The mycelium plus sporangiophore(s) constitute a single, multinucleate cell. The cell wall at the growing zone is composed of chitin (poly-acetylglucosamine) approx. 0.5 μm thick. See Bergman, et al. (1969) and Burke (1971) for further information on the ultrastructure of sporangiophores.

The upper drawing shows a sporangiophore avoiding a barrier. The bending angle is defined as the angle between vertical and the upper segment of the growing zone.

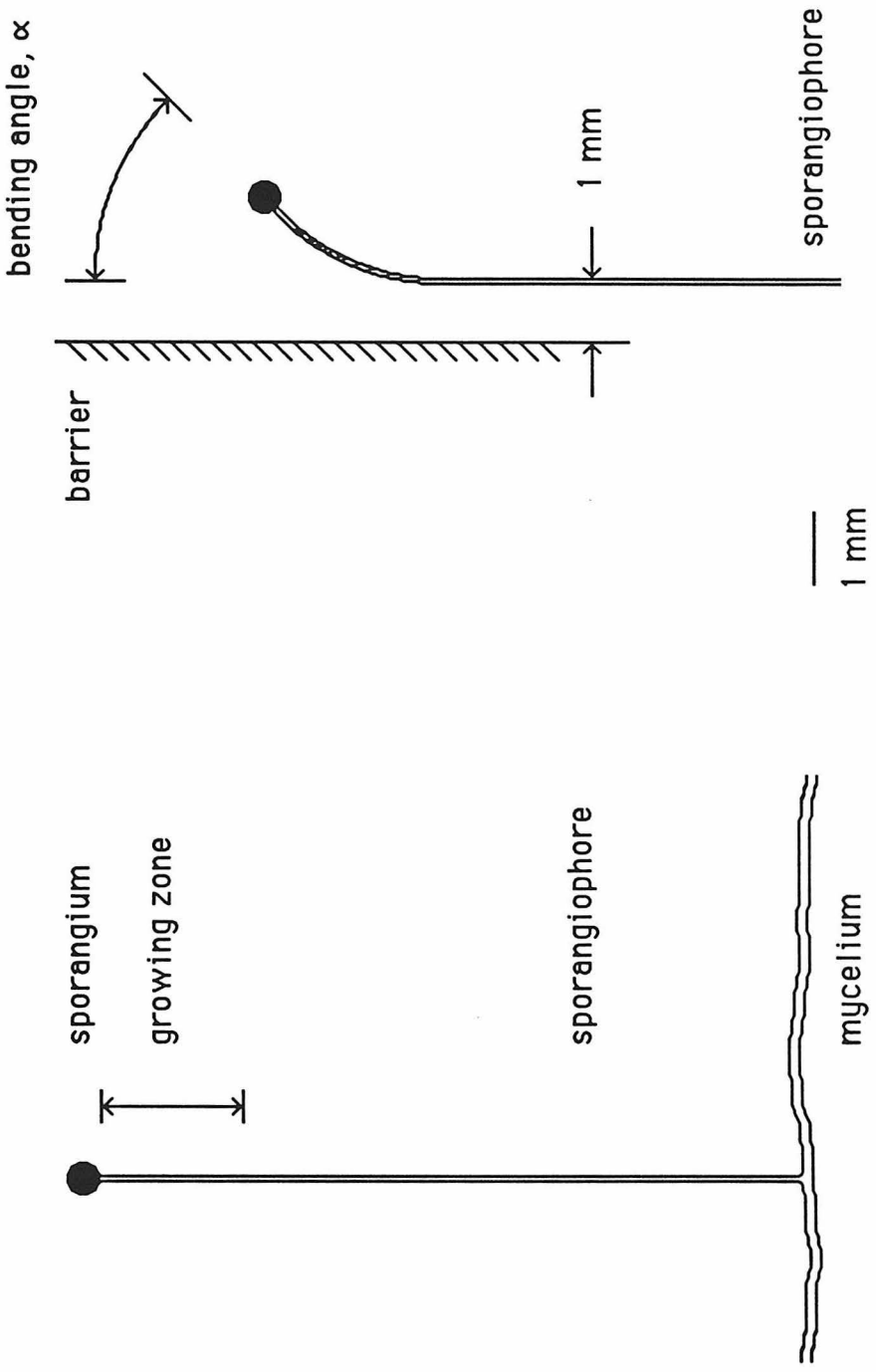
bending angle, ∝
barrier
1 mm
sporangiophore
1 mm
sporangium
growing zone
sporangiophore
mycelium

The avoidance response was rediscovered by Shropshire (1962), who published the first known report of avoidance of a dry surface (glass), along with the first quantitative, minute-by-minute observation of bending angles during an avoidance response. He also reported that the avoidance response is suppressed at relative humidities above 95%.

The response was studied extensively by Max Delbrück and his students at Cold Spring Harbor and at Caltech, from 1965 to 1975 [reviewed by Cohen, et al. (1975), and by Jan (1974)]. Electrostatic fields, magnetic fields, and electromagnetic radiation were ruled out as possible signals for the avoidance response. A number of different barriers and barrier materials were investigated, such as a parallel, aligned sporangiophore, a 50 μm diameter wire, various metals, activated charcoal, KOH, H_2SO_4, water, and oils; all produced measurable avoidance responses. Symmetrically placed barriers did not produce bending, but elicited a brief (15 min) increase in growth rate of sporangiophores. Also, sporangiophores bent upstream into a wind current of 10 cm/sec at a rate of about 1°/min. They exhibited growth responses to changes in wind speed as small as 1/2 cm/sec, growing more slowly after a step-up in wind speed, and vice-versa.

The first published model for the avoidance response, the Chemical Self-Guidance Hypothesis (CSGH), is consistent with these results. The CSGH according to Bergman, et al. (1969) is :

"...a gas evaporates from the growing zone (e.g., water, CO_2, organic molecule) which develops a higher concentration on the side of the sporangiophore proximal to the barrier than on the distal side. A concentration gradient across the growing zone might then cause bending, and a step-up in concentration (with bilateral barriers), a transient growth response."

The CSGH according to Cohen, et al. (1975) is :

"A volatile growth effector is emitted by the organism. The barrier causes a concentration gradient across the sporangiophore and therefore the

differential growth rate. Bilateral barriers result in symmetric changes in concentrations, and hence cause a transient growth response."

Cohen, et al. (1975) rejected the simple version of the CSGH in which the barrier merely blocks the diffusion of a stable, growth-promoting (effector) molecule, for three reasons : they were unable to detect the hypothetical effector in a bioassay, the avoidance response away from activated charcoal was about as strong as the response away from glass, and a 50 μm diameter wire produced a measurable avoidance response at a distance of 0.5 mm. They proposed instead that an effector gas is emitted by the sporangiophore growing zone, but is readsorbed by the growing zone and does not diffuse more than a fraction of a millimeter away, on average. Since ambient air currents are suppressed by viscous drag within a few millimeters of any solid object (their velocity dropping to zero at the surface of the object itself), the effector would still accumulate on the (less windy) side of the sporangiophore facing the object, causing the sporangiophore to bend away.

Conclusive evidence against this Wind Gradient Model, and further evidence against the simple CSGH are presented in Chapter 4. No further modifications to the CSGH have appeared in the published avoidance literature since the work of Cohen, et al. (1975).

Johnson and Gamow (1971) claimed that the avoidance response does not occur in still air, but that an 0.2 mm/sec air current is sufficient to sustain the response. They also postulated that ambient wind is necessary to produce a "reflection gradient" of a signal gas across the sporangiophore, and that this gas is water vapor. None of this can be correct (Chapter 4).

Lafay, et al. (1975) measured the distance dependence of the response in open air for flat metal barriers 2 mm and 20 mm in diameter. They found that the avoidance bending rate decreases with distance as $[1/r]^{0.6\pm0.1}$, for distances, r, between 0.12 mm and 2.2 mm. Ambient air movement in their setup probably steepens the distance dependence by suppressing the

response as the sporangiophore is moved away from the barrier [see Cohen, et al. (1975, Fig. 5)]. Fig. 8 from Cohen, et al. (1975), shows a $[1/r]^{0.3\pm0.2}$ dependence for a 50 μm diameter wire barrier placed at a distance, r, between 0.03 mm and 1.0 mm from the sporangiophore. Matus (1985) has found that for a plane barrier, in the absence of wind, the avoidance rate is constant out to about 4 mm and then drops off sharply beyond that (Chapter 4, Section VII).

Russo, et al. (1977), and Russo (1977) found that ethylene and ethane both elicit short, positive growth responses and also inhibit the avoidance response, at concentrations of 10 to 100 ppm (for C_2H_4) in air. They claimed that ethylene must be the effector gas emitted by the sporangiophore in the "emission-readsorption" model of Cohen, et al. (1975), because they found that the sporangiophore emits ethylene at a rate of approximately 2.4×10^7 molecules per sporangiophore per second. However, a calculation in Appendix 4, Section III, shows that this emission rate would yield a concentration of at most 10^{-5} ppm ethylene at the growing zone surface, so ethylene itself cannot be the signal gas. Unfortunately, Russo, et al. (1977) tried to avoid this problem by proposing that the concentration of ethylene could be in the 10-100 ppm range somewhere inside the sporangiophore (the "site of action" of ethylene) and yet be controlled by changes of 10^{-5} ppm on the outside, for example, during an avoidance response. But if that were true, they would have seen a threshold of 10^{-5} ppm for eliciting growth responses, and not 10 ppm as observed in their experiments. So their argument that ethylene could act as the signal gas in this way is incorrect.

Cohen, et al. (1979) discovered that the sporangiophore exhibits a transient negative growth response when exposed to any one of 22 different volatile organic substances, at concentrations as low as 0.1 ppm. Many of the substances are the same ones that attracted sporangiophores in Elfving's experiments, which makes sense, because the concentration of a

growth-inhibiting gas will be higher on the side of the sporangiophore facing a source of the gas, so the sporangiophore should bend toward it. Non-specific olfactory chemotropism is probably a distinct tropic response of Phycomyces. It may have adaptive value, since Phycomyces is often found growing on rodent dung in nature.

Lafay (1980) and Lafay and Matricon (1982) found that sporangiophores avoid a moving barrier (e.g., a 30 cm long conveyor belt moving at 2 cm/sec) about as fast as they avoid a stationary one. This is evidence against the Wind Gradient Model of Cohen, et al. (1975), since the ambient wind velocity decreases with distance away from a moving barrier, and in that model the sporangiophores should bend toward such a barrier. However, their result still leaves open the possibility that the sporangiophore detects an object by emitting a large, long-lived signal molecule which gets trapped in the boundary layer next to the surface of the object (whether moving or not). There is now strong evidence against any model in which the sporangiophore uses ambient wind to detect an object (Chapter 4).

Lafay and Matricon (1982) also investigated the earlier finding - that air currents can inhibit the avoidance response (Cohen, et al. 1975). They reported that while the sporangiophore avoids a 250 μm mesh stainless steel screen placed 1 mm away at 2°/min, and bends upwind into a 1 cm/sec wind current at 0.3°/min, it will not avoid the screen at all if the same 1 cm/sec wind current is blown through it. Perhaps the effector molecules emitted by the sporangiophore are so large they cannot diffuse more than a fraction of a millimeter upstream against such a wind current. If so, such an experiment could be used to determine their diffusion coefficient.

Gamow and Böttger (1982a) discovered that during an avoidance response, the sporangiophore does not bend in the direction perpendicular to the barrier, but instead exhibits an "aiming error" of zero to 60° clockwise, when viewed from above. The same effect has been observed for phototropic

responses, and it is due to the 15˚/min clockwise rotation of the growing zone in mature stage 4b sporangiophores. This aiming error angle must be measured and compensated for to obtain reproducible measurements of the avoidance rate (Chapter 4, Section III).

Gamow and Böttger (1982b) and Gyure, et al. (1984) have adhered to the simple model of the CSGH in which the barrier acts by merely blocking the diffusion of an effector gas, which they believe to be water vapor. This model cannot explain why a second sporangiophore and a thin wire are equally effective as barriers (Appendix 4).

Recent, unpublished results obtained at Caltech from 1979 to 1985 are described here. These include: construction of a wind-free environmental chamber for avoidance experiments; observation of avoidance responses in the complete absence of air currents; controlling the environment and the experimental procedure to obtain bending rates reproducible to within ±10% for different sporangiophores; measurement of the humidity dependence of the avoidance response between 76% and 98.5% relative humidity; discovery that cleaning the experimental apparatus inhibits the avoidance response; discovery and measurement of a time dependence of the response during observations for 2 hr to 4 hr periods on a single sporangiophore; tests of activated charcoal, a second sporangiophore and a thin wire, and metals of different redox potential as barriers; and calculation of the hypothetical distribution of a signal gas emitted by the sporangiophore near a barrier, for different versions of the CSGH.

When confronted in 1979 with the result that a sporangiophore avoids a 120 μm diameter platinum wire about as fast as it avoids another sporangiophore, Max Delbrück exclaimed, "the barrier must emit the gas!" This is now one version of our working hypothesis (Chapter 4).

2. History

I. Discovery of the avoidance response in Phycomyces

Wortmann (1881) studied the avoidance of single sporangiophores by carefully pushing aside all but one or two of the mature sporangiophores in a growing culture with a needle and then lowering a glass plate onto the culture, allowing the remaining sporangiophore(s) to protrude undisturbed through a "quite small" hole drilled in the glass plate. A wet piece of pasteboard was mounted vertically on the top surface of the glass plate next to the protruding sporangiophores and the entire setup was covered with a large, black pasteboard cylinder to exclude light. After 4 hr to 6 hr the sporangiophores had clearly bent away from the wet piece of pasteboard in all cases, sometimes at an angle of "almost 90°." Wortmann (1881) did not report the actual distance between the sporangiophores and the pasteboard, nor the size of the pasteboard, nor the ambient relative humidity. If the pasteboard was mounted at an angle above the growing sporangiophores, they bent out of its way before colliding with it. Dry pasteboard gave "not the slightest" bending (again, distance not specified). Wortmann (1881) concluded that the avoidance responses he observed were due to hydrotropism, i.e., bending away from a wet surface.

Elfving (1881) observed the growth of sporangiophores placed under damp pieces of plaster, in an experimental setup covered with a pasteboard cylinder to exclude light. When the plaster was mounted at an angle from the horizontal, the sporangiophores veered off before reaching the plaster and grew parallel to its surface. When the plaster was mounted horizontally, the sporangiophores turned at right angles and grew horizontally with some nutation. When the plaster was removed, the sporangiophores bent upward and again grew vertically. A moist zinc plate gave similar results; however, the sporangiophores grew directly into dry glass that had been

cleaned with alcohol.

Until the rediscovery of the avoidance response by Shropshire (1962), there is no known report of Phycomyces sporangiophores avoiding a dry surface.

II. Responses to water vapor

Steyer (1901) repeated Wortmann's observations and found that sporangiophores would avoid wet filter paper (during a 9 hr exposure period) only if placed within 0.5 cm from it, at an ambient relative humidity of 50%. The relative humidity was 85%-90% at a distance of approximately 1 cm from the filter paper, measured using a small, calibrated "hygrometer spiral."

Walter (1921) observed growing Phycomyces cultures inside a horizontal box approximately 30 cm long with wet filter paper (relative humidity ≈ 100%) mounted inside the box on one end and pieces of calcium chloride (relative humidity ≈ 30 %) held behind a copper grid on the other end. He observed no significant bending toward either the wet wall or the dry wall, unless the sporangiophores were placed "quite close" to the wet filter paper (distance not specified), in which case they avoided the filter paper.

Evidently, Phycomyces sporangiophores exhibit hydrotropism (bending away from a source of water vapor) at high local relative humidity. This may be a side effect of the avoidance response, since saturating the growing zone surface with water (at high humidity) should have the same effect as bringing a barrier up close to the growing zone. If this is true, then step changes of relative humidity from less than 70% to above 90% should elicit strong positive growth responses.

Walter (1921) observed positive growth responses in response to a step-up in relative humidity from 15% to 90%. After a 5 min latency, the growth rate was increased by about 20% for 15 to 30 min following the step. He also observed negative growth responses to a step-down in relative humidity from 90% to 15%, but with 15 min latency. Cohen, et al. (1975) could not repeat these results. However, it is not clear that the apparatus depicted in their Fig. 15 provided the necessary humidity step, since they evidently did not measure the relative humidity at the output of their wind tunnel during the experiment, as was done by Walter (1921) and by Gyure, et al. (1984). Gyure, et al. (1984)

show but do not comment on the positive growth responses in Fig. 5 of their paper, for sporangiophores located in their wind tunnel and stepped up from 30% relative humidity and no wind to 90% relative humidity and 2.5 cm/sec wind speed; the step-up in wind speed alone should elicit a negative growth response. They did not observe a negative growth response to a step-down in relative humidity from 90% to 50%, perhaps because of its longer latency or because their humidity step-down took 15 min to complete.

The "hydrotropic" response and the growth responses to step changes in humidity need to be examined more carefully.

III. Discovery of olfactory chemotropism in Phycomyces

Elfving (1890, 1893, reviewed 1917) reported that sporangiophores bent towards pieces of rusted iron, sealing wax, or rosin, placed immediately above a growing Phycomyces culture. The sporangiophores were attracted at a distance of up to 3 cm from such objects, bending toward them at a rate of at most 20°/hr (Elfving 1917, p. 2, p. 23, and Fig. 3., p. 26). Errera (1892) and Steyer (1901) believed that this attraction was due to hydrotropism, i.e., bending towards hygroscopic surfaces. However, Elfving (1917) showed that hygroscopic materials such as NaOH or KOH, and plaster or charcoal plates saturated with $CaCl_2$ solution did not attract sporangiophores. The relative humidity is less than 1% at the surface of NaOH or KOH, and 35% at the surface of saturated $CaCl_2$ solution (Weast 1975, p. E41, p. E46). Also, many of the attractive compounds listed below are not hygroscopic, e.g., aromatic oils.

Elfving (1917, p. 23-24) found that a 2.5 x 4 cm sheet of platinum did not attract sporangiophores, if it was degassed by heating it red-hot beforehand and allowing it to cool. If a degassed sheet of platinum was then placed for 24 hr in a small, sealed glass box containing a volatile chemical substance (without touching the substance), removed, and mounted vertically, directly above a growing culture of Phycomyces sporangiophores, it then attracted the sporangiophores in the same manner as described above. Similar results were obtained with a drop of a volatile liquid spread on a ground glass surface that had been previously cleaned in a solution of potassium dichromate and sulfuric acid, rinsed, and dried; glass cleaned in this way did not attract sporangiophores.

The following substances attracted sporangiophores in these experiments.

acids: nitric and hydrochloric acids.

halogens and halogenated compounds: bromine, ß-bromo-camphor, chloroacetone, chloroform, iodine, iodoform, and a solution of iodine and potassium iodide in water.

sulfur compounds: carbon disulfide and hydrogen sulfide.

organic compounds: acetal (1,1-diethoxyethane), acetone, 1-hydroxyacetone, ammonia, amyl acetate, amyl ether, biphenyl, 2-butenal, butyric acid, cedarwood oil, cyclohexanone, diethylamine, diethyl ether, ethanol, ethyl acetate, ethyl formate, ethyl nitrate, ethyl salicylate, methyl phenyl ketone, pentanal, petroleum, pyridine, turpentine, turpentine oil, and xylol.

A few milligrams of a solid, weakly volatile (odor-producing) organic compound, held on the end of a copper wire or needle with a drop of wax and positioned directly over a growing culture (Elfving 1917, Fig. 4, p. 28), was also effective, for the following compounds:

L-borneol, isoborneol, camphene, camphene hydrate, camphenilone, methylcamphenol, camphor, L-camphor, menthol, alpha-santenol, beta-santenol, santenone, phenol, alpha-terpenol, and beta-terpenol.

The following compounds did not attract sporangiophores, or attracted them only very weakly in Elfving's experiments:

acetic acid, osmic acid, 2-methylpyridine, 2-hydroxybenzamide, and nitro-salicylic acid.

A roughly filed iron plate was not effective, whether used immediately or kept for one month inside a sealed glass box. But if it was exposed to the laboratory air for three days, it attracted sporangiophores. If an iron plate was activated in this way and then kept inside a sealed, light-tight zinc box for three weeks, it was again no longer effective. Elfving attributed these results to laboratory odors adsorbed by and then released from the iron

surface. Platinum or glass exposed to the ozone produced by a Wimhurst machine also attracted sporangiophores, for up to one week following the exposure (Elfving 1917, p.16, p.18-21, p.43-44).

Elfving (1917, p. 33) believed that all of the above chemicals acted by inhibiting growth on the side of the sporangiophore growing zone facing the chemical, relative to the opposite side. He did not examine whether any of the chemicals were growth inhibitors. Recently, Cohen (1979) found that many volatile organic substances act as growth inhibitors, at concentrations as low as 1 ppm in air. Cohen does not mention Elfving's results, and there has been no account of olfactory chemotropism in the Phycomyces literature since 1917.

IV. Zinc and Aluminum

Elfving (1917, p. 10) reported that a brightly polished, unoxidized surface of either zinc or aluminum attracted sporangiophores, while a polished iron surface did not. In addition, 11 other metals did not attract sporangiophores (Cd, Co, Ni, Sn, Pb, Sb, Bi, Cu, Ag, Pt, and Au). All of these inactive metals are weaker reducing agents than iron, which has a standard oxidation potential, E°, of 0.44 volts - this means that 0.44 electron-volts of energy are released per electron in aqueous solution when one atom of metallic Fe donates two electrons to two H^{+} ions, producing H_2 and Fe^{+2}, at $[H^{+}] = [Fe^{+2}] = 1$ M and $pH_2 = 1$ atm. Zinc and aluminum are much stronger reducing agents than iron, with E° equal to 0.76 and 1.7 volts, respectively. The thermodynamic data are from Latimer (1952).

Clean surfaces of strongly reducing metals may attract sporangiophores by blocking an oxidation step required for the avoidance response (Chapter 4, Section VII).

V. Sporangiophore flaring

Elfving (1917, p. 47-53) reviewed earlier work on the "flaring" of a forest of sporangiophores, in which the peripheral sporangiophores bent centrifugally away from the center of the forest, at a rate of at most 2°/hr. The flaring was weaker both in very dry and in very moist air. It was enhanced by placing a small piece of camphor next to the forest.

Passing a current of humidified room air at approx. 3 cm^3/sec vertically up or down through a forest of sporangiophores growing in a 300 cm^3 glass bell jar did not affect the rate of flaring, or reduced it only slightly - the wind velocity in this experiment would have been between 0.05 and 0.5 cm/sec (Elfving 1917, Fig. 7 and p. 51). Elfving mistakenly concluded from this result that since the wind would blow away any gas produced by the sporangiophores, the flaring was not mediated by the emission and detection of a signal gas. However, diffusion can easily compete with convection over a distance of 1 cm at these wind speeds, for any gas with a diffusion coefficient greater than 0.02 cm^2/sec.

Presumably, the flaring of a forest of sporangiophores is due to the mutual avoidance responses of sporangiophores away from each other. The mutual avoidance of a pair of aligned sporangiophores has been studied (Chapter 4, Section VII).

3. General Methods

Unless otherwise stated, the following is the standard method used in all experiments.

I. Culture conditions

Sporangiophores of wild type Phycomyces strain NRRL 1555 (mating type "minus") were grown in shell vials, 8.5 mm diameter by 30 mm tall, containing 1.1 ml of 4% potato dextrose agar (Difco Laboratories, Detroit, Michigan) with 6 μg/ml thiamine:HCl (Sigma Chemical Co., St. Louis, Missouri). Following Bergman, et al. (1969), spores suspended in 2 ml distilled water at a concentration of about 50 viable spores/ml were heat-shocked at 49°C ± 1°C for 15 min ± 5 min. One drop of this suspension was then inoculated into each vial (.05 ml containing an average of about 3 spores). The vials were incubated inside 10 cm diameter by 8 cm tall Corning 3250 glass culture jars at 97% ± 2% relative humidity (Section V) at 19°C ± 1°C, and under continuous overhead room light (four 40 watt fluorescent bulbs located 2 m above the cultures). Stage 4b sporangiophores usually appeared after 3 days, and the sporangiophores were plucked daily so that a fresh crop was ready the next day. In general, only the third through sixth crop of sporangiophores were used in the experiments. In the experiments demonstrating reproducible avoidance rates under fixed conditions, and in the measurement of the humidity dependence of the response (Chapter 4, Sections III and IV), only third-crop sporangiophores were used, from cultures aged 120 to 150 hours since inoculation.

II. Experimental procedure

A vial containing a vertical, 1.5 cm to 3 cm tall sporangiophore was selected and all unwanted sporangiophores (stages 1 through 4) were removed with forceps. To keep the mycelium out of the system, it was covered with a 1 mm deep layer of paraffin oil (J.T. Baker, Phillipsburg, New Jersey). The vial was placed in a delrin holder and inserted into the experimental chamber from below. This chamber is described in detail below (Section III). The sporangium was positioned to lie in the plane containing the axes of the chamber's horizontal ports, and located within 2 mm of the axis of the chamber's vertical observation port. Once in place, static charge was neutralized by holding a polonium-210 source inside the chamber, 1 cm away from the sporangiophore, for 15 sec.[1] The sporangiophore was then allowed to adapt to its new environment for at least 30 min before the barrier was moved into place.

[1]Polonium-210 emits alpha particles with an energy of about 5 MeV (Weast 1975, p. B315). These alpha particles ionize air molecules, forming a conductive path that neutralizes any static charge present on nearby surfaces. The initial activity of the source (Staticmaster IC200, Nuclear Products Co., South El Monte, California) was 200 microcuries. The half life of polonium-210 is 138 days (Weast 1975, p. B28), and the source was replaced every 2 years. This source was handled only with forceps, never with fingers. Weast (1975) reports that 10^{-11} gm of polonium-210 is about as toxic as 10^{-6} gm of plutonium-239. These are roughly the maximum permissible doses for an adult, 0.05 microcurie in either case.

A photograph of the chamber and the surrounding experimental setup is shown in Fig. 2. The sporangiophore was viewed horizontally from the front of the chamber with a low-power microscope equipped with a goniometer for measuring the bending angle of the sporangiophore accurate to ± 0.5° (Gaertner Scientific Corporation, Chicago, Illinois). A 20 watt collimated microscope lamp run at 5 watts provided dim back illumination; before entering the experimental chamber, this light passed through two Schott KG-3 infrared filters 2 mm thick to prevent heating of the sporangiophore, and then through two Schott RG-610 red glass filters 3 mm thick (mounted in the rear observation port) to prevent phototropic responses. The culture vial was seated in a delrin holder mounted on the shaft of a vertical, non-rotating micrometer, whose bottom half is visible in Fig. 2. The growth of the sporangiophore was measured by lowering it approximately every 10 min, and adjusting the micrometer (accurate to ±10 μm) so that the top of the sporangium was maintained level with a horizontal hairline inside the microscope eyepiece.

The microscope was mounted on a micrometer-driven x-y-z stage (accurate to ±10 μm), and the diameter of the sporangium and the diameter of the sporangiophore's stalk 1.0 mm below the base of the sporangium were measured at the beginning of each experiment using a vertical hairline inside the microscope eyepiece. The point 1.0 mm below the sporangium was located using a calibrated reticle inside the microscope eyepiece, with its divisions spaced 60 μm apart in the focal plane. The distance between the axis of the sporangiophore's growing zone (at a point 1.0 mm below the base of the sporangium) and the barrier surface was measured in the same way.

The sporangiophore was viewed from above with another low-power microscope, mounted on a micrometer-driven x-y stage (accurate to ±10 μm) and equipped with a crosshair inside the eyepiece. For these observations, the intensity of the rear illuminator was temporarily increased (to

full power, 20 watts) and the sporangiophore was viewed by its reflected light. The horizontal position of the sporangiophore was measured once before bringing the up the barrier and once again at the end of the avoidance response, 20 min to 30 min later. Sometimes the horizontal position was checked during the response also. The sporangiophore's aiming error was estimated from these data.

Fig. 2. Photograph of the experimental setup

The environmental chamber is visible in the center of the picture, along with the hollow observation plugs inserted in the front and top ports, and the solid aluminum plugs inserted in the left and right horizontal ports. Part of the chamber temperature control circuit (Section III, Part B) is visible on the left side behind the setup.

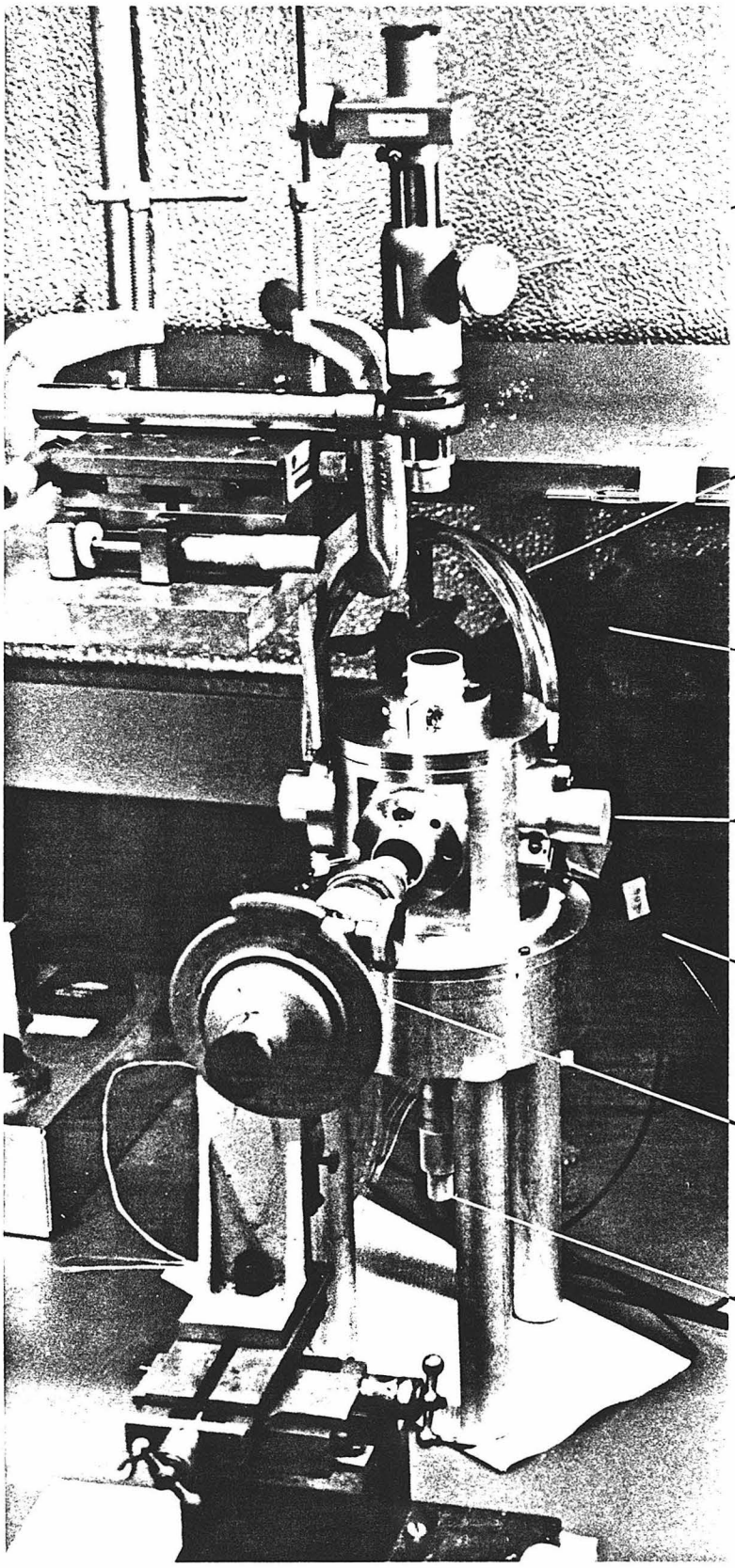
vertical microscope
coolant lines
illuminator
plug with barrier
thermistor cables
horizontal microscope
(with goniometer)
micrometer

III. Apparatus for the avoidance response

A. Mechanical design

A small environmental chamber was built to control convective flow, composition, pressure, temperature, and relative humidity of the air, electrostatic charge, and ambient light.

An outline drawing of the chamber is shown in Fig. 3. This is a cross-sectional view through the center of the chamber in a plane normal to the axis of the horizontal telescope. The chamber was machined from a cylindrical piece of 2024 aluminum alloy (4.4% Cu, 1.5% Mg, 0.6% Mn), 4 inches in diameter by about 4 inches high. It has six 1-inch diameter ports centered on orthogonal axes. The top port contains a hollow cylindrical plug machined from 6061 aluminum alloy tubing (1.0% Mg, 0.6% Si, 0.25% Cu, 0.2% Cr) and fitted with two red cutoff filters (Schott RG-610 glass discs, 21.8 mm diameter by 3 mm thick, cut to order by Industrial Glass Industries, Los Angeles, California) which allow the sporangiophore to be viewed from above, even in room light, without invoking a phototropic response. The front and back ports contain plugs identical to the top plug. The bottom port contains a micrometer with a non-rotating shaft (Mitutoyo 153-203, MTI Corp., City of Industry, California) that carries a delrin support for the sporangiophore and allows its height to be adjusted for growth. The micrometer is mounted on a circular plate which can be moved in the horizontal plane, and which rests on a sliding O-ring seal, so that the sporangiophore can be centered with the chamber remaining airtight. The left and right ports contain cylindrical plugs (machined from 2024 alloy aluminum rod stock) carrying vertical barriers.

Fig. 3. Cross-sectional view of the environmental chamber

The drawing is to scale, within 1.5% in linear dimensions. Legend: a) top plug, b) clamp for plug, c) red cutoff filter, d) side plug, e) round glass coverslip, f) sporangiophore, g) glass vial, h,h') top and bottom electrical heater coils, non-inductive spiral winding, i) paraffin oil, j) delrin holder for vial, k) water-cooling coil, ℓ) glass-distilled water or saturated salt solution, m) main body, mm) non-rotating micrometer head, n,n') press-fit rings, o_1) o-ring seal, o_2,o_3) sliding o-ring seals, p) bottom housing, r) sliding circular plate which supports the delrin holder, s) clamp-down bolts for the sliding circular plate, total of three spaced equally at 120° angles around the vertical axis of the chamber (only one is visible in cross section but two have been shown for clarity), ss) set screw (note: a second set screw clamping the delrin holder to the micrometer shaft is shown but is not labeled).

Not shown: 1) horizontal sensing holes for the upper and lower thermistor probes, 2.2 cm deep, and located 0.65 cm below the top heater coil and 0.65 cm above the bottom heater coil; 2) horizontal vent hole, 0.5 cm below the bottom edge of the side ports, closed on the outside with a stainless steel screw (opened during movement of plugs); 3) cooling coil tubing entering and leaving the apparatus through vertical holes - sealed with epoxy - in the edge of the bottom press-fit ring; 4) oil drain line in bottom housing; 5) three support legs, attached to the underside of the bottom housing.

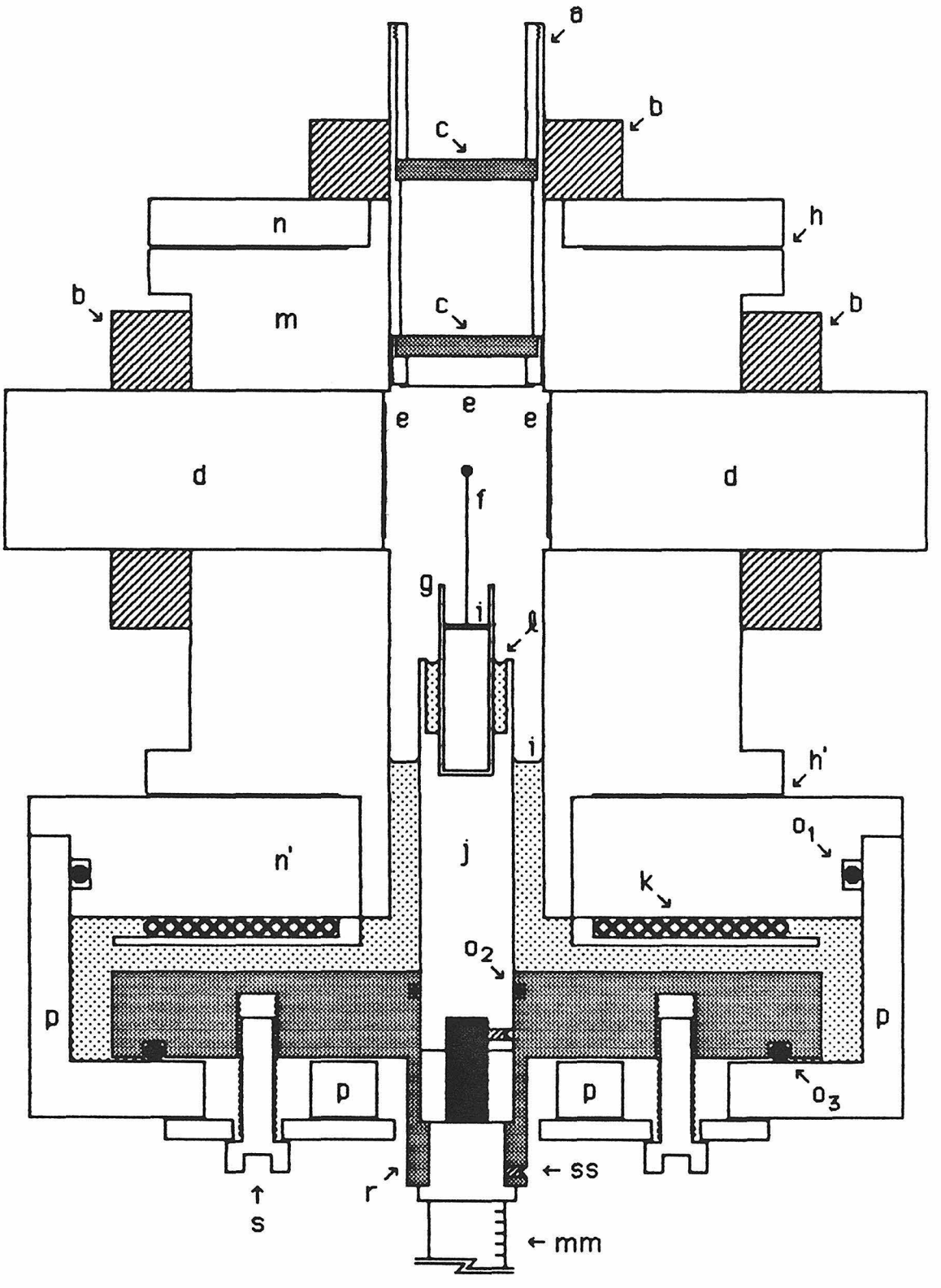
a
b
c
n
h
b
m
c
b
e
e
e
d
d
f
g
i
l
i
h'
n'
j
o1
k
o2
p
p
p
p
o3
r
ss
s
mm

The ports and plugs were lapped to a close tolerance and assembled with silicone high-vacuum grease (Dow Corning, Midland, Michigan; no type number specified) to provide an airtight seal and adequate thermal conductivity. The plugs are held in place by clamps and can be positioned at will. Normally, the inside faces of the plugs were recessed 1 mm as shown in Fig. 3. A vent (not shown), closed by a stainless steel needle valve inserted from the outside, allows air to enter or leave the chamber when the plugs are moved. This vent is .099 inches in diameter, 1.5 inches long, and drilled in a direction normal to the vertical axis of the chamber, 0.5 cm below the bottom edge of the side ports (3.5 cm above the bottom heater coil). The bottom part of the apparatus was usually filled with paraffin oil (J.T. Baker, Phillipsburg, New Jersey) to a level 0.5 cm above the bottom heater coil. Thus, the only materials normally exposed to a sporangiophore during an experiment were aluminum, stainless steel, glass, delrin, silicone grease, paraffin oil, and a salt solution in an annular well in the delrin holder at the base of the vial that was used to control the relative humidity (see below). The inside volume of the chamber is approximately 25 cm^3, with oil added and with the plugs positioned as shown in Fig. 3.

B. Temperature control

The chamber is nearly isothermal: it is controlled at 20.00°C at the bottom (by cooling and heating) and at 20.05°C at the top (by heating). This small thermal gradient completely suppresses convective stirring (Section IV).

The chamber temperature is regulated by the circuits shown in Fig. 4 and Fig. 5. Only one of the two regulating channels is shown. A small thermistor (Fenwal GB31J1) is coated with silicone heat sink compound (type Z9, GC electronics, Rockford, Illinois) and seated at the bottom of a 2.2 cm deep hole drilled in a direction normal to the chamber's vertical axis 0.65 cm below the top heater coil. The thermistor's resistance increases with decreasing temperature: its resistance is 1300 ohms at 22°C and 750 ohms at 37°C. A 120 cm length of RG-174 miniature coaxial cable connects the thermistor to the bottom of one leg of a bridge circuit located in a control box next to the chamber. See Fig. 4. The other leg of this bridge consists of a 10-turn potentiometer with a dial calibrated in 1/100 ths of a turn. The outputs of this bridge circuit are fed to the (+) and (-) inputs of an LM312 op-amp whose differential voltage gain is set by a feedback resistor connected from its output to its (-) input. Its resistance had to be determined by trial and error, to give the maximum stable closed-loop gain. For a typical potentiometer setting, this gain is about 300 for the upper channel. The op-amp output provides base current via a series resistor and diode to a heat-sinked MJE 1102 power transistor, shown in Fig. 5. This transistor acts as a current amplifier, with the top heater coil and an ammeter (1 amp full scale) connected in series from a +23 volt supply to its collector, and with its emitter grounded. Thus, as the thermistor's temperature decreases below a certain point (set by the 10-turn bridge potentiometer), the op-amp's output voltage rises proportionally from the bottom supply rail (-15 volt) to the top rail (+15 volt); when it gets above +1.2 volt, the output transistor turns on and the heater current increases proportionally from zero to saturation, which is about 1.8 amp.

Fig. 4. Temperature-sensing bridge and amplifier circuit

Only the upper channel circuit is shown. The 2.49 volt regulated supply is common to both channels. The lower channel circuit is identical, except that the op-amp feedback resistor is 900 K instead of 348 K, giving a differential voltage gain of 1000 instead of 300. The room temperature sensing circuit is similar (cf. Fig. 6), except that a LF355 op amp is used, with a 500K feedback resistor, and a 0 to 11 volt output swing, instead of -15 to +15 volts. Point "M" connects to the 1N459 diode in Fig. 5, or to pin 13 of the CA3059 integrated circuit in Fig. 6.

The solid black arrow is the common ground return for all of the power supplies.

All resistances are in ohms. "K" denotes 10^3 ohms. "Meg" denotes 10^6 ohms. All resistors are metal film, 1/4 W, ±1% tolerance, unless noted.

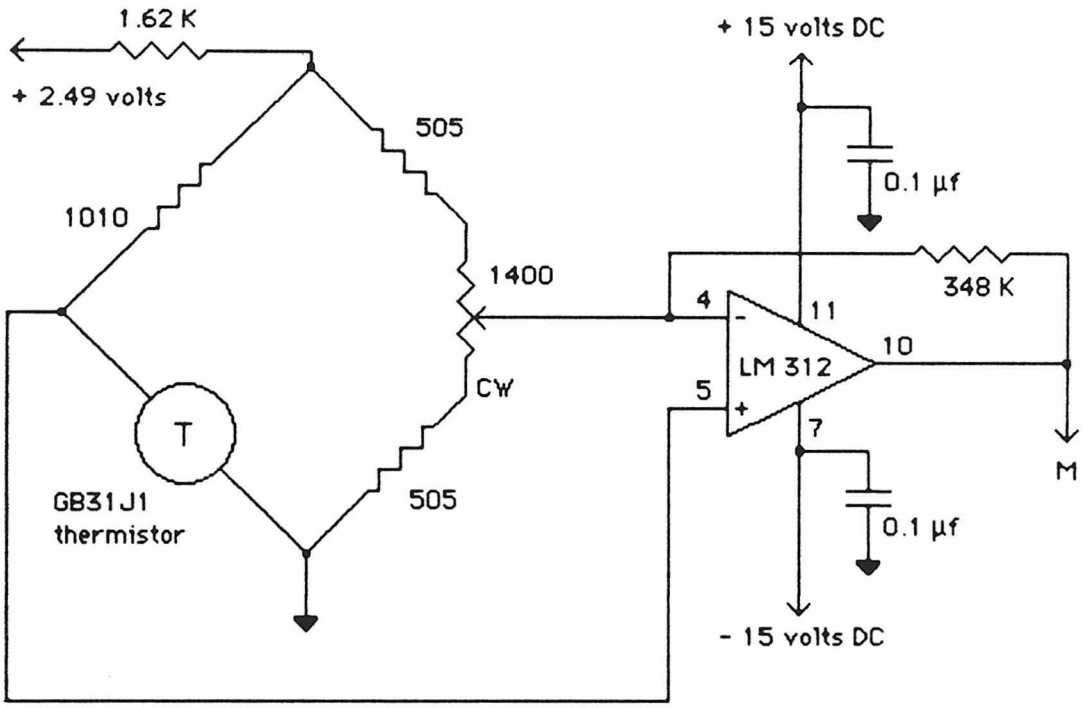
1.62 K
+ 2.49 volts
505
1010
1400
CW
505
T
GB31J1
thermistor
+ 15 volts DC
0.1 µf
348 K
4
11
10
LM 312
5
7
M
0.1 µf
- 15 volts DC

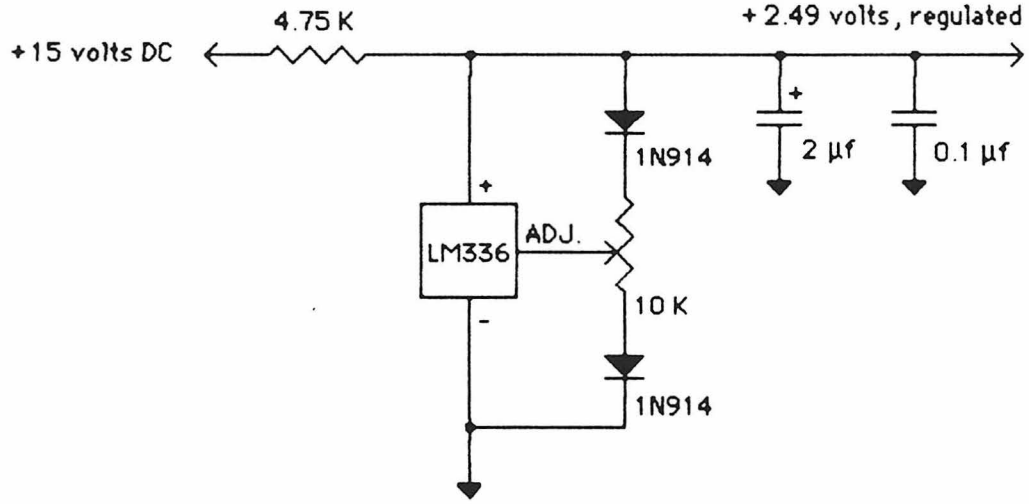
4.75 K
+15 volts DC
+2.49 volts, regulated
1N914
2 µf
0.1 µf
LM336
ADJ.
10 K
1N914

Fig. 5. Current amplifier for heater coil

Only one of the two identical amplifiers is shown. The circuit details are the same as for Fig. 4.

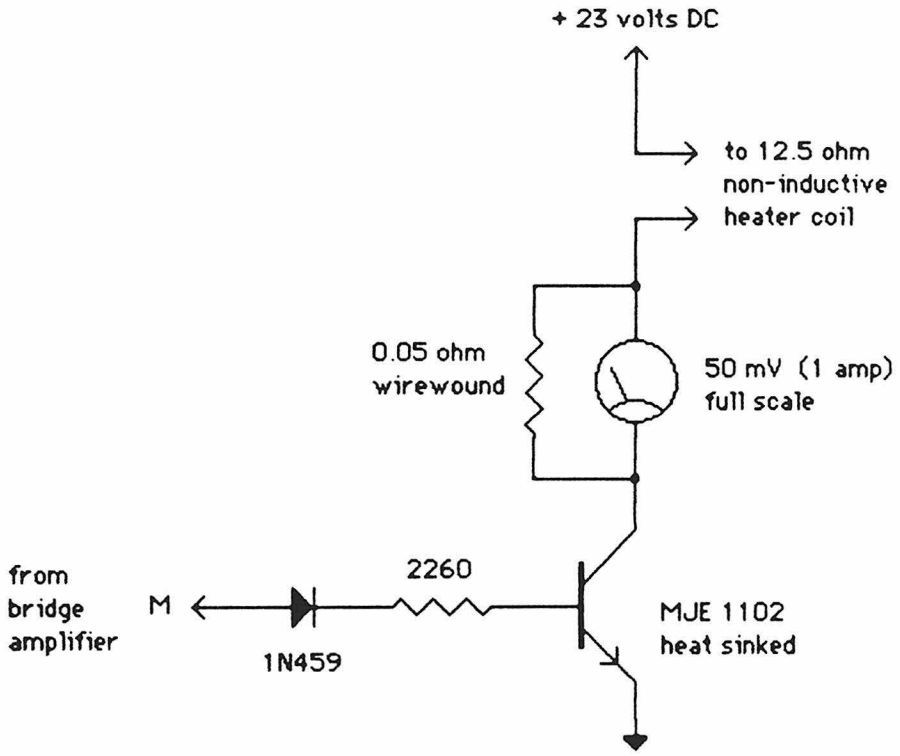
+ 23 volts DC
to 12.5 ohm
non-inductive
heater coil
0.05 ohm
wirewound
50 mV (1 amp)
full scale
from
bridge
amplifier
M
2260
1N459
MJE 1102
heat sinked

The heater coil itself consists of a 65 foot length of #32 enameled wire (Belden 8082 heavy polythermaleze) wound in a flat spiral spanning 1 radial inch in the 0.014 inch wide slot shown in Fig. 3. To minimize the self-inductance of the winding, the midpoint of the wire was tied down at the base of the slot with 100% polyester thread (size 50), and the two halves of the wire were wound outward together in 54 bifilar turns. The winding was vacuum-impregnated with paraffin to improve the thermal contact with the walls of the slot. The resistance of the winding is 12.5 ± 0.5 ohms. The bottom heater coil was constructed in the same way with the temperature sensed by a second thermistor positioned 0.65 cm above it and regulated by an independent, but identical circuit.

Both circuits were calibrated separately against a precision thermometer (CMS 227-637, ruled in 1/10 ths of a °C, calibrated in turn against a U.S. National Bureau of Standards platinum resistance standard) by immersing the thermistor and the thermometer in a water bath and plotting the bridge potentiometer setting (at 0.25 amp heater current) vs. the bath temperature over the range 18°C to 25°C. The potentiometer setting increased linearly with temperature (to within 1% over this range), by about 1/100 dial turn per 0.06 °C rise in temperature. The gain of the feedback circuit (with the output transistor conducting but not saturated) gave a 0.25 amp increase in heater current for a 0.01 °C drop in thermistor temperature. This was the highest gain at which the circuit remained stable. The circuit holds the temperature at the bottom heater coil constant to within ± 0.005 °C (measured every 20 sec over a 20 min interval).

Heat is removed from the chamber by a flat spiral copper cooling coil cemented with epoxy (to improve thermal contact) against the base of the chamber, 3/4 inch below the bottom heater coil, as shown in Fig. 3. The coil was wound from 1/8 inch o.d. copper tubing in the same way as the heater coils (bifilar winding with its midpoint at the center), to minimize any radial

temperature gradient that might be produced by the difference in temperature between the inlet water and outlet water. The cooling water is maintained at a average temperature of 19.0°C by a Lauda K-2/RD water bath (Lauda/Brinkmann instruments, Westbury, New York) and is circulated through the coil at a rate of 2.8 cm^3/sec.

The experiments are carried out inside a thermally insulated incubation room, of approximate dimensions 2 m by 3 m wide by 2.5 m tall. The room temperature is kept at 20.0°C ± 0.15°C by two refrigeration units run continuously and a 1500 watt resistive heater, switched on and off with a period of 1.5 sec by a pair of MAC 10-4 triacs in parallel. The sensing circuit is similar to Fig. 4, above. The triac drive circuit is shown and explained in Fig. 6. The duty cycle is controlled by another thermistor, a Fenwal GB31J1, mounted inside a 5 inch length of 0.25 inch o.d., 0.18 inch i.d., 6061 alloy aluminum tubing, about 1 foot upstream from the air intake of one of the refrigeration units, and 2 inches below the ceiling. This placement gave the fastest response and the greatest stability for the feedback circuit. The thermistor is connected in a bridge circuit as described above, but using an LF355 op-amp (see Fig. 4).

Fig. 6. Triac drive circuit for the room air heater

A pair of 10-amp triacs are switched on and off at a constant rate by the CA3059 zero-voltage switch. Switching occurs only at the zero-crossings of the AC line voltage. The switching rate, about 0.7 Hz, is set by the "rate control" potentiometer located on the lower left side of the figure. The duty cycle of the CA3059 switch is controlled by the input to pin 13, from the temperature sensing amplifier circuit (Fig. 4). The duty cycle increases from 0% to 100% as the voltage at pin 13 increases from 3.3 to 8 volts. The 0.2 ohm, 50 watt resistors balance the currents between the triacs, whose on-state resistance is on the order of 0.05 ohm.

The gain of the overall circuit increases the heater duty cycle by about 10% (150 watts) for a 0.25°C drop in thermistor temperature. During an experiment, the heater duty cycle is nearly constant at some value between 15% and 30%. After any disturbance, such as opening the door to the room for 1 min, the system returns to equilibrium within 10 to 15 min.

The circuit details are the same as for Fig. 4.

The solid black arrow denotes the ground return for all of the power supplies, including the "cold" side of the AC line. It is not connected to the chassis. The heater duty cycle is monitored by a separate circuit, not shown, and displayed on two panel meters, one inside the temperature-controlled room and the other on the outside.

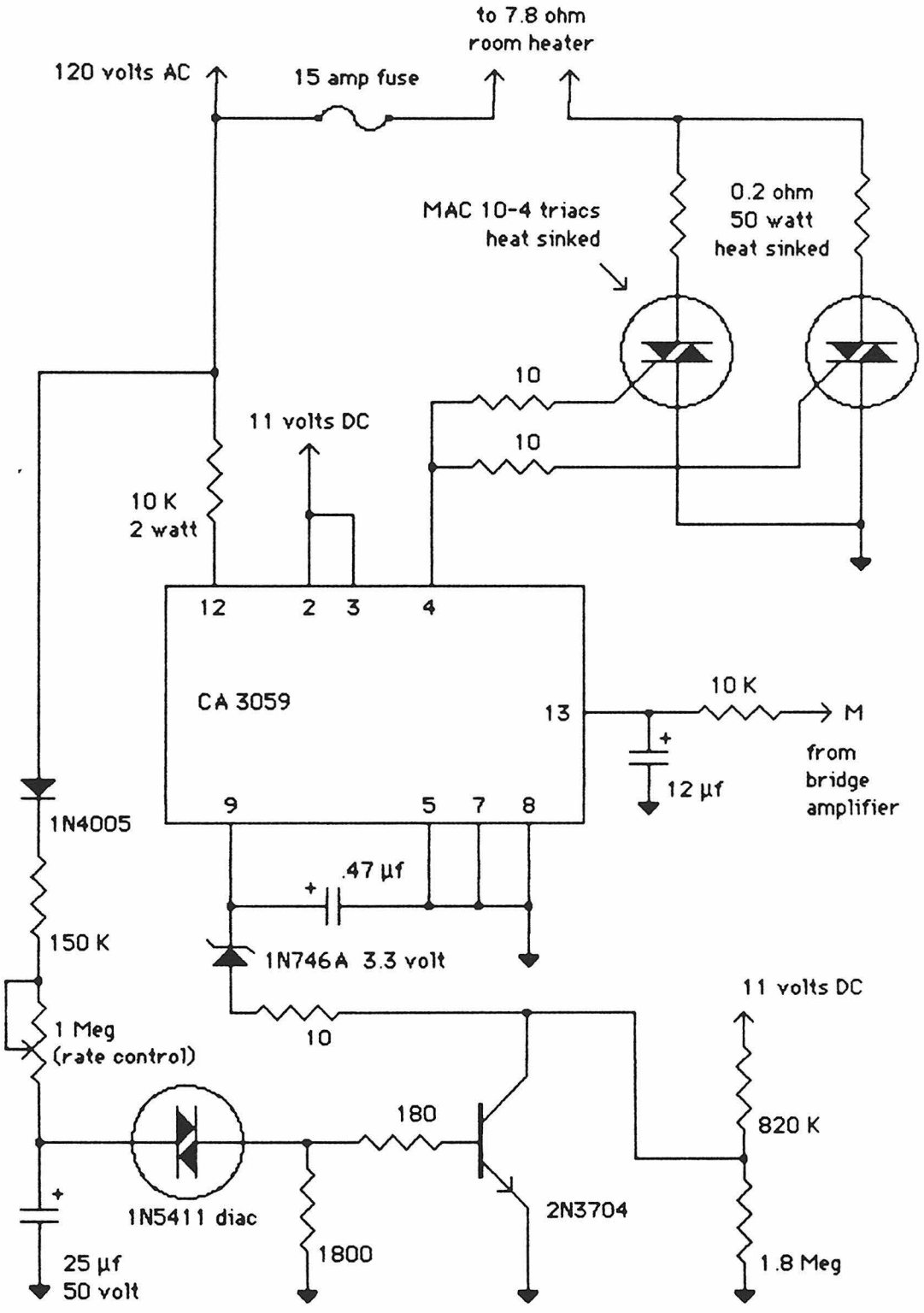
to 7.8 ohm
room heater
120 volts AC
15 amp fuse
0.2 ohm
50 watt
heat sinked
MAC 10-4 triacs
heat sinked
10
10
11 volts DC
10 K
2 watt
12
2
3
4
CA 3059
13
10 K
M
from
bridge
amplifier
12 µf
9
5
7
8
1N4005
.47 µf
150 K
1N746A 3.3 volt
11 volts DC
1 Meg
(rate control)
10
180
820 K
1N5411 diac
2N3704
25 µf
50 volt
1800
1.8 Meg

The thermal conductance of the aluminum body of the chamber was estimated as follows:

The room air and the bottom thermistor in the chamber were both held at a constant temperature of 20.0°C. The power fed to the top heater coil was found to increase as the set temperature of the top thermistor was increased, at about 10 watt/°C.

The top heater circuit was switched off. The power fed to the bottom heater coil, still regulating at 20.0°C, increased as the temperature of the cooling water bath was decreased, at about 4 watt/°C.

With the top heater switched off, the cooling water bath temperature was held constant at between 17.5°C and 19.5°C, and the bottom thermistor was held at 20.0°C. The power fed to the bottom heater coil increased as the room air temperature was decreased, and vice-versa, at about 1.3 watt/°C.

With the top of the chamber held at 20.05°C, the bottom at 20.00°C, the room at 20.00°C ± 0.15°C, and the cooling water at 19.0°C, the bottom heater coil was normally dissipating 4.0 watt ± 0.2 watt, and the top coil 0.5 watt ± 0.2 watt. The variations in heater power were caused by small changes in room temperature.

IV. Measurement of air movements

Convective stirring was monitored by injecting a 10 ml suspension of smoke particles into the chamber, in some cases with a sporangiophore inside avoiding a flat barrier at a distance of 1 to 2 mm. The particles were produced by burning a 1 inch length of 1/8 inch wide, 0.007 inch thick magnesium ribbon (Sargent-Welch, Skokie, Illinois) inside a 500 ml flask containing 5% O_2 and 95% N_2 at above 90% relative humidity. The particles were illuminated with the 1 mm diameter beam from a 1 mW helium-neon laser (Spectra Physics #133, Mountain View, California), by passing the beam horizontally through one of the hollow observation plugs inserted in the horizontal port directly opposite the barrier. The particles were viewed in the front horizontal telescope by their reflected light, 1 mm above the sporangium, and 1 mm away from the barrier. If no sporangiophore was present, the particles were observed 1 mm from the barrier and 1 mm above the midpoint of the chamber - the intersection point of the axes of the horizontal ports.

In each observation, the velocities of 10 to 20 different smoke particles were measured in the vertical direction by timing their movement along two minor divisions (a distance of 130 μm) of the reticle inside the horizontal telescope. Steady horizontal movement of the particles was negligible. The mean sedimentation rate of the particles was estimated from observations made within 0.5 mm. of the barrier surface. It varied anywhere from 1 to 10 μm/sec. It was subtracted from the average vertical velocity to give the values reported below. Both Brownian motion and sedimentation of the particles introduced an error of up to ±10 μm/sec into the measurement of wind speed near the sporangiophore.

The mean particle velocity 1 mm from the barrier was determined in 15 separate observations, as a function of the vertical temperature gradient inside the chamber. The results are plotted in Fig. 7. A sporangiophore was present in the chamber during the three observations with the temperature

cooler on top by 0.015°C, and during the two observations with the temperature 0.045°C and 0.16°C warmer on top. With the vertical temperature gradient in the chamber anywhere between zero from top to bottom, to 0.1°C warmer on top than on the bottom, the wind speed was always less than the measurement error of ±10 μm/sec. As the temperature gradient was increased beyond 0.1°C from top to bottom, downward convection was observed, e.g., 150 μm/sec downward at a temperature difference of 0.3°C. Thus, a temperature difference of 0.05°C, warmer on top, was normally used in the avoidance experiments.

An inverted temperature gradient was obtained by cooling the room air to 19.0°C and turning off the upper heater coil, using the upper thermistor and bridge circuit to measure the chamber temperature on top. This also produced stirring, 25 μm/sec upward with the top of the chamber 0.015°C cooler than the bottom.

The wind speed was also checked once after every 50 to 100 experiments, at the end of an experiment, with the plugs inserted symmetrically in the standard configuration shown in Fig. 3, with the sporangiophore still in place, and a vertical temperature gradient of 0.05°C, warmer on top. The laser beam was directed by a 90° prism, vertically down through the top observation port. The smoke particles were observed in the same focal plane as the sporangiophore, 1 mm on either side of it. In all cases, the wind speed at the growing zone was less than the measurement error of ± 5 μm/sec to ± 20 μm/sec.

The wind speed inside the chamber as a function of vertical temperature gradient has also been measured by Matus (1985) using the procedure just described (vertical illumination, standard configuration shown in Fig. 3). In this case, smoke particles were obtained by burning, inside a 500 ml flask, approximately 50 mg of Whatman #5 filter paper placed inside a 5 turn, 1/4 inch diameter, 1/2 inch long helical coil of #22 nichrome wire

(Consolidated Wire, Chicago, Illinois) connected across a 2.5 volt AC power supply. Results similar to those shown in Fig. 7 were obtained.

Fig. 7. Wind velocity inside the experimental chamber as a function of vertical thermal gradient

The experimental procedure is described in the text. Each data point represents the average vertical component of the velocities of 10 to 20 smoke particles. The standard deviation for each point was on the order of ± 30 μm/sec for the points above 0.15°C, and ±10 μm/sec for the remaining points.

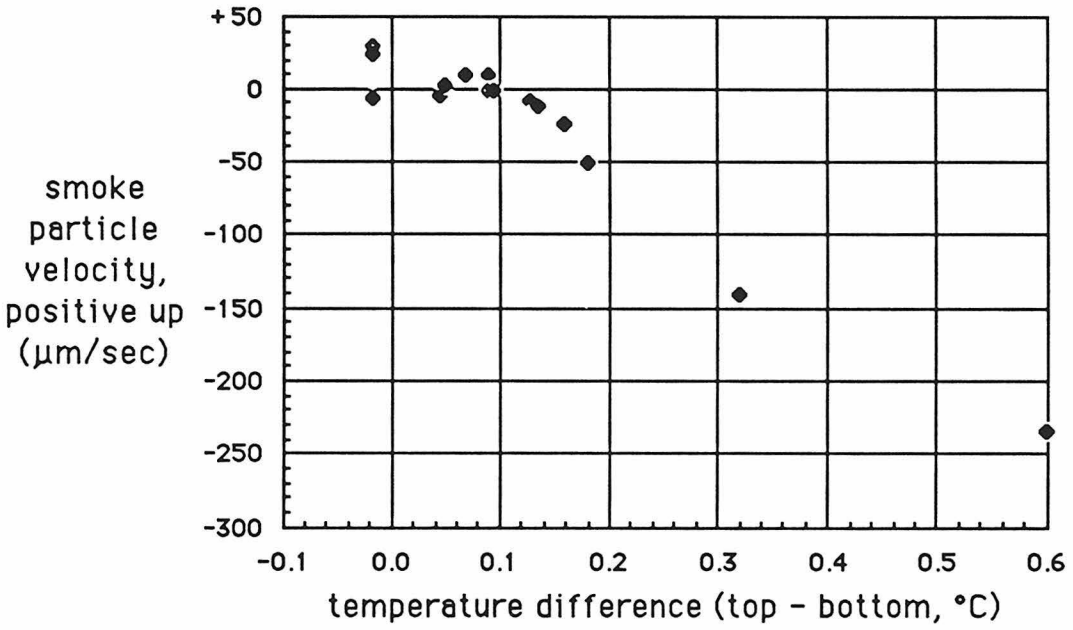

V. Measurement and control of relative humidity

A. Experimental procedure

The relative humidity inside the chamber was controlled by placing 0.5 ml of a saturated salt solution inside an annular well at the base of the sporangiophore's vial (Section III, Part A). Since water vapor can diffuse 3 cm in 20 sec, on average, the chamber humidity should come to within a few percent of its equilibrium value in a few minutes after the chamber is closed.

The relative humidity at 20°C at the surface of the saturated aqueous solutions of the different salts used in the experiments is as follows (Weast 1975, p. E46):

Na_2SO_4, 93%; K_2HPO_4, 92%; $Na(CH_3COO)$, 76%; NaBr, 58%.

This relative humidity is equal to the water activity of the salt solution, by definition (Eisenberg and Crothers 1979, Chapter 7).

The first observations of avoidance responses in the chamber were made without filling the bottom of the chamber with paraffin oil. These included the demonstration of reproducible avoidance rates under fixed conditions, as well as the measurement of the humidity dependence of the response. In this situation, since the base of the chamber was held 0.5°C to 1.0°C colder than the upper part of the chamber by the cooling coil, the vapor pressure of water was lower in the base, so that water may have diffused down from the annular well in the upper part of the chamber and condensed on the inside surfaces of the base of the chamber. This problem was avoided in later experiments by filling the base of the chamber with paraffin oil to 0.5 cm above the bottom heater coil.

B. Correction for cooling the base of the apparatus

The temperature of the cooling water in the copper cooling coil was always between 19.0°C and 19.5°C, in the experiments. Thus, the inside surfaces of the chamber below the bottom heater coil were held at a temperature between 19.0°C and 19.5°C by the cooling coil, while the inside surfaces above the bottom heater coil were controlled at a temperature between 20.00°C and 20.05°C by the circuits in Fig. 4 and Fig. 5. The vapor pressure of water falls off with decreasing temperature, so that water may have condensed in the base of the chamber when it was not filled with oil, reducing the relative humidity in the upper part of the chamber near the sporangiophore. Here we estimate the relative humidity at the level of the sporangiophore, in the experiments where the base was not filled with oil.

The vapor pressure of water at 20.0°C is 17.5 mm Hg, and at 19.0°C it is 16.5 mm Hg (Weast 1975, p. D180). This is a difference of about 6%. Thus, if the water activity of a salt solution placed in the annular well is less than 100% - 6% = 94%, and its temperature is 20°C, the partial pressure of water vapor at its surface will be less than 16.5 mm Hg. There should be no condensation of water in the base of the chamber, and relative humidity in the chamber should be equal to the water activity of the solution, given above.

If, instead, distilled water is placed in the well, the relative humidity in the chamber should be somewhat less than 100%. Suppose the base of the chamber is at 19.0°C, and the upper part of the chamber above the bottom heater coil is nearly isothermal and at 20.0°C. The partial pressure of water vapor at the level of the sporangiophore should be between 16.5 mm Hg and 17.5 mm Hg. Then the relative humidity should be between 94% (100% - 6%), and 100%. As a rough estimate, and for the purpose of plotting the humidity dependence (Chapter 4, Section IV) we take 97% as the relative humidity at the level of the sporangiophore with distilled water in the well and the base at 19.0°C, and 98.5% with the base at 19.5°C.

This estimate was obtained as follows. The concentration of a gas falls off as a/r away from a spherical source of radius a. The i.d. of the annular well is 0.8 cm and its o.d. is 1.0 cm. The diameter of the experimental chamber is approximately 2 cm. Thus, with the base at 19.0°C, the partial pressure of water on the inside wall of the chamber adjacent to the well is on the order of 17.5 - (1cm/2cm)·(17.5-16.5) = 17.0 mm Hg, or 97% relative humidity at 20.0°C. The sporangiophore growing zone is always located at least 3 cm above the surface of the solution in the well. Since there are no sources or sinks of water vapor above the annular well in the chamber (we ignore the growing zone, whose total surface area is of the order of 1 mm^2), the vertical flux of water vapor must be weak, and downward at any point on the inside wall above the well. Thus, the partial pressure of water vapor at the level of the sporangiophore cannot be less (nor much greater) than 17.0 mm Hg, the value just calculated.

C. Direct measurement of the relative humidity

The relative humidity inside the experimental chamber was measured with no oil in the base of the chamber, with the cooling water at 19.5°C, with a sporangiophore in the chamber, and with the horizontal plugs in their retracted position shown in Fig. 3. A 1 cm^2 piece of Whatman GF/A glass fibre filter paper (W&R Balston, Ltd., England) weighing 5 mg was stuck to one face of a 18 mm diameter circular cover glass, thickness #1, weighing 105 mg (VWR, San Francisco, California) using approximately 10 mg of silicone grease. One drop of water, weighing initially 25 mg to 45 mg was placed on the filter and allowed to soak in. The coverslip was weighed, then placed inside the chamber for up to 4 hr, resting on two small horizontal brass screws protruding from the face of one of the horizontal plugs and not shown in Fig. 3, and then weighed again. When outside the chamber, the coverslip was kept inside a small, 2 cm dia culture dish to minimize evaporation. This procedure was repeated many times, with the coverslip kept in the chamber for only 1 min on several occasions, to correct for the mass of water evaporated during weighing, approximately 0.7 mg. The filter evaporated 0.4 to 0.6 mg/hr, while inside the chamber. This procedure was also repeated with a different glass fibre filter, soaked in a saturated solution of Na_2SO_4. In this case the filter evaporated 0.5 mg during weighing, and <u>increased</u> in mass (i.e., adsorbed water) by about 0.1 mg/hr while inside the chamber. Plotting the rate of evaporation (or condensation) vs. the water activity of the test solution on the filter, it appears that zero water loss or gain should have occurred with a test solution of water activity 94% ± 1%. Hence, the relative humidity inside the chamber at the surface of the horizontal plug was approximately 94%. This is lower than the value of 98.5%, predicted above. This discrepancy has not been explained.

The relative humidity inside the chamber with a saturated solution of Na_2SO_4 in the annular well, with the base filled with paraffin oil, and the

base temperature at 19.5°C, was measured in the same way, and found to be 90% ± 2%, as expected.

In all cases, the relative humidity with a salt solution in the well was assumed to be the water activity of the solution, given above.

The relative humidity inside the culture jars was measured by weighing small capillary tubes (1.3 ± 0.1 mm i.d., 1.5 ± 0.2 cm long, weighing approximately 80 mg) half-filled with either distilled water or a sucrose solution (weighing 10 mg) and placed in an open petri dish inside the jar. A tube containing distilled water typically evaporated about .04 mg/hr while in the jar; weight loss during each weighing was about 0.1 mg. On the other hand, a tube containing 2.3 M sucrose, whose water activity is 95% at 20°C, increased in mass (i.e., adsorbed water) at about .025 mg/hr while in the jar. The relative humidity inside the jar was estimated to be 97% ± 1% by plotting the rate of water loss or gain vs. the water activity of the capillary solution, for several different solutions placed inside the jar at the same time, and interpolating. According to Raoult's Law, for dilute solutions, the water activity is proportional to the mole fraction of water in the solution [the number of water molecules divided by the total number of molecules (Daniels 1948, p. 202)]. The water activities of 0 to 5 M sucrose solutions are less than those predicted by Raoult's Law, by as much as 3%. Exact values were obtained from Eisenberg and Crothers (1979, Fig. 7-9, p. 299).

VI. Cleaning the apparatus

The lower half of the apparatus was not usually cleaned, since it was filled with fresh oil at the beginning of each experiment. The bottom port and the vent hole in the upper half of the apparatus were also not usually cleaned, because they were never greased. The remaining inside surfaces of the chamber were cleaned and degreased as follows.

The visible silicone grease on the inside surfaces of the 4 horizontal ports and the top port, on all surfaces of the 2 solid plugs, the delrin sporangiophore holder, and the 3 internal Schott filters, and on all surfaces and in all 90° inside corners on the 3 Schott filter retaining rings and the 3 hollow plugs, was wiped off by hand using Kimwipes (5" x 8.5", #34155, Kimberly-Clark Corp., Roswell, Georgia). Traces of silicone grease on the inside surfaces of the top port and the 4 horizontal ports were removed by wiping the ports with a Kimwipe dipped in reagent-grade n-heptane (Mallinckrodt, Inc., Paris, Kentucky), held with a disposable PVC glove, and then immediately wiping them dry with a fresh Kimwipe. This was repeated for all 5 ports once again with heptane, twice with filtered RBS-35 alkaline detergent solution (Pierce Co., Rockford, Illinois; filtered through Whatman #5 filter paper, to prevent the plugs from jamming inside the ports), and twice with glass distilled water. The two solid plugs, the delrin holder, the stainless steel needle valve, the 3 Schott filters and their retaining rings, and the 3 hollow plugs were rinsed several times in heptane and dried with Kimwipes, until the filter glasses showed no visible traces of grease. All of these parts were then soaked in a 20% solution of filtered RBS-35 in glass distilled water, at 90-92°C, for approximately 30 sec. Disposable PVC gloves were used to handle the parts in this and the following steps. Any hydroxide layer formed on the surface of the aluminum parts was immediately wiped off by hand and all of the parts were quickly immersed in glass distilled water at room temperature. They were rinsed 5 to 10 times in glass distilled water, until a

soap bubble no longer appeared inside a retaining ring when it was removed from the rinse solution. All of the parts were then dried uncovered overnight in room air, by placing them on a double layer of 15" x 17" Kimwipes (#34255), with the surfaces that normally face the sporangiophore in the apparatus facing upward and not touching the Kimwipe.

VII. Barrier preparation

Normally, 2.2 cm diameter round microscope cover glasses, thickness #1 (VWR Scientific, Inc., San Francisco, California), were used as barriers. They were cleaned prior to an experiment by soaking 50 of them overnight in 50 ml of 90% fuming nitric acid (Aldrich Chemical Co., Milwaukee, Wisconsin) at room temperature and then removing them from the acid one by one with a pair of Dumont stainless steel #7 forceps, and rinsing them twice in glass distilled water (so that the water wet the surface of the glass evenly). In each rinse each cover glass was shaken with the forceps in the water for about 5 sec and then allowed to soak with the rest of the glasses in 100 ml of glass distilled water for about 20 min. The glasses were then stored under fresh glass distilled water in a pyrex beaker covered with parafilm.

4. Experiments, Results and Interpretations

I. Outline of the results and interpretations

Our goal is to determine the physical mechanism used by the Phycomyces sporangiophore to detect nearby objects. The strategy has been: 1) to characterize the avoidance response in a well-controlled environment; 2) to test critically the prior versions of the Chemical Self-Guidance Hypothesis (CSGH) (Chapter 1); and 3) to develop and test new versions of this hypothesis that agree with all of the results to date. The results obtained in each of these three areas and presented in this chapter (in chronological order) are outlined here.

In the first experiments using the wind-free environmental chamber, a normal avoidance response was observed with an ambient wind speed of less than 10 μm/sec (Section II). By controlling certain experimental conditions (age of the sporangiophores, culture conditions, barrier, temperature, wind, humidity, and static electricity), the experimental protocol and the methods of data analysis, it was possible to obtain as low as a ± 5% variation in the avoidance rate observed for different sporangiophores avoiding clean, unused glass barriers in successive experiments (Section III). The dependence of the avoidance rate on the relative humidity inside the growth chamber was determined under these controlled conditions between 76% and 98.5% relative humidity (Section IV). The avoidance response was inhibited by cleaning the chamber with an alkaline detergent. This result, along with some unsuccessful attempts to determine the cause of this inhibition, are described in Section V. Under certain conditions, the avoidance rate increased with the time that the sporangiophore had spent inside the apparatus since the beginning of the experiment (Section VI). Preliminary evidence that the avoidance rate depends on the chemical composition of the barrier is presented in Section VII, along with a description of an early

measurement of avoidance of a thin vertical wire, as well as a summary of recent measurements of the distance dependence of the response performed by Matus (1985).

Our current working hypothesis for the avoidance response is still the CSGH, but modified to account for a number of facts that were either not known or not recognized in 1975. Two previous versions and three new versions of the CSGH are outlined below.

A. The Growth Promoter-Reflection Model

The sporangiophore emits a stable, growth-promoting gas whose diffusion is blocked by the object, producing a concentration gradient across the sporangiophore growing zone that is then detected by the sporangiophore. If this were true, the hypothetical gas would have been detected in one of the bio-assays of Cohen, et al. (1975). Given that these assays failed to detect any such gas, if the sporangiophore emits a signal molecule, then either it must decay, or it must be readily adsorbed by surfaces, e.g., the inside surfaces of the bio-assay apparatus. Another prediction of this model is that the avoidance rate away from a 25 μm diameter, parallel, aligned wire placed 2 mm away from the growing zone should be about 250 times less than the avoidance rate away from a large plane barrier, parallel and placed 5 mm away (Appendix 3). In fact, a sporangiophore avoids either of these barriers at about the same rate (Section VII).

B. The Wind Gradient Model

The sporangiophore avoids an object by detecting the damping of ambient air currents near the surface of the object, as postulated by Cohen, et al. (1975). This cannot be correct; sporangiophores avoid a glass barrier placed 1 to 5 mm away in a wind-free environmental chamber (wind speed less than 5 μm/sec) at at least the same rate as in open air (Section II).

Since the signal gas cannot simply reflect off of the barrier surface, and since barriers cannot act just by their aerodynamic effect, there is only one alternative for the CSGH, namely, that the sporangiophore emits a gas which is adsorbed by the barrier surface for a certain length of time.

C. The Growth-Inhibitor Adsorption Model

The sporangiophore emits a growth-inhibiting gas which is then adsorbed by the barrier. This model was ruled out by Cohen, et al. (1975), who argued that if it were true, sporangiophores would exhibit a positive (instead of negative) wind growth response, bend downwind instead of upwind, and bend toward one another instead of away. These arguments do not hold, however, if: 1) the sporangiophore emits a physiologically inert gas with a high vapor pressure; and 2) this gas decays in a matter of seconds in the atmosphere (e.g., by oxidation), producing a growth inhibitor with a low vapor pressure; and 3) this inhibitor - but <u>not</u> its precursor - is completely adsorbed by (or condensed onto) surfaces, including the surface of the sporangiophore growing zone itself. The concentration of the inhibitor would increase with distance from a barrier, and the sporangiophore would then grow faster on the side facing the barrier and bend away from it. See Chapter 5 and Appendix 3 for further discussion of this and the following two models.

D. The Atmospheric Growth - Inhibitor Adsorption Model

Another possibility is that the barrier acts by adsorbing growth-inhibiting gases already present in the atmosphere - consider the result of Cohen, et al. (1979), that most volatile organic compounds are growth-inhibitors. In this case, one must assume that a source of the hypothetical inhibitor is normally present somewhere inside our sealed experimental chamber, and that the barrier surface does not become saturated with the substance during an experiment.

E. The Barrier Emission Model

A third, and final possibility is that the sporangiophore emits a physiologically inert gas which then undergoes a chemical reaction (e.g., by oxidation) slowly in the air, and rapidly while adsorbed to the barrier surface, producing a growth-promoting gas which is emitted by the barrier. If this growth-promoting gas decays to a (once again) inert gas while in the air, its concentration will decrease exponentially with distance from the barrier (see Appendix 3), and the sporangiophore will bend away from the barrier.

II. Avoidance in the absence of ambient wind

Chapter 3 described the construction and testing of a wind-free environmental chamber. In all physiological experiments, the top of this chamber was maintained 0.05°C warmer than the bottom, which guarantees an ambient wind speed of less than 10 μm/sec in the vertical direction, parallel to the barrier and 1 mm away from it (Chapter 3, Section IV, Fig. 7). Section III in this chapter describes a series of experiments done under these conditions in which the avoidance rate is 2.4°/min away from a glass barrier placed 1 mm from the sporangiophore. This value is not less than those published for avoidance responses observed with approx. 1000 μm/sec ambient wind, for example, in Cohen, et al. (1975).

This result shows that ambient wind cannot provide the signal for the avoidance response by modifying the distribution of a signal gas in the vicinity of the sporangiophore. The extremely weak air currents in the apparatus cannot compete with diffusion. For example, a large gas molecule (molecular weight ≈ 300) would have a diffusion coefficient of at least 0.01 cm^2/sec in air. Such a molecule will diffuse a root-mean-square distance of 0.2 cm (e.g., out to the barrier and back) in $(0.2\ cm)^2/2(0.01\ cm^2/sec) = 2$ sec. Yet convection at 10 μm/sec will have carried the molecule a distance of 20 μm, only 1/100 the length of the growing zone, during this time. The concentration difference of signal gas induced across the growing zone by a "wind gradient" (increasing wind speed with distance from the barrier) would thus be exceedingly small. It is estimated in Appendix 3 to be less than 1 part in 10^8.

It could be that the sporangiophore nevertheless detects and amplifies this small signal, but if that were the case, one would expect the avoidance rate to increase with ambient wind velocity, since higher velocity wind should compete better with diffusion and thus increase the concentration gradient of signal gas across the sporangiophore. But the avoidance rates in

< 10 μm/sec winds that we measured were similar to those observed earlier in 1000 μm/sec winds (e.g., by Cohen, et al. 1975). In addition, when an artificial air current of approximately 150 μm/sec was generated inside our apparatus by setting the vertical temperature difference to 0.3°C, a sporangiophore inside the apparatus avoided a glass barrier 1 mm away at the same rate (within 20%) as it did with the temperature difference set to 0.05°C, i.e., at ambient wind speeds of less than 10 μm/sec (Matus 1985).

III. Reproducible avoidance rates

An effort was made to control environmental variables, experimental procedure, and methods of data analysis in order to minimize the variation in the rate of avoidance among different sporangiophores. Under the following conditions, the mean avoidance rate was 2.4˚/min, with a standard deviation of 0.1˚/min (4 % of the mean) for 11 different sporangiophores tested between June 30 and July 23, 1982. Data from 10 other sporangiophores tested during this period were rejected for reasons outlined below. The barrier in all cases was a 2.2 cm diameter glass coverslip placed 1.0 mm from the midpoint of the sporangiophore growing zone. Unless noted, the experimental setup and procedure were as described in Chapter 3, except that the bottom of the chamber was not filled with paraffin oil.

A. Environmental controls

1. Sporangiophores were used only from cultures that had been inoculated 120 to 150 hours prior to the beginning of an experiment (i.e., "third-crop" sporangiophores).
2. The annular well surrounding the sporangophore vial was filled with glass-distilled water, and the cooling water (circulating in the copper coil at the base of the chamber) was maintained at 19.0 ± 0.1°C, giving a relative humidity inside the chamber of 97%.

B. Experimental procedure

1. The front, top, and back ports contained "window" plugs (Chapter 3) used for observation; these plugs were not moved during an experiment, nor were they disturbed or removed between experiments. The coverslips mounted on the inside surfaces of these plugs were usually not replaced. If they were replaced, the avoidance bending rate in the next experiment deviated > ± 20% from the average value for the conditions described here. This was the case for three experiments done between June 30 and July 23, 1982, so data from these experiments were ignored.
2. The right- and left-side horizontal ports each contained a solid plug with a 2.2 cm diameter microscope coverslip greased to its inside surface; both of these coverslips were replaced with fresh, air-dried coverslips at the beginning of every experiment.
3. The plug on the right (south, in our setup) was always used as the barrier.
4. A new sporangiophore was used in each experiment, and only one avoidance response was observed.
5. No measurement of the horizontal position of the sporangium (requiring horizontal, bright illumination to observe the sporangium from above by reflected light) was made within 10 min after bringing the barrier up to the sporangiophore. The avoidance bending rate was reduced by up to 30% when this measurement was made less than 10 min after positioning the barrier next to the sporangiophore. See Fig. 10. Data from three sporangiophores tested between June 30 and July 23, 1982 were rejected for this reason.

6. At the end of every experiment, the solid plugs were removed and stored inside a pyrex culture jar (Corning #3250); the delrin support was removed and the bottom port was left open; each of the open side ports was stuffed with a Kimwipe (5 inch x 8.5 inch, #34155, Kimberly-Clark Corp., Roswell, Georgia) to prevent dust from entering the apparatus.

C. Data analysis

1. The vertical component of the growth of the sporangiophore, v, in μm/sec, was estimated from observations made every 5 to 10 min (Chapter 3, Section II). See Fig. 8a. This growth rate, v, was then corrected for the bending angle and bending rate of the sporangiophore, to give the true growth rate in the direction of growth, instead of its vertical component. The following correction formula was used (Appendix 1):

$$v_c = [v + z_o\alpha(d\alpha/dt)] / \cos\alpha$$

where

v_c = corrected growth rate in μm/min,

v = vertical component of the growth rate in μm/min,

z_o = 0.56 μm/(degree)^2,

α = bending angle away from vertical in degrees (°)

$d\alpha/dt$ = bending rate away from vertical in °/min.

2. The largest avoidance bending rate (averaged over a 10 min interval) after bringing the barrier up to the sporangiophore was determined from a plot of the angle, with respect to vertical, of the top 0.5 mm segment of the growing zone versus time; this rate is called the "observed bending rate," or $d\alpha/dt$. See Fig. 8b.

3. The aiming error angle, θ, during this 10 minute period was estimated from a plot of the position of the sporangium in the horizontal plane (observed approximately every 10 min through the top port). See Fig. 8c.

4. A corrected bending rate was calculated by compensating for the growth rate and the aiming error (Appendix 2) of the sporangiophore, according to the following formula:

$$(d\alpha/dt)_c = \{ (d\alpha/dt)(v_s/v_c) / \cos\theta \} + k ,$$

where

$(d\alpha/dt)_c$ = corrected bending rate in °/min,

$d\alpha/dt$ = observed bending rate in °/min (para. #2),

v_s = "standard" growth rate, 50 µm/min,

v_c = corrected growth rate, µm/min (para. #1),

θ = aiming error angle, ° (para. #3),

k = correction factor for age of the apparatus; see next paragraph.

5. The avoidance bending rate (calculated using k=0 in the preceding formula) was found to decline linearly by about 0.03°/min. from one experiment to the next, for the 11 sporangiophores tested during the two week period described above. This decline was accounted for by letting k equal +(0.03°/min)·N, where N was the number of the experiment during this two week period. The avoidance rate returned to its initial value if the chamber was allowed to rest unused for at least one week, maintained as described in Part B, #6, above.

6. The results of an experiment were ignored if the aiming error was outside the range $0^\circ \leq \theta \leq 35^\circ$ clockwise, viewed from above, or if the growth rate was outside the range 35 μm/min $\leq v_c \leq$ 65 μm/min, or if the initial angle of the sporangiophore towards the barrier (when the barrier was brought up to it) was outside the range $1^\circ \leq \alpha \leq 15^\circ$. Data from four sporangiophores tested between June 30 and July 23, 1982 were rejected for one of these reasons.

Fig. 8 Data from a typical experiment

a) corrected growth rate as a function of time,

b) observed bending angle as a function of time,

c) position of the center of the sporangium in the horizontal plane (the vertical axis of the chamber is at the origin).

The right barrier was brought to within 1.0 mm of the midpoint of the growing zone at time B, 13 min. The 10 min period of maximum bending rate occurs between t = 24 and 34 min (graph b).

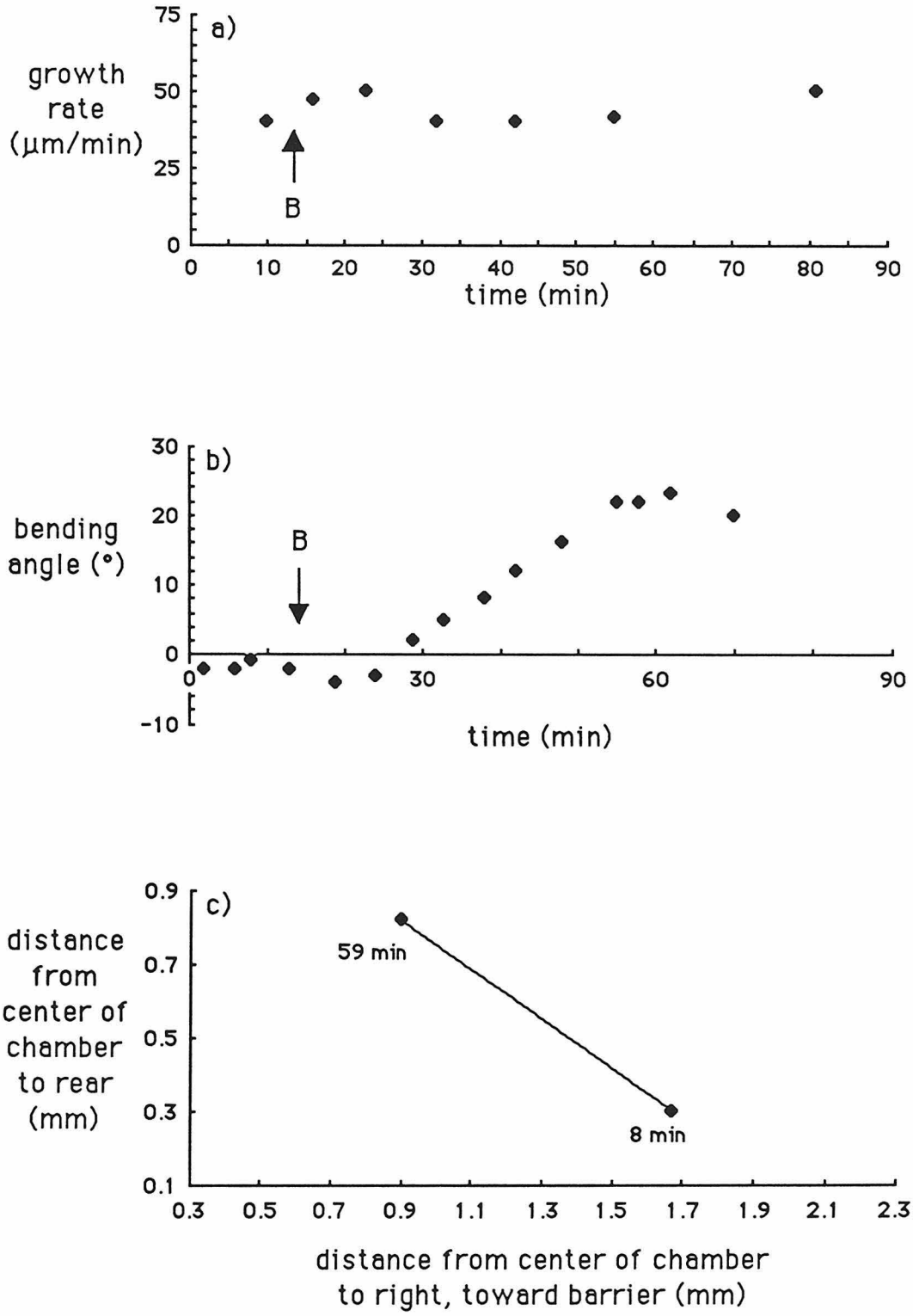
a)
growth rate (μm/min)
75
50
25
0
B
0 10 20 30 40 50 60 70 80 90
time (min)
b)
bending angle (°)
30
20
10
0
-10
B
0 30 60 90
time (min)
c)
distance from center of chamber to rear (mm)
0.9
0.7
0.5
0.3
0.1
59 min
8 min
0.3 0.5 0.7 0.9 1.1 1.3 1.5 1.7 1.9 2.1 2.3
distance from center of chamber to right, toward barrier (mm)

D. Results obtained with reproducible avoidance rates

Fig. 9 shows the corrected avoidance bending rate, $(d\alpha/dt)_c$, for the 11 sporangiophores tested under the above conditions. Also shown are the corrected bending rates observed for two other sporangiophores (also under these conditions) with the barrier placed 0.50 mm and 2.0 mm away. The distance dependence of the avoidance response appears to be much weaker than the published value of $(1/r)^{0.6}$ (Lafay, et al. 1975). Matus (1985) has confirmed this weak distance dependence, in experiments with the barrier at 0.5, 1, 2, 3, 4, and 6 mm. See Section VII, Part C, below.

Fig. 10 shows the corrected avoidance bending rate as a function of the the time delay between placing the barrier next to the sporangiophore and the next measurement of the sporangiophore's horizontal position (using bright illumination and observing the sporangium from above, as described earlier). The avoidance rate is reduced by up to 30% if the horizontal measurement is made too soon - within 10 min after bringing up the barrier. This effect has yet to be fully explained. In some of the observations described in this section, the avoidance rate following measurements of the sporangiophore's horizontal position was reduced by up to 50% for 5 to 10 min following the measurement, but usually only for measurements done within 10 min after bringing the barrier up to the sporangiophore. Perhaps bright red light interferes with the signal transduction mechanism. Harris and Dennison (1979) reported that a 1 min pulse of bright blue light (100 watt tungsten bulb, Corning 5-61 filter, 315 $\mu W/cm^2$ intensity) inhibits or inverts the avoidance response for 5 to 10 min after the pulse.

Fig. 9. Avoidance rate at 0.5, 1.0, and 2.0 mm from the barrier

The experimental procedure is described in the text.

Corrected avoidance bending rates are plotted.

Each point represents data from one sporangiophore. The number in the parentheses above each data point indicates the number of sporangiophores used.

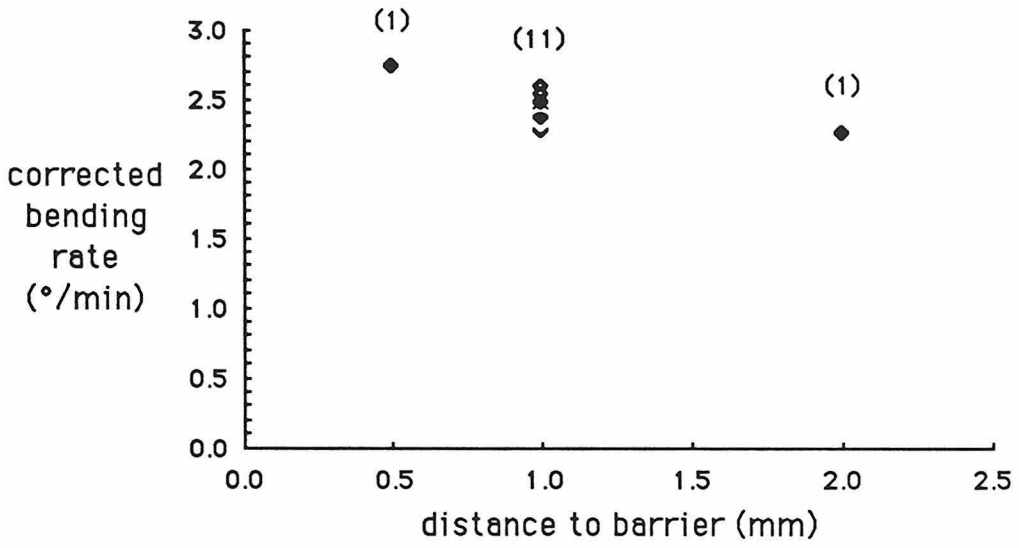

Fig. 10 Avoidance rate as a function of the time delay between the positioning of the barrier and the first measurement of the horizontal position of the sporangium

The experimental procedure is described in the text.
Corrected avoidance bending rates are plotted.
Each point represents data from one sporangiophore.

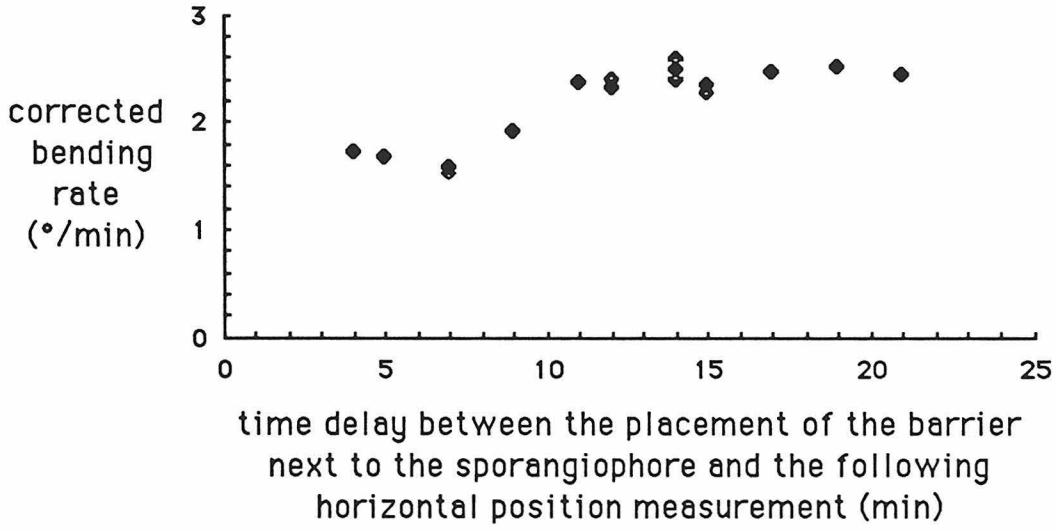

The avoidance rate of the sporangiophore was found to be independent of the diameter of the sporangiophore's growing zone. This is shown in Fig. 11 for the 11 sporangiophores described above.

Since data from sporangiophores with large aiming errors (greater than 35°) were not reliable and had to be ignored, an effort was made to find which (if any) experimental variables correlated with the aiming error. Possibilities tested included the diameter of the growing zone; the diameter of the sporangium; the height of the sporangiophore; its growth rate; the age of the mycelium; the relative humidity in the experimental chamber, from 76% to 98.5%; the length of time the sporangiophore was allowed to adapt to the chamber before bringing up the barrier; the number of the experiment in a succession of up to 3 experiments performed on different sporangiophores on a given day; the time of day; and whether or not the coverslips mounted on the three window plugs were replaced. None of these factors had a significant effect on the aiming error. The aiming error did depend somewhat on the initial angle of the sporangiophore towards the barrier (at the time when the barrier was positioned), as shown in Fig. 12. These data are for 49 sporangiophores tested under the above conditions but with the relative humidity between 76% and 98.5%. Nine of the specimens showed aiming errors of 40° to 60°, and all of these had initial angles of $> 6°$ toward the barrier. 25 of the specimens had initial angles of $\leq 6°$, but only one of them showed an aiming error of $\geq 40°$. Why a large initial angle tends to result in a large aiming error is not known. In future experiments, using only sporangiophores with an initial angle of $\leq 6°$ may eliminate large aiming errors.

Fig. 11 Avoidance rate as a function of stalk diameter

The experimental procedure is described in the text.

Each point represents data from one sporangiophore.

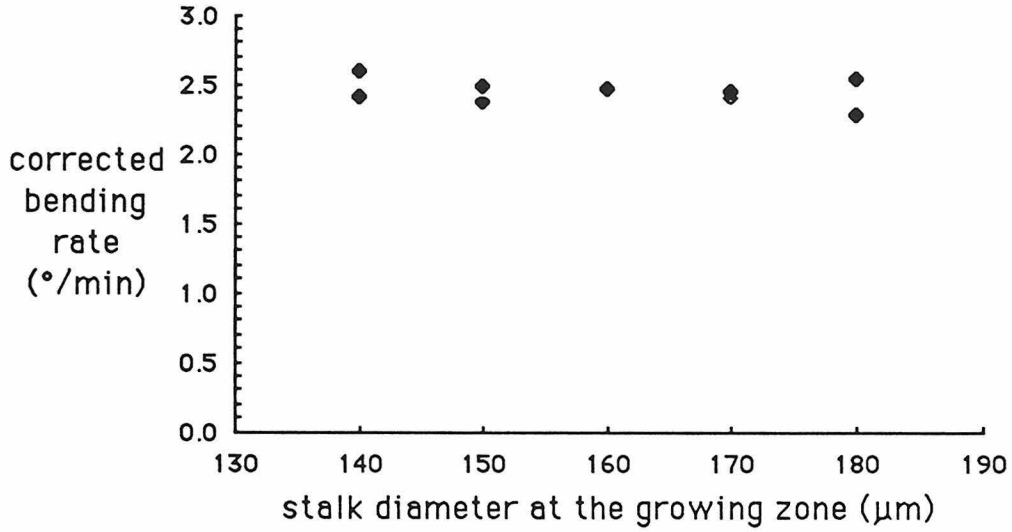

Fig. 12 Aiming error as a function of the initial angle of the sporangiophore with respect to the barrier

The experimental procedure is described in the text.

Each point represents data from one sporangiophore.

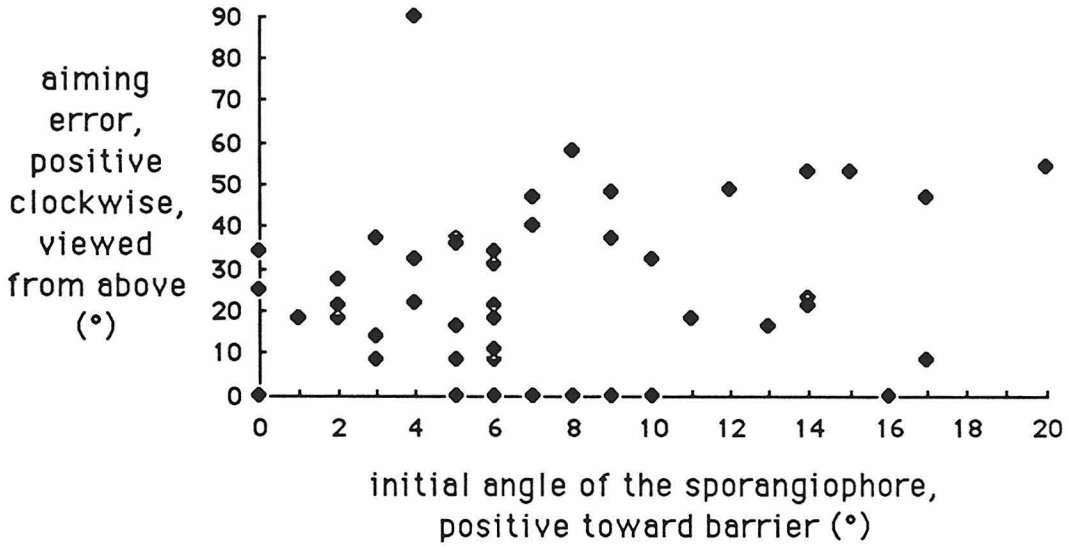

IV. Humidity dependence

The avoidance bending rates of 15 different sporangiophores were measured under the conditions described in Section III, at 76%, 92%, 93%, 97%, and 98.5% relative humidity. The corrected bending rates are plotted in Fig. 13 as a function of relative humidity. Evidently, the avoidance rate falls off with increasing relative humidity. In particular, Fig. 13 shows that the humidity must be controlled to within better than ±1%, to keep the variation in avoidance rates below ±5%.

Matus (1985) has found that the avoidance rate does not fall to zero at above 99.5% relative humidity - as Fig. 13 might suggest - but instead is only about 30% lower than its rate at 93% relative humidity.

Water may saturate the cell wall at high humidity, blocking the diffusion of signal gases necessary for the avoidance response.

If this is true, then if the sporangiophore is placed in a concentration gradient of water vapor at high ambient relative humidity (above 90%), its growing zone ought to become more saturated on the high-humidity side, and it should bend away from the source of water vapor. This is consistent with Elfving's (1881) finding that sporangiophores readily avoid a wet plaster plate placed above them at a 45° angle, but not a dry glass plate. No studies or observations of this "hydrotropism" (above 90 % relative humidity) have been published since 1921. Hydrotropism might have adaptive value for Phycomyces, boosting the avoidance response away from wet surfaces.

Fig. 13 Avoidance rate as a function of relative humidity

The experimental procedure is described in the text.

Each point represents data from one sporangiophore. The numbers in parenthesis above the data points indicate the number of sporangiophores used, at each value of relative humidity.

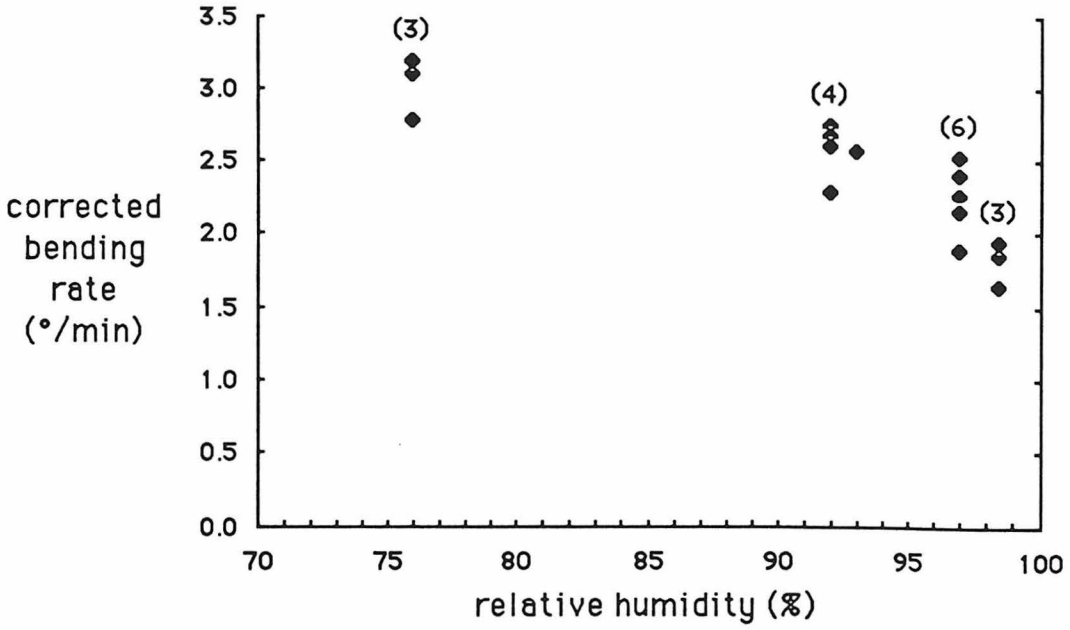

V. Inhibition of the avoidance response by cleaning the apparatus

In an effort to prevent the slow decrease in the rate of avoidance in successive experiments (Section III), the chamber was cleaned before each experiment as described in Chapter 3, Section VI.

Unfortunately, this cleaning inhibited the avoidance response, giving reduced bending rates and a shorter duration for the response. The latency of the response might have been increased, as well. These observations were made under the conditions described in Chapter 3, Section II, and Chapter 4, Section III, with the bottom of the chamber filled with paraffin oil, and with all of the plugs removed from the chamber and kept in the open air, and the chamber itself left uncovered between experiments. Third- through sixth-crop sporangiophores were used, from cultures 120 to 216 hours old. The relative humidity was 93%. The results from two typical experiments are plotted in Fig. 14, the first with no cleaning in the four preceding experiments, the second with the chamber and plugs cleaned immediately before the experiment. If the chamber and plugs were not cleaned the average bending rate was 0.87°/min, and the average maximum angle away from the barrier after 45 min was 14.6° (data from 12 experiments), while if the chamber and plugs were cleaned before each experiment the bending rate fell to 0.46°/min, and the average maximum angle in 45 min fell to - 0.6°, i.e., <u>toward</u> the barrier (data from 19 experiments). In the second case, the sporangiophore typically bends away from the barrier at some non-zero rate, from its initial angle of 5° to 10° toward the barrier, until it is vertical.

Fig. 14 Typical avoidance response after cleaning the chamber with alkaline detergent, and typical response without cleaning

The experimental procedure is described in the text. The barrier was brought up to the sporangiophore at time B.

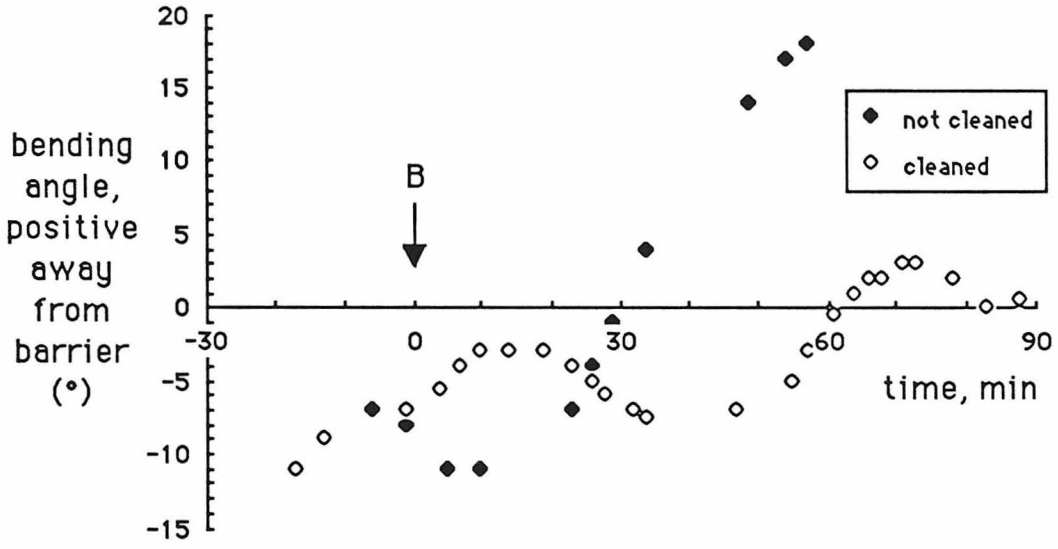

In a "clean" chamber, after the barrier was placed next to the sporangiophore, in some cases no response was observed for at least 30 min. In this situation, passing ≈ 100 ml of fresh air in 2 min through the chamber always initiated a normal avoidance response with the usual latency, speed, and duration. Both room air, and "ultra-high purity" air from a gas cylinder were effective ("ultra-high purity" air = 20% ± 1% O_2, balance N_2, no CO_2, typically less than 10^{-5} ppm hydrocarbons, but less than 0.5 ppm hydrocarbons guaranteed; Big Three Industries, Inc., Long Beach, California). Since removing and injecting 2 ml of the chamber air with a ground-glass syringe 50 times in 2 min did not restore the response, this effect was not due to stirring up the air. In this experiment, the syringe was connected to the vent with an airtight seal, and the chamber remained airtight. In this and all other experiments, the paraffin oil in the base of the chamber was connected to a vertical paraffin oil column outside the chamber (not shown in Fig. 3, but visible in Fig. 2 directly above the left-side plug clamp, as a 15 cm long, thin, white, vertical tube), which rose and fell as the pressure in the chamber changed.

It might be that in a "clean" chamber, either some substance emitted by the sporangiophore or by the residue of detergent left behind after cleaning accumulates rapidly and interferes with the avoidance response. Another possibility is that some substance required for the response is normally present in the atmosphere and on the surfaces of the "dirty" chamber but is not present inside the "clean" chamber. However, this seems unlikely, since injecting less than 30 ml of room air did not restore the response.

The detergent by itself did not seem to be the culprit, since attaching a 3 mm thick, 20 mm diameter aluminum disc with silicone high-vacuum grease to the inside face of the plug opposite the barrier did not inhibit the avoidance response, whether or not the disc was cleaned immediately before the experiment as described in Chapter 3, Section VI, and

whether or not the aluminum alloy was 6061 or 2024. The control in these experiments was a glass coverslip instead of the aluminum disc; in either case, the chamber and plugs were not cleaned. A time-dependent effect was discovered during these experiments, and is reported in the following section.

VI. Time dependence of the response

The rate of the avoidance response increased with the length of time that a sporangiophore spent inside the chamber, under the following conditions: The same experimental procedure was used as outlined in Section V, with the chamber and plugs left uncovered and in the open air between experiments, but not cleaned prior to an experiment. In general, the barrier was used repeatedly, and not replaced between experiments. In some of these experiments an aluminum disc was attached to the plug opposite the barrier (Section V), but this had no effect on the avoidance rate (less than ±10 %).

These observations were made in the following way: after a 30 min adaptation period (or longer), the barrier was brought up to 1.0 mm from the midpoint of the growing zone, and the avoidance response was recorded. Some 30 to 40 min later, the barrier was pulled away and the sporangiophore was allowed to bend back toward vertical (which it almost always does, and at nearly the same rate at which it avoids the barrier; this reaction has never been explained). In some cases, after another 30 to 60 min, the barrier was brought up again, and the avoidance response was recorded once more. This measurement procedure was repeated a third time on some sporangiophores. The avoidance rates observed for 22 such measurements on 12 sporangiophores are plotted in Fig. 15 (black squares) versus the time elapsed from the beginning of the experiment, i.e., when the last plug was inserted and the vent was closed, to the midpoint of the avoidance response, i.e., the midpoint of the 10 min interval defined in Section III.

Fig. 15 Avoidance rate as a function of the elapsed time during the experiment

The experimental procedure is described in the text. Each point represents data from one of several measurements on one sporangiophore.

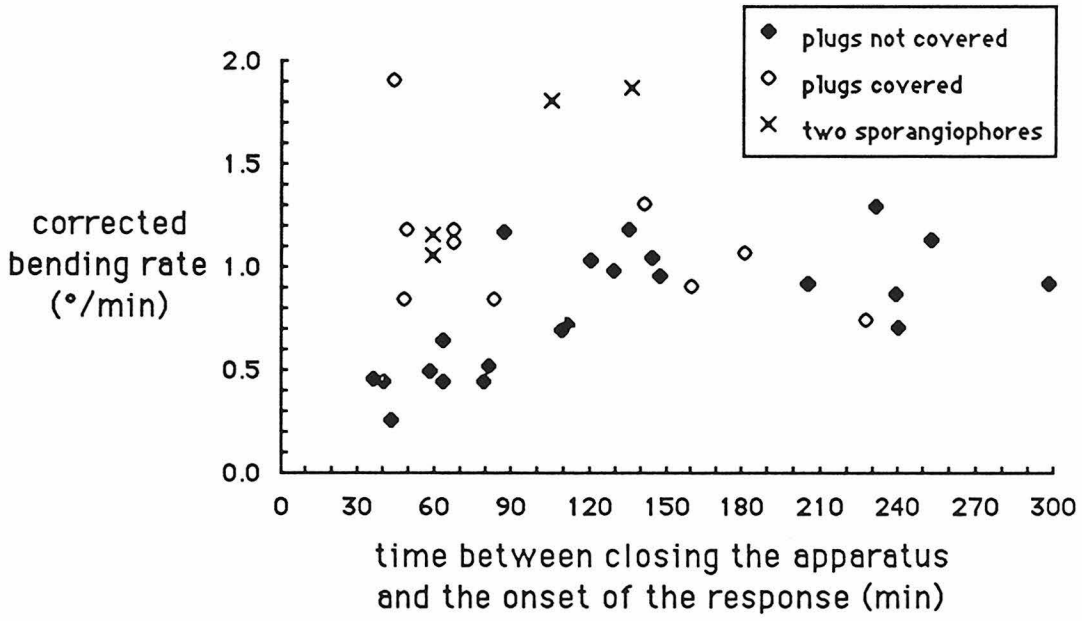

The rate appears to increase linearly from zero to 1°/min during the first 2.5 hours that the sporangiophore has spent inside the chamber, and then remains almost constant. Note that 2 avoidance measurements were made (and plotted) on 6 of these 12 sporangiophores, and 3 measurements were made on 2 of them. So this increase in avoidance rate with time does not depend on whether the sporangiophore has exhibited an avoidance response once already inside the chamber.

In two separate experiments, two sporangiophores growing out of the same vial, 0.6 cm apart, were placed in the chamber, aligned so that they were the same distance from the barrier at the beginning of the experiment, and tested (simultaneously) as described above. These results also appear in Fig. 15 (crosses). In these experiments, the avoidance rate of three of the four sporangiophores increased twice as fast as would be predicted by Fig. 15 for a single sporangiophore, to 2 degrees per minute in 2.5 hours, on average. The remaining sporangiophore exhibited an abnormally large aiming error - over 40° - so its data were rejected (Section III). These experiments should be repeated, since they would show for the first time that one sporangiophore can increase the avoidance rate of another one nearby.

If the plugs and the chamber were kept in room air between experiments, but kept covered with a Kimwipe, or if all of the plugs except the bottom one were left inserted in the chamber between experiments, the avoidance rate no longer increased from zero at the beginning of the experiment, but started out high and remained fairly constant at about 1.0 ± 0.2°/min. Data from 11 measurements made on 7 sporangiophores under these conditions also appear in Fig. 15 (white squares).

The time dependence has not been explained. It can be avoided entirely, however, by keeping the inside surfaces of the chamber covered between experiments, as was done in the series of controlled experiments described in Section III.

The bending rate (at 1 mm) in these controlled experiments (Section III) was 2.4°/min, or twice that shown for single sporangiophores in Fig. 15. This difference was not due to a change in the sporangiophores themselves, since they did avoid at about 2°/min when two of them were placed in the chamber. The difference may have been due to the fact that the barrier was not replaced between experiments, or that the bottom of the chamber was filled with paraffin oil, in the experiments just described. Matus (1985) has found that a fresh barrier gives a stronger avoidance response than one which has been used 1 or 2 days prior to the experiment. He has also found an average avoidance rate of 1.4°/min - as opposed to the value of 2.4°/min reported in Section III - under the conditions of Section III, but with paraffin oil in the base of the chamber.

VII. Recent results supporting the new working hypothesis

A. Dependence on chemical composition

Note: most of the experiments described in this part (A) were performed by Ivan Matus (1985).

A slab of magnesium metal 1.2 cm square and 0.3 cm thick was stuck to the inside face of one of the solid aluminum plugs with silicone high-vacuum grease and positioned with its exposed face 1 cm away from the sporangiophore on one side, while a clean glass coverslip was positioned in the same way on the opposite side at the same distance. The sporangiophore bent toward the magnesium at about 0.1°/min. When the magnesium was replaced by a copper slab of the same dimensions, no such bending was observed. The chamber relative humidity was 93%. The exposed face of the metal was sanded bright immediately before the experiment using fresh 600 grit sandpaper (3M company, "wet-or-dry" "tri-M-ite" paper). The experimental conditions were the same as described in Chapter 3 and in Section VI of this chapter, with only the bottom port left open between experiments.

This result is consistent with that described by Elfving (1917) and reviewed in Chapter 2, namely, that the sporangiophore exhibits weak bending at a distance of several cm toward brightly polished surfaces of strongly reducing metals such as zinc (standard redox potential, $E^\circ = 0.76$ volt at pH = 0 in aqueous solution) but not toward polished iron ($E^\circ = 0.44$ volt) or other less strongly reducing metals such as Cd, Co, Ni, Sn, Pb, Sb, Bi, Cu, Ag, Pt, or Au (in order of decreasing E°).

The result described here suggests that the response might be slightly weaker for a strongly reducing barrier, perhaps because the oxidation step which produces the active signal gas - as proposed in one version the new working hypothesis - is inhibited on the surface of such a barrier. Another possibility is that the fresh magnesium surface is hygroscopic and is producing a hydrotropic response (Section IV). This alternative can be tested by

comparing magnesium to glass at two different relative humidities, say, 70% and 99%. If the metal acts by adsorbing water vapor, it should attract the sporangiophore more strongly at 99% relative humidity than at 70%. If it acts by reversing the gradient of the signal gas used in the avoidance mechanism, the opposite should occur, since the avoidance response is inhibited above 90% relative humidity (Section IV).

In addition to magnesium (E° = 2.37 volt), and copper (-0.34 volt), also zinc (0.76 volt), chromium (0.74 volt), gallium (0.53 volt), iron (0.44 volt), and gold (-1.5 volt) could be tested, to accurately determine the redox potential below which bending toward metal is no longer observed. Elfving's (1917) result implies that this value will be between 0.44 and 0.76 volt. To insure that the effect is not due to some impurity picked up from the sandpaper, alternate methods for cleaning the metal surface should also be tried, such as dipping the metal in reagent grade fuming HNO_3 and rinsing it in glass-distilled water.

B. Avoidance of thin wires

In November, 1980, before the wind-free chamber was constructed, three measurements were made of the avoidance rate away from a parallel, aligned 120 μm diameter platinum wire, or "dummy sporangiophore," positioned 0.6 to 0.7 mm away from a test sporangiophore, inside a 1inch x 1 inch x 3 inch tall glass house. The sporangiophores and the wire were inserted ≈ 1 cm into the house through a 0.5 cm x 2 cm rectangular slot in its base. The house was humidified by wet tissue paper. The bending rate away from the wire was about 2˚/min. The mutual avoidance of a pair of parallel, aligned sporangiophores positioned 0.6 to 0.7 mm apart was also observed inside this house - the sporangiophores bent away from each other at about 2˚/min.

A similar result is described by Cohen, et al. (1975), for a horizontal wire aligned perpendicular to the growing zone of a sporangiophore. They observed avoidance rates of about 0.5˚/min for either a 50 μm diameter wire located 0.6 mm from the growing zone, or another, parallel, aligned sporangiophore positioned 0.6 mm away. See Figs. 8 and 12 in their paper.

Matus (1985) has found that in our environmental chamber sporangiophores avoid a 50 μm diameter parallel glass fiber, placed 2 mm away from the growing zone, at nearly the same rate (1.0˚/min) as they avoid a 22 mm diameter glass coverslip placed 5 mm away (1.4˚/min). Such rapid bending away from a thin wire is not consistent with the Growth-Promoter Reflection Model (Appendix 3).

C. Distance dependence in a wind-free environment

Matus (1985) has found that the avoidance response away from clean glass coverslips is constant at about 1.4˚/min (± 10%), from 1 mm distance out to about 4 mm distance, with the response falling off rapidly between 4 and 6 mm. The experimental procedure was as outlined in Chapter 3, Section II, and in this chapter, Section III, but with the base of the experimental chamber filled with paraffin oil.

The reason for this "saturation" of the response at distances closer than 4 mm (or 2 mm for the fiber) is not known.

With a parallel, aligned 50 μm diameter glass fiber as a barrier, no saturation of the response is observed. The avoidance rate falls off gradually with distance, from 1 mm out to 5 mm. The rate is about 1.0˚/min at a distance of 2 mm.

In Appendix 3, for our 5 versions of the CSGH, we estimate the gradient of signal gas across the growing zone - and predict the bending rate from this - due to barriers placed at distances large enough that the response would not be saturated, and such that the avoidance rate would be about 1˚/min: 5 mm for the plane, and 2 mm for the glass fiber barrier.

5. Discussion

The experiments discussed in the preceding sections establish the following facts about the avoidance response of Phycomyces sporangiophores:

(1) A normal avoidance response occurs with an ambient wind speed of less than 10 μm/sec.

(2) The variation in avoidance rates for different sporangiophores tested under identical conditions can be kept to less than ±10%. The following were controlled:
   (a) the age of the Phycomyces culture,
   (b) the temperature and relative humidity in the experimental chamber,
   (c) replacement and cleaning of the coverslips used as barriers and as windows in the experimental chamber,
   (d) exposure of the sporangiophore to high light intensity during the experiment - even "physiologically inactive" red light,
   (e) protection of the inside surfaces of the chamber between experiments,
   (f) the time delay between the start of the experiment and the placement of the barrier,
   (g) correction for the aiming error angle,
   (h) correction for any slow, uniform drift of the avoidance rate in successive experiments.

(3) The avoidance rate falls off with increasing relative humidity.

(4) Cleaning the inside surfaces of the experimental chamber in hot alkaline detergent inhibits the response - the maximum bending angle is limited to within a few degrees of vertical, on average.

(5) The avoidance rate may depend on the chemical composition of the barrier.

(6) The avoidance rate does not depend strongly on the distance from the barrier.

(7) A thin wire is effective as a barrier - even at large distances from the sporangiophore.

The simpler versions of the CSGH cannot explain this last result, nor the avoidance in the absence of air currents (Chapter 4, Section I, and Appendix 3). Thus, if the sporangiophore detects objects by emitting or adsorbing a signal molecule, and this molecule cannot just be reflected by the barrier, our only alternative is that it must be adsorbed by the barrier surface for a certain length of time.

If this is true, then poorly adsorbing barriers (e.g., teflon, boron nitride) should give relatively weak avoidance responses, while barriers with a high specific surface area (e.g., activated charcoal, glass fiber filters) may give stronger, or longer lasting responses. Also the response may depend on the chemical composition of the barrier. Finally, the avoidance rates away from thin wire barriers and plane barriers should agree with what the new working hypothesis predicts, and they do - see Appendix 3, Fig. 24.

The different versions of the new working hypothesis can be distinguished experimentally. For example, the Growth-Inhibitor Adsorption Model predicts that a test sporangiophore will exhibit a negative growth response when exposed (without any intervening adsorbing surfaces) to the effluent from a forest of sporangiophores, while the Barrier-Emission Model predicts a positive growth response in this experiment, and the Atmospheric Growth-Inhibitor Adsorption Model predicts no growth response.

Another experiment will distinguish between the two Growth-Inhibitor models, assuming that one of them is correct. In the Atmospheric Growth-Inhibitor Model, a sporangiophore should exhibit a strong growth response (a decrease) when retracted a few millimeters from between two fixed, parallel plane barriers, spaced much closer than their width. This is

because the hypothetical inhibitor gas is produced outside the space between the two barriers in our experimental chamber. If, instead, the growing zone itself produces the inhibitor (Growth-Inhibitor Adsorption Model), then much weaker responses should be seen. Separating the two barriers a fraction of a millimeter should give a strong growth response (decrease) in either case, and should be used as a control.

The reasons why cleaning the inside surfaces of the experimental chamber inhibits the response, and why covering - or not covering - these surfaces between experiments affects the avoidance rate, are still unknown.

With the set of working hypotheses narrowed down to one strong candidate, and given reasonable estimates of the decay time of the signal molecule and its rate of adsorption to surfaces, it should be possible to detect and isolate this molecule using a bio-assay, and then identify it. This would decide once and for all the question: "How does the sporangiophore detect nearby objects?"

Appendix 1

Derivation of the corrected growth rate

We want to calculate the approximate speed of elongation of the growing zone, v_c, in μm/min.

In an experiment, we measure in the focal plane as a function of time, the vertical velocity of the sporangium, v, in μm/min, the bending angle of the growing zone, α, in degrees (°), and the bending rate, $d\alpha/dt$, in °/min.

We assume that the aiming error is small, and that α and $d\alpha/dt$ are close to their actual values - that would be measured in the plane of bending (Appendix 2).

We approximate the growing zone of the sporangiophore as shown in Fig. 16a. The growing zone is assumed to be straight, non-bending, and of fixed length z_o = 2 mm. We assume that all growth occurs at the base of the growing zone, and that all bending occurs at a "hinge," which moves up continuously to remain just below the base of the growing zone.

There are two independent contributions to the vertical velocity of the sporangium, v. Call them v_1 and v_2 (where $v = v_1 + v_2$). v_1 is due to the elongation of the growing zone at a rate v_c, and angle α, and is equal to $v_c \cdot \cos\alpha$ (Fig. 16b). The second component, v_2, is due to bending at the hinge. If z is the vertical distance from the hinge to the top of the growing zone, then $v_2 = dz/dt$. Since $z = z_o \cdot \cos\alpha$ (Fig. 16c), we take a derivative and get $v_2 = -z_o \cdot \sin\alpha \cdot d\alpha/dt$. If we take $\sin\alpha \approx \alpha$ (this is accurate to within 5% for $\alpha < 30°$), we get $v_2 = - z_o \cdot \alpha \cdot d\alpha/dt$.

Adding v_1 and v_2 and rearranging, we get:

$$v_c = [\, v + 0.61 \cdot \alpha \cdot d\alpha/dt \,] / \cos\alpha \qquad (1)$$

in μm/min, where v is in μm/min and α is in degrees. This formula (1) was used to estimate v_c in the experiments.

Fig. 16 View of the sporangiophore (a), the vertical component of its growth rate as a function of bending angle (b), and the vertical elevation along the growing zone as a function of bending angle (c).
All views are in the focal plane.
The growing zone in (a) is assumed to be 2 mm long.
The variables are defined in the text.

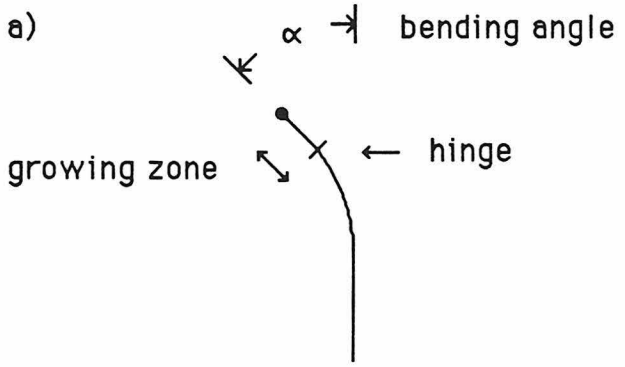

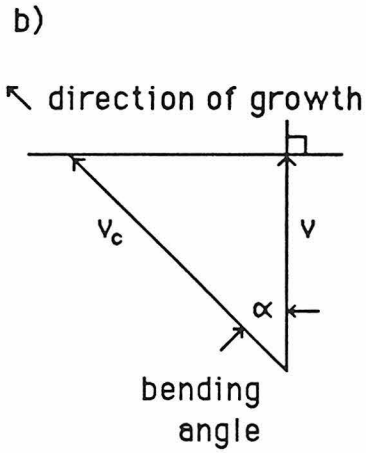

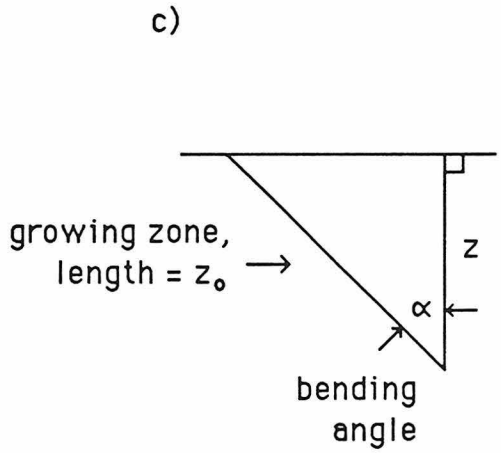

Appendix 2

Derivation of the corrected bending rate, in the plane of bending

In the experiments, we measured the bending rate of the growing zone in the focal plane. If a sporangiophore bent away from the barrier in a direction other than parallel to the focal plane, then its actual bending rate - in the plane of bending - was larger than the measured rate by some factor. Here we estimate this factor from the aiming error angle, θ.

This angle is defined in Fig. 17a as the angle between the focal plane (normal to the barrier) and the plane of bending (the actual path taken by the sporangium).

Let α be the bending angle of the growing zone measured in the focal plane, and let α_c be its actual bending angle in the plane of bending. Then:

$$\tan\alpha_c = r_c/z \,, \qquad (1)$$

where r_c is the horizontal component of the growing zone, and z is its vertical component (Fig. 17b). If the growing zone is rotated by the aiming error angle, θ, as represented in Fig. 17a, then z is unchanged, but the observed value of r_c is decreased to:

$$r = r_c \cdot \cos\theta \,, \qquad (2)$$

as can be seen from Fig. 17a.

In the same manner as for α_c, the measured bending angle, α, can be expressed as:

$$\tan\alpha = r/z. \qquad (3)$$

Substituting (2) and (3) into (1), we get:

$$\alpha_c = \tan^{-1}(\tan\alpha/\cos\theta). \qquad (4)$$

If α is small (less than 30°, so that $\alpha \approx \tan\alpha$), then a good approximation to (4) is $\alpha_c = \alpha/\cos\theta$. The time derivative of this is:

$$d\alpha_c/dt = (d\alpha/dt)/\cos\theta. \qquad (5)$$

This is the formula that was used to obtain the actual bending rate (in the plane of bending) from the aiming error, in the experiments.

Fig. 17 The path of the sporangium as viewed from above (a), and the vertical and horizontal components of the growing zone (b), viewed in the plane of bending

The variables are defined in the text.

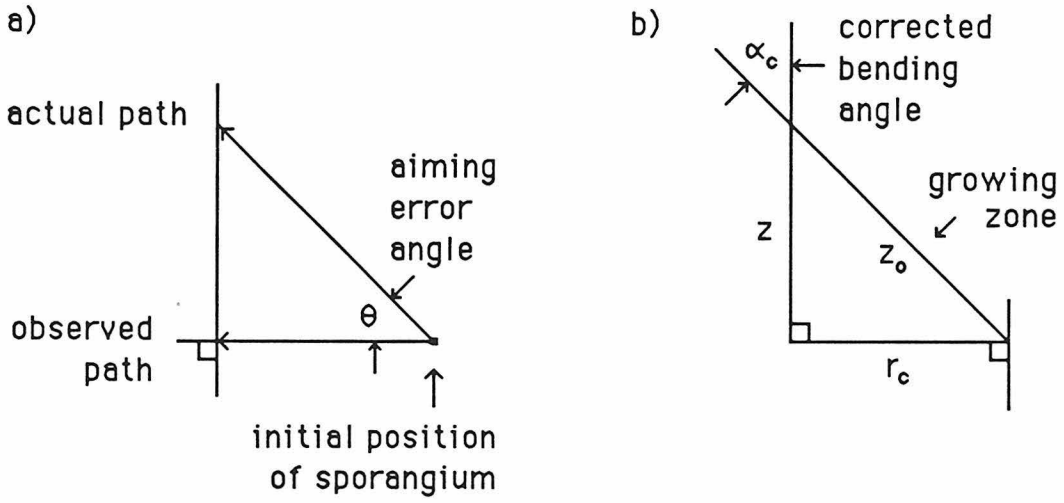

Appendix 3

Mathematical modeling of the response

I. Introduction and Definitions

For each of the models proposed in Chapter 4, we will calculate the effect of barriers on the distribution of an effector gas at the surface of the sporangiophore growing zone.

In Section II we solve Laplace's equation for a gas emitted or adsorbed by a sphere of radius a, in open, quiet air, for the boundary conditions imposed by each of our models, except the wind gradient model.

In Section III we solve Laplace's equation for a gas emitted by a long, thin cylinder of radius a, and length L, in open, quiet air. We also give an estimate of the concentration of ethylene at the surface of the growing zone, from the emission rate measured by Russo, et al. (1977).

In Section IV we estimate the relative difference in concentration, $\Delta c/c$ (or flux, $\Delta F/F$), of the signal gas, induced across the growing zone by a large plane surface located 5 mm away or a 50 μm diameter parallel wire located 2 mm away, for each of the models.

In all of our calculations, we ignore the fact that the sporangiophore bends and moves away from the barrier during the response. All calculations are for the steady state: $\partial c/\partial t = 0$, where c is the gas concentration. We ignore the effect of the ≈ 0.05 cm diameter sporangium. Unless noted, we assume that the ambient wind speed is zero. We use cgs units. "log" always denotes natural logarithm, to the base e.

We approximate the growing zone of the sporangiophore by:

1. a sphere of radius a = 0.005 cm, or
2. a cylinder of the same radius, a, and length L = 0.2 cm.

A glossary of variables and notation is provided on p. xi, immediately preceding p. 1 of Chapter 1.

Fig. 18 The coordinate system used in the calculations

The center of the sphere, and the midpoint of the cylinder are located at the origin.

The x-axis is normal to the barrier. It is positive away from the barrier.

The y-axis is not labeled.

The axis of the cylinder coincides with the z-axis, positive upward.

r is the distance from the z-axis.

R is the distance from the origin.

θ is measured counterclockwise from the positive x-axis, viewed from above.

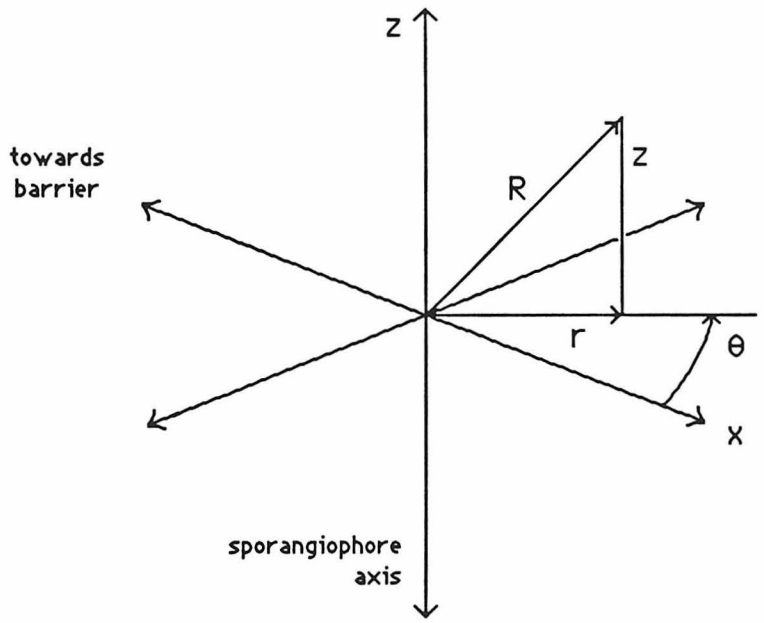

II. Solutions to Laplace's equation in open air: emission or adsorption of a gas by a sphere

We approximate the growing zone by a sphere of the same radius, a. This is a good approximation if only a short segment of the growing zone is emitting and sensing the effector gas. We consider the following cases:

A. Emission of a non-decaying gas
B. Adsorption of a gas
C. Emission of a decaying gas
D. Emission of a decaying gas whose decay product is adsorbed by the sphere.

The derivations in Parts A and B follow those in Berg (1983). The derivations in Parts C and D are original.

A. Emission of a non-decaying gas

Consider a sphere of radius a emitting a non-decaying gas at a uniform, constant rate on its surface, in open, quiet air. In the steady state, the concentration of the gas must obey Laplace's equation, $\nabla^2 c = 0$, or:

$$\partial^2 c/\partial R^2 + (2/R)\partial c/\partial R = 0 \qquad (1)$$

in spherical coordinates, with no angular dependence, where R is the distance from the origin (Berg 1983, p. 21).

The general solution to (1) is:

$$c(R) = c_\infty + (c_0 - c_\infty)(a/R) \qquad (2)$$

where c_∞ is the concentration of gas at $R = \infty$ (i.e., far from the sphere), and c_0 is its concentration in the air at the surface of the sphere. Equation (2) satisfies both uniform-concentration and uniform-flux boundary conditions.

The outward flux, F, of gas at any point is given by Fick's first equation, $F = -D\partial c/\partial R$ (Berg 1983, p. 18). From (2), we get:

$$F = (c_0 - c_\infty)(Da/R^2) \qquad (3)$$

in molecules/cm^2/sec. D is the diffusion coefficient of the gas, in cm^2/sec.

B. Adsorption of a gas

Now suppose that the sphere adsorbs a gas from its environment. If the background concentration of the gas, c_∞, is non-zero, and if its concentration is $c_0 < c_\infty$ at the surface of the sphere, then equation (2) above is still correct. If the sphere is a good adsorber, c_0 will be a small fraction of c_∞. If the sphere is a poor adsorber, c_0 will be almost equal to c_∞.

How good is "good?" In the simplest case, if the gas is adsorbed by and removed from the surface of the sphere at a rate proportional to c_0, in other words, if the adsorbed flux (-F) equals kc_0 at R = a, then equation (3) gives:

$$c_0 = c_\infty / [1 + ak/D] \qquad (4)$$

where k is in cm/sec. If k is large compared to D/a, then the sphere is a good adsorber.

C. Emission of a decaying gas

Consider again the case in which the sphere emits a gas, but let the molecules decay in air with a time constant τ, in sec. If we isolate a small volume of this gas (containing no sources or sinks), the concentration will fall off at the rate:

$$\partial c/\partial t = -c/\tau \qquad (5)$$

in molecules/cm^3/sec. Fick's second equation is $\partial c/\partial t = D\nabla^2 c$ (Berg 1983, p. 21). $D\nabla^2 c$ is the rate at which the concentration increases in the small volume, due to diffusion. In the steady state, this increase must balance the loss due to decay, so that:

$$D\nabla^2 c = c/\tau\,. \qquad (6)$$

If we require that c go to zero at infinity, then in spherical coordinates, (6) is satisfied by :

$$c(R) = c_o\,[a/R]\,e^{-(R-a)/R_d} \qquad (7)$$

where c_o is the concentration at the surface of the sphere, and R_d is the decay length, $(D\tau)^{1/2}$. If D = 0.1 cm^2/sec and τ = 10 sec, then the decay length R_d equals 1 cm. The outward flux at any point is:

$$F = D\,[1/R + 1/R_d]\,c(R) \qquad (8)$$

in molecules/cm^2/sec, where c(R) is given in (7), above.

D. Emission of a decaying gas whose decay product is adsorbed by the sphere

Suppose that the sphere emits a precursor gas which decays in the air to an effector gas, as in the "growth-inhibitor adsorption" model. One precursor molecule generates one molecule of effector. This effector does not decay, but is adsorbed by surfaces, including the sphere itself. Here we get a intriguing result, because the effector concentration can be zero at the surface of the sphere, rise to some maximum value at a critical distance R_{MAX} [which depends only on the radius of the sphere and the precursor decay length], and then fall off as 1/R beyond R_{MAX}.

The precursor gas concentration is already given by (7), above :

$$c_P(R) = c_{OP} [a/R] e^{-(R-a)/R_{dp}} \qquad (9)$$

where R_{dp} is the decay length of the precursor gas, and c_{OP} is its concentration at the surface of the sphere. In any small volume, precursor is decaying at the rate $c_P(R)/\tau_P$, from (5). Since one precursor molecule generates one molecule of effector, effector must be produced in this small volume at the same rate, $c_P(R)/\tau_P$. In the steady state, this must equal its loss due to diffusion ($-D\nabla^2 c$), so that:

$$-D\nabla^2 c = c_P(R)/\tau_P \qquad (10)$$

where c is the effector concentration (unknown function of R), and $c_P(R)$ is the (known) precursor concentration (9). A particular solution of (10) is just $c = -[D_P/D]\, c_P(R)$. This is because $c_P(R)$ is a solution to (6). If the effector concentration, c, goes to zero at infinity, the solution to the corresponding homogeneous equation [with $c_P = 0$ in (10)] is just $c = c_O [a/R]$, where c_O is a constant, to be determined by the boundary condition on c(R) at the surface of

the sphere. Because (10) is linear, its general solution is the sum of these two solutions (Mathews and Walker 1965, p. 7):

$$c(R) = c_O [a/R] - c_{OP} [D_P/D] [a/R] e^{-(R-a)/R_{dp}} \quad (11)$$

If c = 0 at R = a (the sphere is a good adsorber), then $c_O = c_{OP} [D_P/D]$, and the concentration of effector is:

$$c(R) = c_{OP} [D_P/D] [a/R] [1 - e^{-(R-a)/R_{dp}}] . \quad (12)$$

This is just as predicted. The effector concentration, c(R), is zero at the surface of the sphere (R = a), increases with R for small R, and decreases as 1/R for large R. It is proportional to the precursor concentration at the surface of the sphere, c_{OP}.

What is R_{MAX}, the distance from the sphere where c(R) is a maximum? Setting the derivative of c(R) equal to zero, and using the first 3 terms, $1 + x + x^2/2$, in the series expansion for e^x to simplify the resulting equation, we get:

$$R_{MAX} = (2aR_{dp})^{1/2} \quad (13)$$

valid only for $R_{dp} >> a$, where R_{dp} is the precursor decay length, $(D_P\tau_P)^{1/2}$. If the radius of the sphere, a, is 50 μm, and the decay length, R_{dp}, is 1 cm, then R_{MAX} is about 1 mm.

We will use this result in the following section, to determine a lower bound on R_{dp} for the Growth-Inhibitor Adsorption model.

The concentration of precursor gas as a function of R and the concentration of effector gas as a function of R are plotted in Fig. 19, using the above parameters.

Fig. 19 The concentration of an emitted precursor gas and an adsorbed effector gas

The open symbols represent the precursor gas and the closed symbols represent the effector gas. One molecule of precursor decays to produce one molecule of effector. The precursor is emitted by a sphere of radius a = 50 μm, whose center is located at the origin. We also assume that: the precursor decay length, R_{dp}, is 1 cm; the diffusion coefficients of the precursor and the effector are equal; and, the effector concentration is zero at the surface of the sphere (at R = a).

The concentration of either the precursor or the effector is expressed relative to the precursor concentration at the surface of the sphere, c_{OP}. Thus, c_P/c_{OP} and c/c_{OP} are plotted as a function of R, the distance from the center of the sphere.

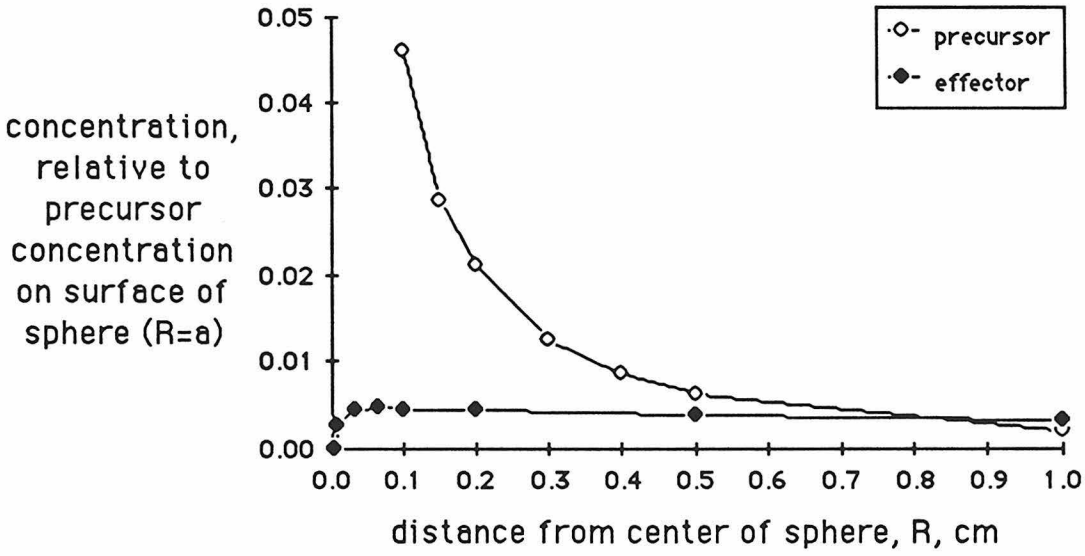

III. Solutions to Laplace's equation in open air: emission or adsorption of a gas by a thin cylinder

We approximate the growing zone by an emitting cylinder located on the z-axis, of radius a, and length L >> a (extending from z = -L/2 to z = +L/2). We assume that the emission rate of gas at the surface of the cylinder is uniform, and equal to F molecules/cm^2/sec.

Suppose we replace the cylinder by a line source of length L, located on the axis of the cylinder. The concentration due to this line source will be the same everywhere as for the cylinder, except in the immediate vicinity of the ends of the cylinder (closer than a few cylinder radii, a).

We determine below the concentration of gas emitted by this line source in the z = 0 plane, as a function of r, using the Green's function in equation (1) below. This is a standard derivation, and it is covered in Smythe (1950) and in other texts. Our result is plotted in Fig. 20.

The emission rate of the line source per unit length must be $2\pi aF$ molecules/cm/sec, to match the emission rate of the cylinder. Then an infinitesimal segment, dz′, of the line source emits at a rate $2\pi aFdz'$ molecules/sec. Since this segment behaves as a point source, the concentration at a distance R′ from the segment falls off as 1/R′. Doing some algebra, and making use of (3) in Section II, we get:

$$c(R') = aFdz'/2DR' \qquad (1)$$

as the concentration at a distance R′ from the segment dz′, all by itself, where a and F were defined above, and D is the diffusion coefficient of the gas, in cm^2/sec.

Since Laplace's equation, $\nabla^2 c = 0$, is linear, we can integrate (1) along our line source to find the concentration due to the entire source. In the $z = 0$ plane, R' is equal to $(r^2 + z'^2)^{1/2}$, where z' is the height of a particular segment, dz', above the origin. The concentration at any point in the $z = 0$ plane at a distance, r, from the midpoint of our line source is then:

$$c(r) = (aF/2D) \int dz' / (r^2 + z'^2)^{1/2} \qquad (2)$$

with the integral evaluated from $z' = - L/2$ to $z' = +L/2$. The integral in (2) is given by Spiegel (1968, p.67) as $\log \{ z' + (r^2 + z'^2)^{1/2} \}$. Evaluating this at the limits $\pm L/2$ and doing some algebra, we get:

$$c(r) = (aF/2D) \log(\xi+1 / \xi-1) \qquad (3)$$

where $\xi = [1 + (2r/L)^2]^{1/2}$. This is approximately the concentration of a gas in the $z = 0$ plane at a distance r from the origin, due to a cylinder of radius a and length $L >> a$, whose axis is the z-axis, emitting the gas at a constant, uniform rate, F, on its surface.

At r << L, close to the cylinder or line source, (3) reduces to:

$$c(r) \approx (aF/D) \log(L/r) ; \qquad (4)$$

i.e., it behaves like an infinite line source, as expected.

At r >> L, far from the source, (3) reduces to:

$$c(r) \approx (aF/D)\cdot(L/2r) ; \qquad (5)$$

i.e., it behaves like a point source, as expected.

In (4), setting r = a, the radius of the cylinder, we find the concentration at the surface of the cylinder at z = 0 (its midpoint):

$$c(a) = (aF/D) \log(L/a) \qquad (6)$$

where a, F, D, and L are all as defined above.

The concentrations given by equations (3), (4), and (5) are all plotted as functions of r, in Fig. 20.

Two points are worth mentioning here.

First, using Smythe (1950, Section 5.28), one can show that the concentration due to a long, thin cylinder given in (3) is nearly identical to the concentration due to a long, thin prolate ellipsoid of revolution of minor radius a, and length L, oriented in the same way, with uniform concentration on its surface. Another way of saying this is that the surfaces of uniform concentration around our line source or cylinder are (approximately) thin prolate ellipsoids of revolution.

Second, how does the concentration of emitted gas at the surface of our cylinder drop off toward the ends of the cylinder? Specifically, what is the concentration at z = L/2 and r = a ? At this location, the distance, R′, to any

point on the line source a distance z′ above the origin is $R' = [a^2 + (L/2 - z')^2]^{1/2}$. Inserting this in (1), integrating in the same manner as eqn. (2), using another integral given by Spiegel (1968, p. 72), and assuming $a << L$, we get approximately half the value given by (6), or $c(r=a, z=+L/2) = (aF/2D)\log(2L/a)$. For $L = 40a$, this is lower than at the middle of the cylinder by about 40%.

This suggests that the concentration and flux of gas at any point, emitted by our cylinder with a uniform surface flux, will be within a factor of two of their values for an identical cylinder which emits the same number of molecules per sec, but with uniform surface concentration.

We make use of this approximation later.

Using (6), above, we can estimate the concentration of ethylene at the surface of the growing zone in the experiments of Russo, et al. (1977). He gives the emission rate per growing zone as $2.4 \cdot 10^7$ molecules/sec. If the radius of the growing zone is 50 μm, and its length is 2 mm, its surface area is about 0.01 cm^2. Thus, the flux, F, of ethylene at the surface of the growing zone is about $2.4 \cdot 10^9$ molecules/cm^2/sec. Using (6), we find that the concentration of ethylene on the surface of the growing zone would be about $0.4 \cdot 10^9$ molecules/cm^3. Given that the concentration of air molecules is 1/25 mole per liter at sea level, this corresponds to about $1.6 \cdot 10^{-5}$ ppm ethylene. This result is used in Chapter 1.

Fig. 20 The concentration of a gas emitted by a thin cylinder

The radius of the cylinder, a, is assumed to be 50 μm, and its length is assumed to be 2 mm. The flux of gas emitted by the cylinder is assumed to be uniform over the surface of the cylinder. The gas concentration is plotted as a function of r, the distance from the cylinder axis in the z = 0 plane. The concentration is expressed as the ratio c(r)/c(a), where c(a) is its value at the surface of the cylinder at its midpoint - i.e., at z = 0. From (6), c(a) = 3.7 (aF/D), approximately.

The exact result (3) is plotted as the heavy line in the figure. Equation (4), the approximation to (3) for r << L, is plotted in the figure using a thin line, and labeled "log(L/r)." Equation (5), the approximation for r >> L, is also plotted, and labeled "L/2r."

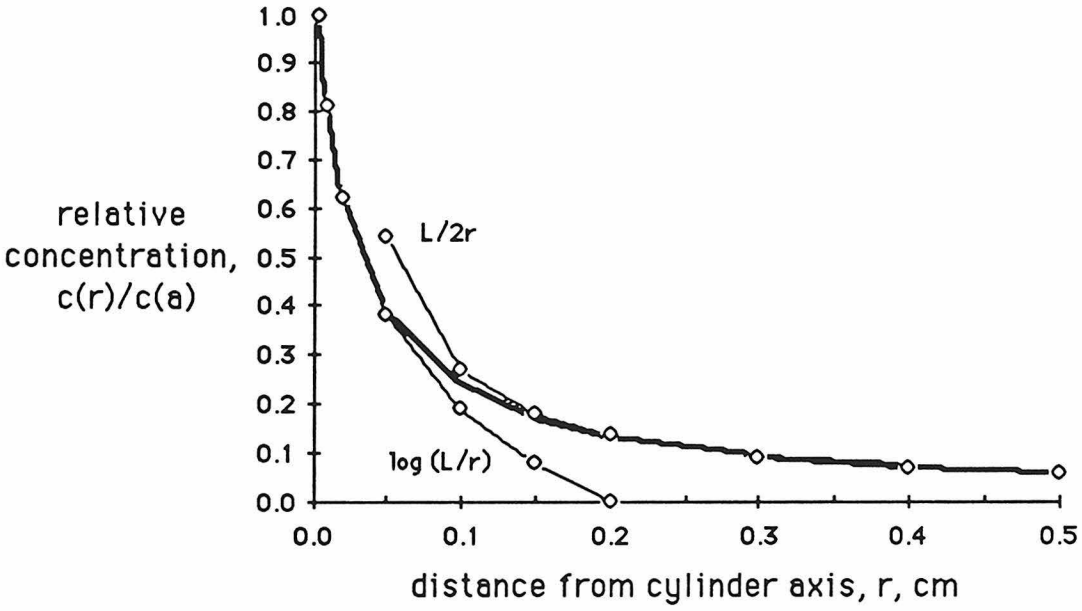

IV. Plane and wire barriers

Here we estimate the fractional difference in concentration, $\Delta c/c$, or the fractional difference in flux, $\Delta F/F$, induced across the growing zone by a 50 μm diameter, parallel wire placed 2 mm away, and a large, flat plane barrier placed 5 mm away from the growing zone.

We do this for each of our 5 models, in order, making reasonable simplifying assumptions along the way. Our results are accurate to within an order of magnitude. They are tabulated at the end of this section, in Fig. 24.

In Parts B, C, and D, below, only the flux difference across the growing zone, $\Delta F/F$, is calculated, because the concentration of the signal gas in each of these models is assumed to be uniform on the surface of the growing zone.

In Part A, below, only the concentration difference across the growing zone, $\Delta c/c$, is calculated, because the concentration of a gas emitted by a cylinder with uniform flux out of its surface was determined accurately in Section III of this Appendix, while only a rough estimate was made for a cylinder with uniform surface concentration (Section III). This is no problem, in this case. In the model discussed in Part A, below, $\Delta c/c$ and $\Delta F/F$ are equal to within an order of magnitude. This is because the concentration difference across the growing zone is on the order of $(a/D)\Delta F$, and the average concentration and outward flux at the surface of the growing zone are related by (6) in Section III. Combining these results gives $\Delta c/c = (1/3.7)\Delta F/F$, for $L = 40a$.

A. The Growth-Promoter Reflection Model

The sporangiophore growing zone emits a growth-promoting gas, and detects the concentration gradient of this gas produced by reflection of the gas off a nearby surface. We assume that the signal gas does not decay in this model, and if the sporangiophore is in an airtight chamber, that the background concentration of the gas does not build up significantly during an experiment inside the chamber. Thus, in the following, we assume that the sporangiophore is in open, quiet air.

We approximate the growing zone by a long, thin, straight cylinder of radius a = 50 μm, and length L = 2 mm. The cylinder emits a non-decaying gas at a uniform rate everywhere on its surface, at r = a, from z = -L/2 to z = +L/2,

To find the concentration of the gas as a function of position, we replace the wire or plane barrier by an appropriate set of image sources and/or sinks. The flux of gas emitted and/or adsorbed by these images cancels the normal component of the flux emitted by our model growing zone at the surface of the barrier. This satisfies the condition that the gas be perfectly reflected by the surface of the barrier. The use of images in solving Laplace's equation is standard (Smythe 1950). The results obtained here with this method are original.

First, we attack the problem of a thin, parallel reflecting wire placed a few mm from the growing zone. We assume that the flux normal to the surface of the wire is zero (total reflection). At the position of the wire, the outward flux due to our emitting cylinder is approximately uniform. Call this flux $F_W(d)$, in molecules/cm^2/sec, where d is the distance between the wire and the sporangiophore. To calculate $F_W(d)$, we use the approximate form of (3) given by (5) in Section III; i.e., we approximate the growing zone by a point source. At r = 2 mm, (5) is only 4% greater than (3), so the approximation is a good one. Using (5), the flux at the wire is:

$$F_W(d) = -D(\partial c/\partial r)_{r=d} = (F/2)\cdot(aL/d^2) . \qquad (1)$$

This flux is directed away from the z-axis (the axis of our emitting cylinder). D is the diffusion coefficient of the emitted gas, F is the outward flux of gas at the surface of the emitting cylinder, a and L are the radius and length of the cylinder, and d is the distance of the wire from the z-axis.

We assume that the flux $F_W(d)$ is uniform in the vicinity of the wire. Let the distance from the axis of the wire be ρ, let the radius of the wire be ρ_o, and let the azimuthal angle around the wire be ϕ, where $\phi = 0$ is defined to be toward the emitting cylinder.

Then the component of F_W normal and into the surface of the wire is just:

$$F = F_W\cos\phi . \qquad (2)$$

The flux at $\phi = 0$ is directed into the surface of the wire, and at $\phi = \pi$ it is out of the surface of the wire.

The trick now is to replace the reflecting wire by an image source whose flux at the surface of the wire cancels the normal component of F_W on

the surface of the wire.

The required image source is a line dipole: a parallel line source and line sink located at the axis of the wire and on opposite sides of it - the source at $\phi = 0$ and $\rho = \varepsilon$, and the sink at $\phi = \pi$ and $\rho = \varepsilon$, where ε is infinitesimal compared to ρ_o, the radius of the wire.

Let the emission rate of the line source in this dipole per unit length be f molecules/cm/sec (this is also the adsorption rate of the line sink in the dipole). Since the source and sink are so close together, the flux of gas out of the dipole at any point is directed away from the dipole (i.e., normal to the surface of the wire), and vice-versa for flux into the dipole. The distance from either the source or the sink to any point at a distance ρ from the axis of the wire is $\rho \pm \varepsilon\cos\phi$, positive for the sink and negative for the source. Summing the fluxes of the source and sink at any point, (ρ, ϕ), and neglecting a term of order ε^2 we get the flux due to the dipole, F_d, as:

$$F_d = (f\varepsilon/\pi\rho^2)\cos\phi \qquad (3)$$

in molecules/cm^2/sec, which is normal to the surface of the wire at any point and is positive for outward flux. (3) is equivalent to the inward normal component of flux due to the emitting cylinder (2), as required. To cancel this flux (2), set it equal to (3) at $\rho = \rho_o$. The required "dipole moment," $2f\varepsilon$, is then:

$$2f\varepsilon = 2\pi\rho_o^2 F_W \qquad (4)$$

in molecules/sec.

If the wire is replaced by a dipole of this magnitude, the flux normal to the surface of the wire, at $\rho = \rho_o$, will be zero. The flux due to the dipole alone, at any point (ρ, ϕ) relative to the axis of the wire, will be (from 3 and 4):

$$F_d(\rho) = (\rho_o/\rho)^2 F_W \cos\phi \qquad (5)$$

in molecules/cm^2/sec, positive outward, where $F_W = F_W(d)$, the cylinder's flux at the location of the wire.

Setting $\phi = 0$ and putting in F_W from (1), we can use (5) to find the flux reflected by the wire, at any distance, ρ, from the wire. This is:

$$F_{refl}(\rho_o, d) = (F/2)(aL\rho_o^2/\rho^2 d^2) \qquad (6)$$

in molecules/cm^2/sec, where ρ_o is the radius of the wire, d is the distance between the wire and the emitting cylinder, F is the outward surface flux at the cylinder, in molecules/cm^2/sec, and a and L are the radius and length of the cylinder.

We assume that the wire's length is much greater than L, the length of the cylinder.

We can integrate (6) with respect to ρ, to find the concentration difference across the cylinder due to the wire. This gives:

$$c(\rho) = (F/2D)(aL\rho_o^2/\rho d^2) . \qquad (7)$$

However, the flux (6), if superimposed on the uniform outward flux at the surface of the cylinder, unbalances it. The cylinder's flux can be returned to uniform, satisfying our boundary conditions specified above, if a second image dipole is added at the axis of the cylinder. We find (without showing the calculation) that the concentration difference produced by this second-order image is of the same sign and magnitude as the difference produced by the flux of the first dipole (6).

The total concentration difference across the cylinder, including this second-order effect, is then:

$$\Delta c = 2\,(aF/D)\,(aL\rho_o^2/d^4) \qquad (8)$$

in molecules/cm^3/sec. The average concentration at the surface of the cylinder is given by (6) in Section II:

$$c(a) = (aF/D)\log(L/a) \qquad (9)$$

in molecules/cm^3/sec. Incidentally, this surface concentration is increased by a factor $(L\rho_o^2/d^3)/2\log(L/a)$, due to the reflection of the gas by the wire, or about 1 part in 50,000 for the values of a, L, ρ_o, and d assumed below. The fractional difference in concentration across the cylinder, induced by the wire at a distance d, is then:

$$\Delta c/c = 2\,(aL\rho_o^2/d^4) \,/\, \log(L/a) \qquad (10)$$

in molecules/cm^3/sec, where a is the radius of the cylinder, L is the cylinder's length, ρ_o is the wire's diameter, and d is the distance between the wire and the cylinder, assumed to be greater than or equal to L (see eqn. 1).

In our case we want to evaluate $\Delta c/c$ for a wire of radius ρ_o = 25 μm, at a distance d = 2 mm from the cylinder. We take a = 50 μm and L = 2 mm as the dimensions of the cylinder. (10) is then equal to $2.1 \cdot 10^{-6}$, so the concentration is only about 2 parts in 1 million greater on the side of the cylinder facing the wire, compared to the opposite side.

Using the above results, we can now easily calculate the concentration difference, $\Delta c/c$, induced across our emitting cylinder by a large, parallel reflecting plane located at a distance d from the cylinder. We assume that the flux normal to the surface of the plane is zero.

As before, we replace the plane by an image source, the "mirror image" of our emitting cylinder, located on the opposite side of the plane at a distance 2d from the actual cylinder.

The normal components of the fluxes of the actual cylinder and its image are equal and opposite at any point on the plane. Thus, if we sum the solutions of Laplace's equation for these two sources, we get approximately the solution for the actual cylinder next to the reflecting plane. We have to correct for the unbalancing of the flux at the surface of the emitting cylinder, by the added flux due to the image, as before. Its effect is to raise the concentration difference across the cylinder by a factor of 2, as before. Without showing the steps involved (they are identical to those above, except with a line source as an image instead of a dipole), the concentration due to the image is:

$$c(\rho) = (aF/D)(L/2)(1/\rho) \qquad (11)$$

where ρ is the distance from the image, and $\rho > 2$ mm. The fractional concentration difference induced across the cylinder by the plane barrier at a distance $d \geq 2$ mm, is:

$$\Delta c/c = (aL/2d^2) / \log(L/a) \qquad (12)$$

where a is the radius of the cylinder, and L is its length.

Notice that this is the same as the result for the wire (9), but increased by a factor $d^2/4\rho_o^2$, where ρ_o is the radius of the wire. Since d is

always 10 to 100 times ρ_o in our experiments, the Growth-Promoter Reflection Model predicts 25 to 2500 times smaller bending rates for a wire, compared to a plane placed at the same distance - assuming that the bending rate is proportional to $\Delta c/c$.

Setting d = 5 mm in (10), we get $\Delta c/c = 0.5 \cdot 10^{-3}$, which is 250 times greater than for the 50 μm diameter wire discussed above.

c(x) is plotted in Fig. 21 for our emitting cylinder both in open air as well as located 2 mm away from a parallel, reflecting plane barrier. Notice that the barrier increases the concentration at the surface of the cylinder by about 7%.

Fig. 21 The concentration of the effector gas in the Growth-Promoter Reflection Model.

The concentration of gas emitted by our model growing zone (emitting cylinder) is plotted vs. distance along the x-axis, which is perpendicular to both the cylinder axis and the barrier, positive away from the barrier. The concentration is given relative to the concentration at the surface at the midpoint of the cylinder in open air. Two cases are shown: no barrier (open symbols), and a large, parallel reflecting plane barrier located at x = -2 mm (filled symbols). The midpoint of the axis of the cylinder is at the origin. The cylinder radius is assumed to be 0.005 cm, and its length 2 mm.

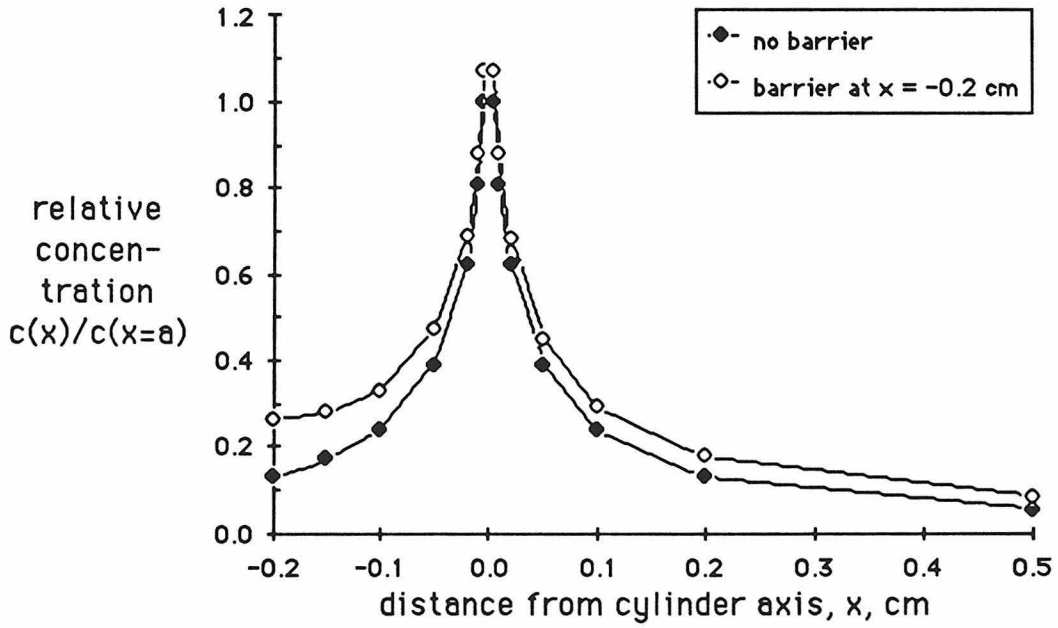

B. The Wind-Gradient Model

In this model, the sporangiophore emits a short-lived, growth-promoting gas which does not diffuse more than a few hundred μm from the surface of the growing zone. The sporangiophore detects an object by keeping the concentration of this gas fixed at the surface of the growing zone, and measuring the difference in the flux of the gas out of the growing zone on the side facing the object, vs. the opposite side. Since ambient wind currents are dampened near the surface of any object, less gas is "blown away" on the side of the growing zone facing the object, so the flux will be slightly less on that side.

We can estimate the relative difference in flux, making reasonable assumptions about the manner in which the gas is convected away from the growing zone. This is an original result.

In quiet air, the surface flux is given (approximately) by (6) in Section III:

$$F = (D/a)\cdot c \qquad (13)$$

in molecules/cm^2/sec, where we have dropped the logarithmic term, and where D is the diffusion coefficient of the gas, a is the radius of the growing zone, and c is the concentration of the gas at the surface of the growing zone, assumed to be uniform. We also assume that the decay length of the gas is on the order of a, and that the wind is directed vertically, parallel to the sporangiophore.

5 mm away from a plane barrier in our environmental chamber, the wind speed cannot be greater than 5 μm/sec. We assume that the difference in wind speed across the sporangiophore is on the order of 0.05 μm/sec.

The flux of gas out of either side of the growing zone due to convection alone can be roughly estimated as follows. Since the gas does not diffuse more than a distance of order a, it can only be removed by convection in a vertical column of cross-sectional area on the order of a^2. If U_1 is the wind

speed on the side of the growing zone facing the barrier, the total convective flow of molecules out of such a column on this side will be approximately U_1a^2c molecules/sec. The extra flux out of the growing zone on this side, due to convection, will be approximately:

$$F_c = U_1a^2c/aL = U_1ac/L \qquad (14)$$

where aL is roughly one-half the surface area of the growing zone.

Taking the difference in flux between the two sides, and dividing by the total flux out of the growing zone given by (13), above, we get:

$$\Delta F/F = (a^2/LD)\cdot\Delta U \qquad (15)$$

for the fractional difference in flux across the growing zone, greater on the side facing away from the barrier, and where a is the radius of the growing zone, L is its length, D is the diffusion coefficient of the gas ($\approx$ 0.1 cm^2/sec), and ΔU is the difference in wind speed across the growing zone, assumed to be 0.05 μm/sec.

Evaluating (15), we get $\Delta F/F = 6\cdot10^{-9}$, for a sporangiophore located 5 mm away from a plane barrier in our experimental chamber. This flux difference is negligible. It is unlikely that the sporangiophore uses wind currents to detect nearby objects.

C. The Inhibitor Adsorption Models

In these models, a growth inhibitor is either produced by the sporangiophore growing zone (Growth-Inhibitor Adsorption Model) or by an external source in the immediate environment (Atmospheric Growth-Inhibitor Adsorption Model), and is adsorbed efficiently by all surfaces, including the surface of the growing zone itself. Here, we assume that its concentration decreases to zero at any surface. Thus, if a barrier is brought up to the growing zone, the flux of inhibitor gas into the side of the growing zone facing the barrier will be less than the flux into the opposite side. The barrier "competes" with the growing zone for adsorption of the inhibitor. We estimate this flux difference below.

If the growing zone itself produces the inhibitor, it must do so by first emitting an inert precursor gas, which is then converted in air to the inhibitor, by oxidation for example. The reasons for this were outlined in Section I of Chapter 4, above. We assume that the precursor is not adsorbed by any surfaces, and we define its decay length to be R_{dp}, as in Section II of this Appendix, above.

It is clear that R_{dp} must be fairly large. From Part D in Section II, above, it was shown that for a spherical "growing zone" of radius a, the inhibitor concentration reaches a maximum at a distance $R_{MAX} = (2aR_{dp})^{1/2}$, and falls off beyond R_{MAX}. Two sporangiophores placed further apart than R_{MAX} should bend toward each other. Since "flaring" of a forest of sporangiophores is observed with a spacing between adjacent growing zones of over 1 cm, we can assume that $R_{MAX} > 1$ cm. Thus, R_{dp} must be greater than 100 cm if the radius of the growing zone, a, is 50 μm.

Since the growing zone is not a sphere of radius a but rather a long, thin cylinder of the same radius, it is probably equivalent - at distances greater than its length - to a larger sphere, say, of radius not more than 10a.

Even so, R_{dp} must still be quite large, i.e., greater than 10 cm.

Given this lower bound on R_{dp}, the precursor concentration must be nearly uniform in our experimental chamber, which only measures 2.5 cm across.

As a result, the two Inhibitor Adsorption models are roughly equivalent. The Growth-Inhibitor Adsorption Model proposes that the production rate of inhibitor will be nearly uniform throughout the volume of our experimental chamber, while the Atmospheric Growth-Inhibitor Adsorption Model assumes that inhibitor is produced at some location in the chamber far from the growing zone; e.g., in the oil in the base of the chamber. In either case the inhibitor concentration is highest in the middle of the chamber, and falls off to zero at the walls and on any surface. We consider only the Growth-Inhibitor Adsorption Model, in what follows, and assume that the results for the other model are similar.

We assume below that the inhibitor is produced uniformly throughout the chamber volume at a rate Q, in molecules/cm^3/sec. We approximate the chamber by a hollow cube with sides of length h = 2.5 cm and with its center at the origin.

All of the results below are original.

First, we calculate the distribution of the inhibitor. Its concentration, c, must obey Laplace's equation, with the uniform production, Q, taken into account. Following (10) in Section II of this Appendix, we get:

$$D\nabla^2 c = -Q \qquad (16)$$

This can be satisfied in 3 dimensions with a series expansion for c of the form:

$\sum a_m \cdot \cos(m\pi x/h) \cdot \cos(m\pi y/h) \cdot \cos(m\pi z/h)$, where m = 1, 3, 5, 7 ... Clearly, c goes to zero on any wall, where either x or y or z $= \pm h/2$. Doing the arithmetic

- plugging the series into (24) and integrating both sides to find the coefficients a_m - it turns out that a_m falls off as m^{-5}, so that the second term in this expansion is $3^5 = 243$ times smaller than the first. Since c is nearly a product of cosines, each of which is of the form $1 - x^2/2 + x^4/24 - \ldots$, solving (16) in one dimension (where c varies as $1 - kx^2$) will give results close to those for 3 dimensions, so we just work with the one-dimensional case here.

In particular, we assume that only two opposing walls adsorb the inhibitor, at $x = \pm h/2$, that one of them is used as the plane barrier, and that the other 4 walls of our box are non-adsorbing. (16) is then satisfied by:

$$c = (Qh^2/8D)\,[\,1 - (2x/h)^2\,] \qquad (17)$$

The concentration at the center of the box ($x = 0$) is $Qh^2/8D$, in molecules/cm^3, and the flux into the surface of one of the adsorbing walls is just $-D(\partial c/\partial x)$ at $x = h/2$, or $Qh/2$, in molecules/cm^2/sec.

If the growing zone is located at the center of the box, what is the flux into its surface? Assume that this flux is about the same as if the growing zone were located in open air with the background concentration of the adsorbed gas equal to $Qh^2/8D$, and with zero gas concentration at the surface of the growing zone. Since the negative of a solution to Laplace's equation is also a solution, this flux is equal to the flux of a non-decaying gas <u>emitted</u> at the surface of a cylinder of radius <u>a</u> and length L in open air, with the gas concentration on its surface held uniform and equal to $Qh^2/8D$, and the background concentration equal to zero.

Equation (6) in Section III of this Appendix gives the concentration at the surface at the midpoint of a cylinder emitting a gas with uniform flux at its surface. This will also indicate approximately the flux at the surface of a cylinder held at some specified concentration (Section III). Setting the concentration (6) in Section III, above, equal to $Qh^2/8D$, we find that the adsorbed flux, F, for the growing zone is roughly:

$$F = (Qh^2/8a) / \log(L/a) \qquad (18)$$

in molecules/cm^2/sec, where Q is the production rate of inhibitor in our box, in molecules/cm^3/sec, h is the width of our box, a is the radius of our model growing zone and L is its length.

To determine the fractional difference in adsorbed flux across the growing zone induced by a nearby plane or wire, we could try to solve Laplace's equation for the concentration and flux near an adsorbing cylinder placed in a concentration gradient. This has been done for a sphere by Berg and Purcell (1977, p. 219). They find that if a perfectly adsorbing sphere is placed in a concentration gradient of magnitude dc/dz, then there is an added inward flux at the midpoint of the front face of the sphere of Ddc/dz molecules/cm^2/sec (and likewise an identical added flux out of the back face of the sphere). This is the same as the flux due to the gradient alone, without the sphere.

Therefore, we make a simplifying assumption. We superimpose the concentration gradient due to the barrier on the concentration due to the adsorbing cylinder by itself. With this, there is no longer a uniform, zero concentration around the surface of the cylinder. An image dipole should be added at the axis of our adsorbing cylinder to correct for this, as was done in Part A of this Section, above. This ought to increase the flux difference across the cylinder by a factor of two, as before. We account for this in our estimate of $\Delta F/F$, below, but not in Fig. 22. For a flux F_g directed perpendicular to the axis of the cylinder, the difference in flux across the cylinder is then $2F_g$, and the fractional difference in flux, $\Delta F/F$, is $2 \cdot 2F_g/F = 4F_g/F$, accounting for the factor of two just mentioned.

Now we estimate $\Delta F/F$ across our model growing zone, due to a nearby plane or wire adsorber.

By analogy with (18), the flux into a thin wire of radius ρ_o, located at a distance d from the wire, where d is much less than the wire's length, is:

$$F_{wire} = (Qh^2/8d) / \log(L_w/\rho_o) \qquad (19)$$

in molecules/cm^2/sec, where Q is the production rate of inhibitor inside our box, h is the width of the box, and d is the distance from the adsorbing wire of radius ρ_o and length L_w.

Because the wire adsorbs the gas, its concentration 2 mm from the wire will be about 15% less than its value with the wire far away (to see this, invert Fig. 20). Thus, the flux calculated in (18) should be correct to well within an order of magnitude.

The fractional difference in flux induced across our model growing zone by the wire is just $4 \cdot F_{wire}/F$, where F is given by (18), above. Hence, if the length, L, of the growing zone is 2 mm and its radius, a, is 50 μm, then:

$$\Delta F/F = (4a/d) \cdot [\, \log(L/a) / \log(L_w/\rho_o) \,] \approx 2.4 \cdot (a/d) \qquad (20)$$

where d is the distance to the wire, assumed to be at least 2 mm, and L_w and ρ_o are assumed to be 1 cm and 25 μm, respectively. Notice that this result is independent of the size of the box as well as the production rate of the inhibitor. It is also only logarithmically dependent on the diameter of the adsorbing wire. If a = 50 μm and d = 2 mm then $\Delta F/F \approx 2.4/40 = 0.06 = 6\%$ for our adsorbing wire 2 mm away.

We can now calculate $\Delta F/F$ for a nearby plane. In this case, one of the walls of our experimental chamber is pushed in so that it is a distance $x = -d$ from the growing zone, which is located at the origin. The opposite wall is located at a distance $x = h/2$ from the origin, where h is the original width of the chamber. Thus, in (17), substituting h by $h^* = d + h/2$, and substituting x by $x - x^*$, where $x^* = h/4 - d/2$, so that the new midpoint of the chamber - midway between the two adsorbing walls - is located at $x = x^*$, we get:

$$c = (Qh^{*2}/8D)\cdot\{ 1 - [2(x-x^*)/h^*]^2 \} \qquad (21)$$

where x is the distance from the origin, and h^* is the new (shrunken) width of the chamber. The concentration at the midpoint, $x = x^*$, is now $Qh^{*2}/8D$, which is lower than before ($h^* < h$) because the two adsorbing walls are closer together.

Equation (21) is plotted in Fig. 22. Its superposition with equation (3) from Section III of this Appendix is also plotted, to give some indication of how the inhibitor concentration falls off in the vicinity of the growing zone. This superposition is obtained by multiplying (21) by $1 - [c(x)/c(x=a)]$, where c(x) is the concentration due to an emitting cylinder, given by (3) from Section III, above.

The flux toward the proximal (pushed-in) wall at the position of the growing zone, $x = 0$, is obtained by differentiating (21). This gives: $F_{wall} = Q\cdot x^*$. Substituting in $x^* = h/4 - d/2$ we get:

$$F_{wall} = Q\cdot(h/4 - d/2) \qquad (22)$$

in molecules/cm^2/sec.

The fractional difference in flux induced across our model growing zone by bringing up the wall to a distance d is just $\Delta F/F = 4F_{wall}/F^{\circ}$. F° is the average flux into the growing zone. It is about 60% less than the value of F calculated in (18), because the inhibitor concentration at the center of the chamber is reduced by about 60% with one of the walls pushed in 5 mm from the center, as indicated by Fig. 22. Thus, $\Delta F/F$ is approximately $(5/2)\cdot 4\cdot F_{wall}/F = 10\cdot F_{wall}/F$, or:

$$\Delta F/F = [40\cdot\log(L/a)]\,(a/h)\,(1/2 - d/h) \qquad (23)$$

where a is the radius of our model growing zone, L is its length, h is the original width of the chamber, and d is the distance between the inserted wall and the growing zone, with $d \geq 2$ mm.

Notice that $\Delta F/F = 0$ if $d = h/2$, as required. If $d = 5$ mm, $h = 25$ mm, $L = 2$ mm, and $a = 50$ μm, then the fractional difference in concentration due to the plane at 5 mm is: $\Delta F/F = 40\ (3.7)\ (0.05/25)\ (1/2 - 5/25) = 0.09 \approx 9\%$.

Fig. 22 The concentration of the inhibitor in the Inhibitor Adsorption Models

The concentration is plotted relative to the concentration at the center of the box with none of the walls pushed in and with the box empty. This reference concentration is $Qh^2/8D$, as given by (17), above. The concentration is plotted as a function of x. The midpoint of the axis of the adsorbing cylinder is located at the origin, which is at the center of the box.

The width of the cubical box is assumed to be 2.50 cm, and only two opposing walls adsorb the inhibitor. One wall is located at x = +1.25 cm, the other is located either at x = -1.25 cm or at x = -0.5 cm.

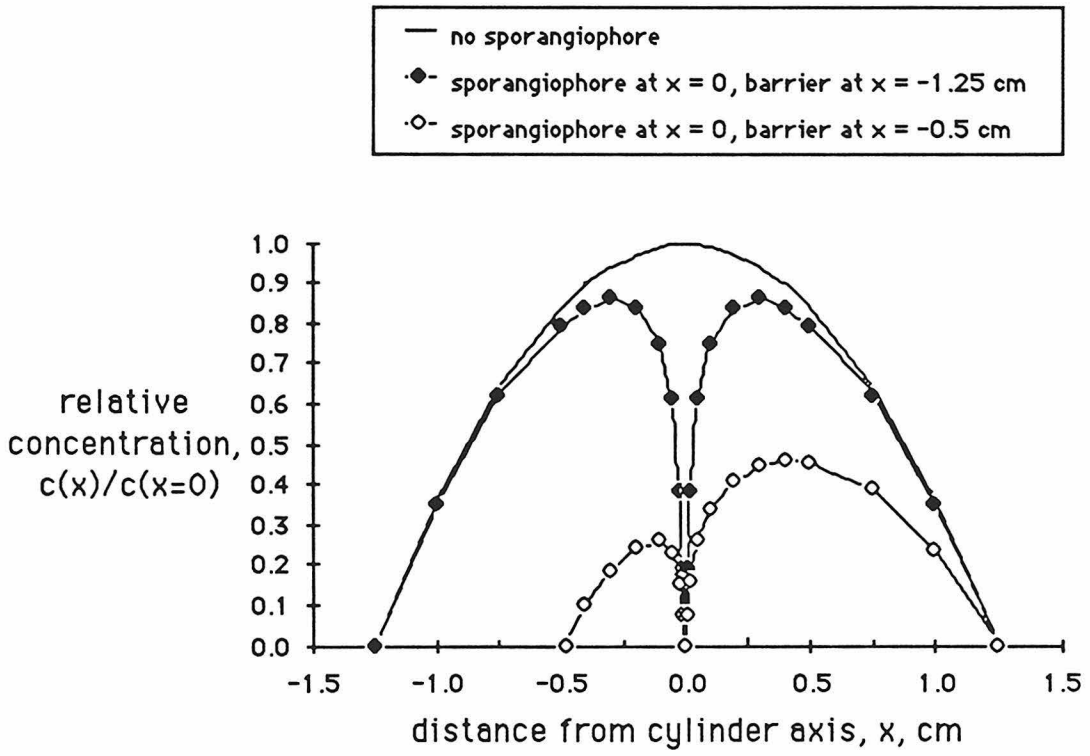

D. The Barrier Emission Model

In this model, the sporangiophore emits an inactive precursor gas which decays preferentially on any surface, including the growing zone itself, to an active, growth promoting gas. This effector must then also decay, to prevent buildup of the gas inside an airtight chamber. Let its decay length be R_d, small compared to the dimensions of the chamber. We assume that the concentration of effector is uniform on all surfaces inside our experimental chamber, including the surface of the growing zone itself, and is equal to c_o. We also assume that the sporangiophore detects an object by measuring the flux of effector emitted by the object, at the growing zone. These assumptions give the best fit to the experimental results.

First, we calculate the flux of effector at the surface of our model growing zone - a cylinder of radius a and length L >> a - under the above conditions. Then, we calculate the fractional difference in this flux induced across the growing zone by a parallel, emitting wire placed nearby. We then do the same calculation for a parallel, emitting plane. All of these results are original.

The flux out of the surface of our growing zone will be about the same as the flux out of an emitting cylinder with the same radius, the same surface concentration, but with infinite length. This is because we assume that the decay length of the effector, R_d, is less than the length of the growing zone, L. The concentration in the vicinity of this infinite cylinder must obey Laplace's equation, modified to take into account the decay of the effector. Using (6) from Section II, above, we get $\nabla^2 c = c/R_d^2$, or, in cylindrical coordinates:

$$\partial^2 c/\partial r^2 + (1/r)\partial c/\partial r - (1/R_d^2)c = 0 \qquad (24)$$

This is satisfied by $c = c' K_0(r/R_d)$ if we require that c go to zero as r goes to infinity, where K_0 is the zero-order modified Bessel function of the second kind (Spiegel 1968, p. 138). c′ is a constant.

This makes sense; $K_0(r/R_d)$ decreases logarithmically with r for small $r << R_d$, where decay doesn't matter, so that the cylinder looks pretty much like a line source; and it decreases exponentially with r for large $r >> R_d$, due to decay of the effector gas.

Requiring that $c = c_o$ at r = a, we get:

$$c = c_o \cdot [\, K_0(r/R_d) / K_0(a/R_d) \,] \qquad (25)$$

Since the derivative of $K_0(x)$ is $- K_1(x)$, from Spiegel (1968, p. 139), the flux of effector out of the surface of our model growing zone is given by $-D(\partial c/\partial r)$ at r = a, or:

$$F = (Dc_o/R_d) \cdot [\, K_1(a/R_d) / K_0(a/R_d) \,] \qquad (26)$$

in molecules/cm^2/sec, where D is the diffusion coefficient of the effector, c_o is its concentration at the surface of the growing zone, R_d is its decay length, and a is the radius of the growing zone.

Now, we calculate the flux induced across the growing zone by a nearby, emitting wire of radius ρ_o, with effector concentration c_o at its surface. This is obtained exactly like (26), so that:

$$F_{wire} = (Dc_o/R_d) \cdot [\, K_1(d/R_d) / K_0(\rho_o/R_d) \,] \qquad (27)$$

where d is the distance to the wire. Since d >> a, this flux (27) is much smaller than the growing zone's own flux (26). Superimposing (27) and (26), and

adding an image dipole to keep the effector concentration uniform at the surface of the cylinder (see Parts A and C, above), we find the fractional difference in flux, $\Delta F/F$, induced across our model growing zone. This is just $4F_{wire}/F$, or:

$$\Delta F/F = 4\cdot[\, K_1(d/R_d) / K_1(a/R_d) \,]\cdot[\, K_0(a/R_d) / K_0(\rho_o/R_d) \,] \qquad (28)$$

This falls off exponentially for $d >> R_d$, as expected.

Taking $R_d = 2$ mm, $d = 2$ mm, $a = 50$ μm, and $\rho_o = 25$ μm, we get $\Delta F/F = 4\cdot(0.6/20)\cdot(3.1/3.8) = 0.094 \approx 9\%$, as the fractional difference in flux of effector across our model growing zone, due to a thin, parallel wire of radius 25 μm located 2 mm away.

The second ratio in (28), of zero-order Bessel functions, is close to unity for any of the values we might assume here. A table of K_0 and K_1, and an approximation for K_0 for small arguments from Spiegel (1968, p. 247 and p. 139), was used to evaluate (28).

Now we calculate $\Delta F/F$ across our model growing zone with a large, parallel emitting plane located at a distance d, with effector concentration c_o at its surface. The concentration of gas emitted by this plane is governed by Laplace's equation in 1 dimension, or:

$$\partial^2 c/\partial x^2 = c/R_d^2 \qquad (29)$$

from (24) above. This is satisfied by:

$$c = c_o\, e^{-x/R_d} \qquad (30)$$

where x is the distance from the plane.

The flux away from the plane at a distance d is just $-D(\partial c/\partial x)$ at r = d, or:

$$F_{plane} = (Dc_o/R_d)\, e^{-d/R_d} \qquad (31)$$

where D is the diffusion coefficient of the effector, c_o is its concentration at the surface of the plane, and R_d is its decay length.

The fractional difference in flux across the growing zone due to the plane is $4F_{plane}/F$, or:

$$\Delta F/F = 4\, e^{-d/R_d} [\, K_0(a/R_d) / K_1(a/R_d) \,] \qquad (32)$$

where a is the radius of our model growing zone. Evaluating (30) at d = 5 mm, with R_d = 2 mm and a = 50 μm, we get $\Delta F/F = 4 \cdot (0.082) \cdot [3.1/20] = 0.05 = 5\%$, as the fractional difference in flux across the growing zone due to a plane at 5 mm.

This is less than the value obtained for the thin wire, 9%, because the wire is only 2 mm from the growing zone. If the plane is moved in to 2 mm, ΔF/F increases to 22%. It is amazing that a 25 μm diameter wire should induce a flux difference across the growing zone almost as strong as that induced by a plane 25,000 μm wide.

Fig. 23 The concentration of the effector in the Barrier Emission Model

The effector concentration is assumed to be uniform and equal to c_o on all surfaces, including the growing zone itself. The decay length of the effector is 2 mm. The growing zone (emitting cylinder) is located at the center of a cubical box of side 2.50 cm, as in Fig. 22.

The effector concentration is plotted relative to c_o, vs. the distance along the x-axis. The concentration at any point on the x-axis is assumed to be the sum of the concentrations due to the 4 walls parallel to it, located at y = ±1.25 cm and z = ±1.25 cm, plus the concentration due to the wall located at x = +1.25 cm, plus the concentration due to the barrier wall located either at -1.25 cm or -0.5 cm, plus the concentration due to the growing zone itself, if present.

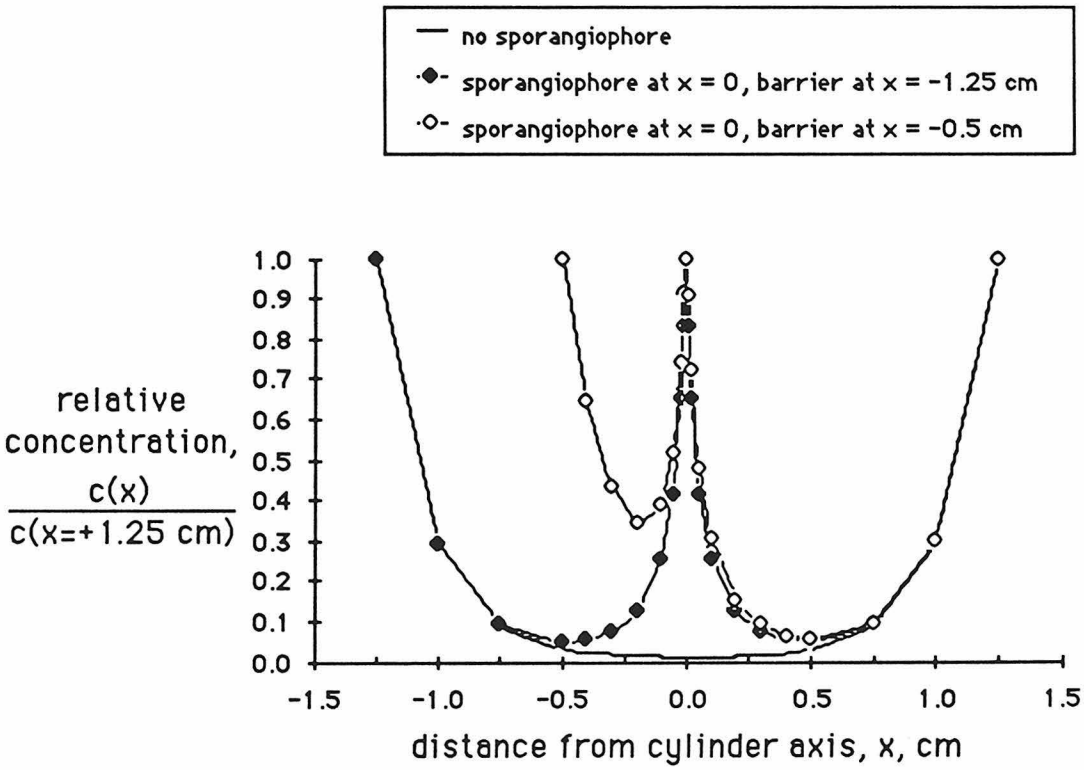

Fig. 24 Summary of the concentration and flux differences predicted for the five proposed models for the avoidance response.

No value was calculated for the wire in the Wind-Gradient Model, but it is probably much less than for the plane barrier.

The Growth-Inhibitor Adsorption Model and the Atmospheric Growth-Inhibitor Adsorption Model are assumed to be identical in these calculations.

The values shown are only accurate to within an order of magnitude.

The models are abbreviated as follows:

GPR = Growth-Promoter Reflection Model
WG = Wind Gradient Model
IA = Inhibitor Adsorption Models
BE = Barrier Emission Model

		fractional increase or decrease in signal produced by:		fractional difference in signal induced across growing zone by:	
model	signal	wire @ 2 mm	plane @ 5 mm	wire @ 2 mm	plane @ 5 mm
GPR	concentration	$2 \cdot 10^{-5}$	0.07	$2 \cdot 10^{-6}$	$5 \cdot 10^{-4}$
WG	flux				$6 \cdot 10^{-9}$
IA	flux	0.15	0.6	0.06	0.09
BE	flux	≈ 0.1	≈ 0.5	0.09	0.05

References

1. Berg, H.C. 1983. Random Walks in Biology. Princeton University Press, Princeton, New Jersey.
2. Berg, H.C., and Purcell, E.M. 1977. Physics of Chemoreception. Biophysical Journal. 20 : 193-219.
3. Bergman, K., Burke, P.V., Cerdá-Olmedo, E., David, C.N., Delbrück, M., Foster, K.W., Goodell, E.W., Heisenberg, M., Meissner, G., Zalokar, M., Dennison, D.S., and Shropshire, W. 1969. Phycomyces. Bact. Rev. 33 : 99-157.
4. Burke, P.V. 1971. "Freezing Phycomyces Sporangiophores in Superfluid Helium for Ultrastructure Studies." Ph.D. Thesis, California Institute of Technology, Pasadena, Calif.
5. Cohen, R.J. 1976. The Avoidance Behavior of Phycomyces blakesleeanus : Is Mediation by Natural Convection Significant ? J. Theor. Biol. 58 : 207-217.
6. Cohen, R.J., Fried, M.G., and Atkinson, M.M. 1979. Olfactory Responses of Phycomyces blakesleeanus. Bioc. Biop. Res. Comm. 86 : 877-884.
7. Cohen, R.J., Jan, Y.N., Matricon, J., and Delbrück, M. 1975. Avoidance Response, House Response, and Wind Responses of the Sporangiophore of Phycomyces. J. Gen. Physiol. 66 : 67-95.
8. Daniels, F. 1948. Outlines of Physical Chemistry. John Wiley and Sons, Inc., New York.
9. Eisenberg, D., and Crothers, D. 1979. Physical Chemistry. Benjamin/Cummings, Menlo Park, California.
10. Elfving, F. 1881. En obeaktad känslighet hos Phycomyces. Botaniska Notiser. no. 4 : 105-107.
11. Elfving, F. 1890. Über physiologische Fernwirkung einiger Körper. Commentationes variae in memoriam actorum CCL annorum. Edidit Universitas Helsingforsiensis.

12. Elfving, F. 1893. Zur Kenntnis der pflanzlichen Irritabilität. Öfversigt af Finska Vetenskaps-Societetens Förhandlingar. 36 : 77-85.
13. Elfving, F. 1916. Phycomyces und die sogennante physiologische Fernwirkung. Öfversigt af Finska Vetenskaps-Societeten Förhandlingar. 59 : 1-56.
14. Errera, L. 1892. On the cause of physiological action at a distance. Annals of Botany. 6 : 373-375.
15. Feynman, R.P., Leighton, R.B., and Sands, M. 1963. The Feynman Lectures on Physics. Addison-Wesley Publishing Company, Reading, Massachusetts.
16. Gamow, R.I., and Böttger, B. 1982a. Phycomyces : Discovery of the Aiming Error in the Avoidance Response. Plant Physiol. 69 : 742-744.
17. Gamow, R.I., and Böttger, B. 1982b. Avoidance and Rheotropic Responses in Phycomyces. J. Gen. Physiol. 79 : 835-848.
18. Gyure, D.C., Böttger, B., and Gamow, I. 1984. Phycomyces : Detailed Analysis of the Anemogeotropic Response. J. Gen. Physiol. 84 : 727-738.
19. Harris, S.S., and Dennison, D.S. 1979. Phycomyces : Interference Between the Light Growth Response and the Avoidance Response. Science 206 : 357-358.
20. Jan, Y.N. 1974. Part 2. "The Avoidance Response, the House Growth Response and the Rheotropic Response of Phycomyces." Ph.D. Thesis, California Institute of Technology, Pasadena, Calif.
21. Johnson, D.L., and Gamow, R. 1971. The Avoidance Response in Phycomyces. J. Gen. Physiol. 57 : 41-49.
22. Lafay, J.F. 1980. "Réponses sensorielles d'un système végétal : réaction d'évitement, anémotropisme, etc... du sporangiophore de Phycomyces blakesleeanus Burgeff (Zygomycètes, Mucorales)." Ph.D. Thesis, L'Université de Paris XI, Centre d'Orsay.

23. Lafay, J.F., and Matricon, J. 1982. Avoidance and Wind Responses of Phycomyces blakesleeanus : Two Distinct Sensitivities. Experimental Mycology. 6 : 244-252.

24. Lafay, J.F., Matricon, J., and Bodéré, C. 1975. The Avoidance Response of Phycomyces : Distance Dependence of the Response. Physiologie Végétale. 13 : 259-263.

25. Latimer, W.M. 1952. Oxidation Potentials. 2nd ed. Prentice-Hall, New York.

26. Mathews, J., and Walker, R.L. 1965. Mathematical Methods of Physics. W.A. Benjamin, Inc., New York.

27. Matus, I.J. 1985. personal communication.

28. Pellegrino, J.J., et al. 1983. Mass Transfer from Phycomyces in the Avoidance and Anemotropic Responses. J. Theor. Biol. 105 : 77-90.

29. Russo, V.E.A. 1977. Ethylene-Induced Growth in Phycomyces Mutants Abnormal for Autochemotropism. J. Bacteriol. 130 : 548-551.

30. Russo, V.E.A., Halloran, B., and Gallori, E. 1977. Ethylene is Involved in the Autochemotropism of Phycomyces. Planta 134 : 61-67.

31. Shropshire, W. 1962. The lens effect and phototropism of Phycomyces. J. Gen. Physiol. 45 : 949-58.

32. Smythe, W.R. 1950. Static and Dynamic Electricity. McGraw-Hill Book Company, Inc., New York.

33. Spiegel, M.R. 1968. Mathematical Handbook of Formulas and Tables. McGraw-Hill Book Company, Inc., New York.

34. Steyer, K. 1901. "Reizkrümmungen bei Phycomyces nitens." Inaugural-Dissertation, Leipzig.

35. Walter, H. 1921. Wachstumsschwankungen und hydrotropische Krümmungen bei Phycomyces nitens. Zeitschrift für Botanik. 13 : 673-718.

36. Weast, R.C., ed. 1975. Handbook of Chemistry and Physics. CRC Press, Cleveland, Ohio. 56 th. edition.

37. Wortmann, J. 1881. Ein Beitrag zur Biologie der Mucorineen. Botanische Zeitung. 39 : 368-374, 383-387.